Senior Design 2

Confidence: 0.9
Range Of Target : 5
Time of Arrival : 8

Lockheed Martin DOMINANCE Challenge: Land Mine

Department of Electrical and Computer Engineering
University of Central Florida
Dr. Lei Wei

Date: 4/19/20
Spring 2020

Group 17
Corey Hogue; *Electrical Engineering*
Joseph Rivera; *Electrical Engineering*
Kristopher Sipe; *Computer Engineering*
Justin Wu; *Computer Engineering*

Sponsor: Lockheed Martin
Contacts: Johnathan Tucker and Andrew Kirk

Table of Contents

List of Figures

1.0 **Executive Summary**

The Lockheed Martin DOMINANCE Challenge calls for a stationary mine system capable of detecting, tracking, and autonomously disrupting Unmanned Aerial Vehicles (UAV), otherwise known as opponent drone teams, that are navigating a stochastically placed obstacle course. The obstacle course includes rings, single pylons, double pylons, and an acoustic waypoint in which the UAV will have to autonomously navigate whilst avoiding the land mine. All teams will have to report Target, Confidence, Range to Target, and Time of Arrival. No team will be allowed to use YOLO based deep learning object detectors. Points will be awarded to drone teams that complete certain objectives, however land mine evaluation hinges solely on the system's ability to remove those drones from play. The competition will be conducted within an indoor laboratory space with GPS denied navigation and a maximum half angle look area to limit search areas between obstacles. The mine system will have to demonstrate four operational features: Auto-Detection, Auto-Tracking, Auto-Disruption, and an Electronic Stop (E-Stop). To meet this challenge, the system will employ the latest computer vision deep learning algorithms, along with fused range information from a stereo camera, to achieve high accuracy detection and localization in three-dimensional space, multi-class classification capability, automatic target tracking, and kill capabilities with a custom net-based kinetic takedown system. Detections will be computed from a state-of-the-art Faster R-CNN deep learning architecture based on a convolutional neural network (CNN) backend. Classification will be exclusively handled by CNNs, due to their intelligent handling of feature extraction from known data through supervised learning and nonlinear mapping to class decisions. Tracking will be accomplished through an optical flow tracker that can capitalize on the object detector's outputs and compute likely positions of identified targets across space and time. The stereo camera allows for both visual, and range to target tracking based on a computed point-cloud of object ranges within the cameras' fields of view. A primary objective of the project will be to evaluate the performance of a fully integrated computer vision system and the ability to deploy deep neural networks in an embedded systems environment with Nvidia's Jetson Nano Developer Kit. The Python programming language will be utilized along with multiple packages like OpenCV, TensorFlow, and advanced optimization libraries like Nvidia's TensorRT and cuDNN to achieve computer vision and deep learning hardware acceleration. Developing a robust game theory is crucial to effectively disabling target drones. In order to counter possible retaliation, the team explored a multitude of disruption and camouflaging techniques. Dummy systems i.e. pop up targets, countermeasures for enemy projectiles, cybersecurity attacks and adversarial sensor exploitation will also be explored. The mine will be equipped with a projectile netting system that utilizes visual servoing, vision-based robotic controls, for aiming, targeting, disabling, and retrieving adversarial drones once they enter the mine's effective range. The goal is to create an Automatic Protection System (APS) able to intelligently decide whether a projectile should be fired based on the target classification and spatial position. The computer vision solution will be able to distinguish between drones, and non-drones to be able to correctly and

safety make autonomous targeting decisions outside of and within the effective range. The focus will be on portability, autonomy, detection accuracy, and kill capabilities. Finally, the safety features like a ground station laptop that will log image data sent directly from the mine through a video datalink, an E-stop kill switch to cut power to the system from a distance. The mine will have three opportunities to compete in 10-minute rounds, and will be unable to repair the mine during round play, and cannot have any human-in-the-loop cued functions.

2.0 **Project Description**

This section is broken in multiple parts: project motivations, goals/objectives, related work, engineering requirement, and an overall design block diagram. The goal of the project description is to give a high-level overview of the senior design project.

2.1 **Motivation**

Multiple concepts were considered before coming to a final decision to attempt the DOMINACE mine challenge. These ranged from reasonable proposals to abstract ideas, but in the end, a project that was sponsored and believed would be reasonable, achievable, and challenging was decided upon. Table 1 illustrates a few project ideas.

Project Idea	Practicality	Originality	Difficulty	Interest
Lockheed Martin Challenge – Land Ordinance Mine	4	2	3	3
Eye Tracking Controlled RC Vehicle	3	4	2	2
Solar Powered Electric Longboard with Bluetooth Control Interface	2	1	1	2
Sentry Drone for Home Security / Protection	4	2	3	2

Table 1: Project Selection Matrix

The DOMINANCE project is a Lockheed Martin sponsored competition that tasks three teams to develop an autonomous drone and one team to develop a mine. The team, consisting of 4 electrical and computer engineering (ECE) majors is assigned to develop a mine that can disrupt autonomous drones and disable them from completing the obstacle course. This project is used to fulfill one of the major requirements to graduate at the University of Central Florida (UCF). In order to fulfill this requirement, we must:

1. Complete a final report of research and findings.
2. Build a working device that meets the customer's (Lockheed Martin) requirements.
3. Take down at least one competing drone.

2.2 **Goals/Objective**

The overall goal of the Lockheed Martin DOMINANCE Mine project is to develop a land stationary mine capable of detecting, tracking, and autonomously disrupt aerial drones on a randomly oriented obstacle course. The following sections outline the main objectives of the project.

2.2.1 **Planning**

This phase is one of the most crucial steps. The goal is to plan out the design the DOMINANCE mine. This section discussed how to take down the drone and what disruption devices could be used. This plans out the short-term tasks for Senior Design one and Senior Design two. Roles are assigned in the development process and tasks are divided according to strengths/weaknesses and interests. A Gantt chart and calendars are crucial to planning out this timeline.

2.2.2 **Research**

One of the most important steps, the goal is to research how to develop the mine. Each group member decides on an "interested" topic and is tasked to research what it was about, how it could be implement, why it was important to the design, and do a part analysis (only if parts were needed). This step is very useful for completing the final document.

2.2.3 **Algorithm Development**

The goal of algorithm development is to develop a solution for pre-processing live video as well as detecting, tracking, and collecting metadata of drones. The plan is to use OpenCV for the pre-processing and TensorFlow for the classification.

2.2.4 **Disruption Development**

The goal of disruption development is to design a device that can disrupt and take down the aerial vehicle. This step is purely hardware based and requires analyzing components and parts for the design.

2.2.5 **Integration/Prototyping and Testing**

After developing the algorithm and disruption device, the task is to integrate the two different components. This is important since this is the last step before the final showcase. In order to integrate the two designs, the knowledge of the two designs are necessary as well as testing.

2.2.6 **Final Showcase**

The mine undergoes thorough unit testing in order to determine any flaws are bugs that might occur. This will be the final evaluation of the project., where the system is demonstrated to customers and the review panel and the system is demonstrated to .

2.2.7 **Block Diagram**

Figure 1 contains a block diagram for the DOMINANCE Mine project. The block diagram represents the crucial components necessary for the DOMINANCE Mine

to detect, track, and disable the UAV within the given proximity. Block diagrams are commonly used to have a visual representation of the tasks needed, the system flow, as well as the responsibility assigned to each member of the team. It is also useful to incorporate the status of each element as knowing the current state helps for time management and provides a checklist of what tasks are still at large.
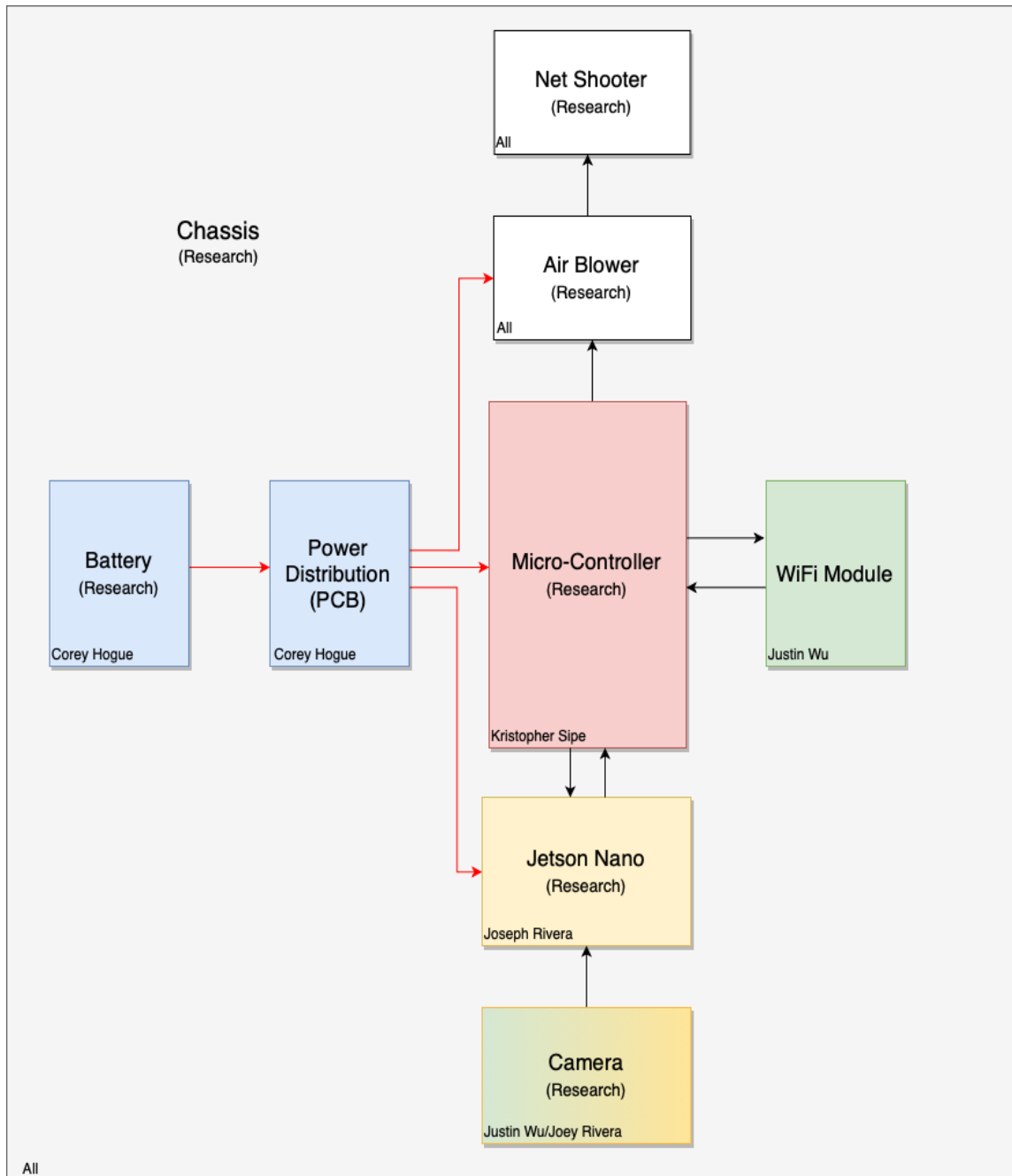
Figure 1: Initial Block Diagram

2.3 Engineering Requirement and House of Quality

This section contains the requirements for the DOMINANCE Mine project. Table 2 displays the final deliverables that will be presented during the final presentation. Table 3 outlines all the requirements necessary to complete the DOMINANCE mine project; containing both customer requirements and standard requirements that will be strictly followed and implemented when designing the DOMINANCE mine.

Requirement	Deliverable
Metadata Box	Metabox Data shall be displayed from the laptop
E-Stop	The E-Stop function shall be displayed as fully operational. (Power on and an immediate stop)
Auto Disruption	DOMINANCE Disruption shall have auto disruption (autonomously utilize blast mechanism to disrupt UAV flight).

Table 2: Deliverables

Requirement Title	Requirement
Design	DOMINANCE shall meet the specified design requirements provided by the customer. It shall not exceed the maximum size of 1.5 ft. x 1.5 ft. x 1.5 ft. (L x W x H). The design of the mine will have all the components self-contained within a single unit.
Material	DOMINANCE shall use materials that are readily available and allow for interchangeability. This requirement is necessary as a "back-up" plan in case the mine is damaged from deterrents the aerial vehicles may have.
Weight	DOMINANCE shall not exceed 50 pounds. This requirement is necessary in order to make the mine portable for 1-2 persons to carry around and placed in the obstacle course.
Cost	DOMINANCE shall stay within the customer's constraints of $700 with an additional $350 for prototyping.
DOMINANCE Sight	DOMINANCE Sight shall be a fixed optical system that can process color information in real-time.

Requirement Title	Requirement
Mode of Operation	DOMINANCE Sight shall meet the required modes of operation provided by the customer.
Automatic Target Detection (ATD)	DOMINANCE Sight shall have auto-detection (autonomously detect UAV). No user interaction is permitted in this process.
Automatic Target Tracking (ATT)	DOMINANCE Sight shall have auto-tracking (autonomously track UAV). No user interaction is permitted in this process.
Automatic Target Recognition (ATR)	DOMINANCE Sight shall have auto-recognition (autonomously classify targets). This will be achieved using the classification capabilities of advanced convolutional Neural Networks.
Detection	DOMINANCE Sight shall be able to detect and identify Unmanned Aerial Vehicles (UAVs).
Metadata Box	DOMINANCE Sight shall be able to generate a large red bounding box overlay centered on the UAV. It shall collect data as it identifies the target.
Confidence	The Metadata Box shall collect normalized ($0 \leq x \leq 1$) confidence data of the UAV.
Range to Target	The Metadata Box shall collect the range to target (in feet).
Time of Arrival	The Metadata Box shall collect the time of arrival (in seconds). This will be an approximation as the path of the target is unknown to the system.
Real-Time	DOMINANCE Sight shall be able to detect and identify the UAV in real-time. This also includes the tracking of said target post detection.
Detection Speed	DOMINANCE Sight shall detect and identify a UAV within 10 seconds of the target visibly entering the frame.
Camera	DOMINANCE Sight shall consist of 4 RGB cameras with 1080p resolution. This camera array approach will ensure full visual coverage of the scene.

Requirement Title	Requirement
DOMINANCE Disruption	DOMINANCE Disruption shall be a slewable system that has the ability to disrupt UAVs such that it falls to the ground.
Mode of Operation	DOMINANCE Disruption shall meet the required modes of operation provided by the customer.
Auto Disruption	DOMINANCE Disruption shall have auto disruption (autonomously utilize blast mechanism to disrupt UAV flight).
E-Stop	DOMINANCE Disruption shall be able to stop all disruption blast mechanisms remotely via user's discretion
Blast Radius	DOMINANCE Disruption shall not exceed the maximum specified blast radius as is denoted on the following page.<table><tr><td>**Horizontal**</td><td>3 feet</td></tr><tr><td>**Vertical**</td><td>10 feet</td></tr></table>
Capacity	DOMINANCE Disruption shall be able to disrupt UAVS a minimum of (1) times before needing a reload.
Projectile Weight	DOMINANCE disruption device shall not launch a projectile exceeding 5 pounds. This would affect the safety hazards of the device if it happened to malfunction.
Projectile Speed	DOMINANCE disruption device shall not blast a projectile exceeding 1200 feet per second.
Stationary	DOMINANCE shall be placed on the obstacle course and remain stationary.
Operational Life	DOMINANCE shall be able to operate for a minimum of one hour while power on.

Table 3: Requirements

Engineering Requirements

Table 4 outlines the requirements that can be physically measured; hence why they are considered "Engineering Requirements". This table is derived from the general requirements table above. While these requirements will not be strictly considered for the final deliverables, they will be important when doing a cross-analysis between market requirements.

Section Title	Requirements
Design	1.5 ft x 1.5 ft x 1.5 ft
Weight	Not exceed 50 pounds
Cost	Not exceed $1050
Detection Speed	Detect and identify in under 2 seconds
Blast Radius	Horizontal: 3 feet; Vertical 10 feet
Operational Life	Minimum of 1 hour

Table 4: Engineering Requirements

House of Quality

Table 5 shows the polarity and correlation of Engineering Requirements and Marketing Requirements, otherwise known as the House of Quality. House of qualities is used to show the correlation between market desires for product development and engineering requirements that must occur in order to develop the product.

			Marketing Requirements							
			Cost	Ease of Use	Durability	Maintenance	Ease of Installation	Target & Disrupt	Dimension	
			-	+	+	-	+	+	-	Target
Engineering Requirements	Design	-	↓	↑	↑	↑	↑	↑	↑↑	1.5 x 1.5 x 1.5 (ft)
	Weight	-	↓		↑					≤ 50 pounds
	Cost	-	↑↑	↓	↓	↓	↓		↓	≤ $1050
	Detection Speed	+	↓	↑				↑	↓	≤ 2 seconds
	Blast Radius	+	↓						↓	Hor: 3 feet; Vert: 10 feet
	Operational Life	+	↓	↑	↑	↑			↓	Min of 1 hour
	Memory Storage	+	↓		↑	↓	↓		↓	Min of 64 GBs
	Power Usage	+	↓		↑	↑			↓	≤ 500 W

Table 5: House of Quality

Legend	
+	Positive Polarity
-	Negative Polarity
↑	Positive Correlation
↓	Negative Correlation
↑↑	Strong Positive Correlation
↓↓	Strong Negative Correlation

3.0 Research and Part Selection

This section contains the bulk of the project as basic research in all areas of technologies were required to meet the design requirements. Conducting applied research over every possible decision in the design process is necessary to develop a fundamental understanding before physically developing the DOMINANCE mine. This section also outlines the part selection. A full analysis of multiple technologies depending on the use of implementation for the design. Factors like cost, power consumption, ease of use, etc. play a role in determining which part to pick. This section contains the justification used for picking the part.

3.1 Control System

The control system incorporated in the design will need to be rather comprehensive as it will be handling both the optics and image processing as well as the turret motion, launching mechanism, and sensing capabilities. It will take a large amount of processing power and programming finesse to achieve this feat, and because of this the possibility of using multiple controllers for this application has arisen; one module to control the optics and image processing and a second to control all secondary features. Another plus to this design consideration is a secondary, more vanilla MCU on the custom-designed PCB (Printed Control Board). This would complicate the design of said component but would fulfill the requirement of designing a PCB that handles some sort of logical operation.

3.1.1 Image Processor Control

The image processor control will run image detection algorithms that will utilize heavy image processing techniques. Not only must it be able to process large amounts of data, but it must also be able to process this data rather quickly since the design must function as a real-time system to be successful in its task. It will also need to be able to handle Wi-Fi communications, via an external Wi-Fi module, to complete tasks such as emergency stops and displaying live camera feeds to an external peripheral such as a nearby laptop. This section analyzes which form of communication works best in each criterion: price, processing power, CPU speed, GPU speed, power consumption, ease of use, general I/O, SW compatibility, and size. This section with be used for the final technology comparison and for the conclusion on which part will be implemented on the final design.

Price
Price is an important factor due to the strictly limited budget to prototype and deliver a final operational product. Development boards can be very pricey, therefore the goal is to find the best cost per computation power. There may be cases that the amount of computation power outweighs the cost of the board, however other factors discussed within this section will be used to confirm the final decisions.

Processing Power
This criterion is very important because of video captured data. In order to pre-process the data and make classifications using a convolutional neural network with TensorFlow, a board that has the ability to do so at a reliable rate without needing to overclock is critical.

CPU Speed and GPU Speed
The central processing unit carries out and controls the instructions by performing input/output operations, basic arithmetic, and logic. The faster the CPU can compute a solution the faster the mine can make decisions on whether or not to disrupt a drone. The graphics processing unit (GPU) is a specialized electronic circuit that accelerates and renders images and videos. The GPU frees up the CPU by computing fast math calculations. Since the primary processing involves live video data, the GPU speed will be the most important of the two [1].

Power Consumption
Power consumption is the amount of energy used per unit of time. Video computation can be very power consuming. Including other external devices, this can be very taxing on the entire system. If a battery power system is decided, research must be made on more cost-efficient development boards or a bigger battery (which will in return reduce the amount of real estate in the development).

Ease of Use
Due to the lack of manpower and time constraints, ease of use and integration will be an important factor to consider. If a development more is brand new to the market it may have less community support than one that has been in the market for a few years. Community support can be useful when integrating the development board with other devices. The less time spent on developing a brand-new methodology the more time can spend on something that has not been developed.

General Purpose Input / Output (GPIO)
General Purpose Input / Output has no predefined purpose and is unused by default. This allows more integration on the circuit with other implementations. If a development board has more GPIO pins can leverage this to the systems advantage by integrating other useful circuits. It can be used to control the servos for the launcher, activate the disruption device, includes a communication device, etc.

Size
Since one of the engineering requirements is to develop the mine with dimensions of 1.5 feet by 1.5 feet by 1.5 feet, it is important to take into consideration how big the development board is. This is not the only part of the design, other factors have to be considered. Ideally, the smaller the form factor (while maintaining other important factors) the better it is for the overall system.

3.1.2 Motion and Secondary Control

The secondary controller that may be utilized in the system must be able to easily communicate with the primary control system and also be able to handle any functions divvied out to it. This controller will not need to process large amounts of data but mainly read sensors and process their data, handle turret motion, control the net launching mechanism, and a few other small-scale tasks required of it. Because of the low amount of processing power required here, it would be possible to use a basic MCU implementation in this case.

Another key point to consider in the selection of this controller is that this chip will be integrated into the PCB design, so it will need to be easily interfaceable with and not require a development board or debug chip to interface with. Knowing this, and what is required of the chip, researching a few options and weighed the pros and cons of each was the best plan.

3.2 Power Solutions

The design for the mine will utilize a decent amount of power due to the controllers used for processing data, motors for rotating the mine body, and the disruption mechanism. Because of this, it is imperative that a power solution that will supply the mine with the power needed while still being efficient is utilized, all while being inexpensive and within budget. For the power solution, there are two main approaches to focus on: Battery power and wall power.

Battery Power
The first possibility explored was to employ a battery to power the system. This would have been a very beneficial solution as it would have allowed the device to be fully contained and therefore completely portable. The team also would have easily been able to find a battery with proper voltage ratings so that the amount of rectifying and stepping down of voltages could have been minimized. Both of those facts made it seem like a simple choice, but when the requirements were again taken into consideration it became obvious that this was the less ideal option. First of all, the battery would have been utilizing most likely would not have been cheap, and definitely would have been more expensive than using wall power that is readily available. Another detrimental fact of using a battery, in terms of the requirements, is that it would have pushed the limits of the sizing constraint. This device is to be no larger than 1.5ft x 1.5ft x 1.5ft, so squeezing an unnecessary component into this tight form factor is definitely less than ideal.

Wall Power (120VAC)
The second possibility for the mine's power source was to use wall power. The team conferred with the sponsors of the DOMINANCE project space and confirmed that it would be acceptable to use power from the facilities there. Once this fact was understood it was clear that this was the obvious path to take as there would be access to a source that could power anything required of it with no worry of power constraints or battery levels dropping to nominal levels. The one negative

that does come with this source, however, is the fact that the voltage will need to be rectified and dropped down drastically; in some instances, even to a small 5VDC. This is not an apparent issue though, as the circuitry involved is relatively low and can be easily constructed.

Conclusion
Out of the two options, wall power would be the best solution. This is primarily due to the ease of usage and design. Using wall power only requires us to include an AC to DC (ADC) converter since standard wall power is 120V at 60 Hz. This will allow us more real estate in the design. If a battery is used, battery size would have to be taken into consideration and the use of a DC to DC converter. This would require us to research battery parts and step-down voltage/current parts.

3.3   **Chassis Solution**

Being that this design will be comprised of multiple electrical components, and since the goal is to ensure the mine fully contained (except for the power source), it is imperative that the design includes a chassis that houses all parts in a compact fashion. This will not only help with the portability of the design but will also help with the overall presentation and in ensuring that the device is compact and stays within the sizing constraints of 1.5ft x 1.5ft x 1.5ft

Completely Manufactured Chassis
One possibility for the creation of the housing unit would be to have it manufactured in the university's manufacturing lab. This would require the team to pass a design onto the employees there and secure the finished product at a later date. This is a viable option, but would most likely require at least minimal funding, which would not be optimal as the budget is already extremely tight for the components alone. Using a material such as metal would also be detrimental to success as the drone's image processing algorithms would most likely be able to spot the device before it would be able to attack, or even before it had entered the blast radius. This could easily be fixed by painting the unit, or even Rhino-Lining it, but again this would cut into the budget. A metal body would also add some heft to the object, even if it is aluminum, and might cause the weight requirement to be met or even surpassed.

3D Printed Chassis
The second option would be to simply design the chassis in a computer-aided design (CAD) software and then 3D prints it. ABS plastic is quite inexpensive, and most likely this operation would be more budget-friendly than having a sheath manufactured. There are also multiple 3D printers that the team could utilize to print this chassis, with the main being the student-driven unit in the innovation lab. One of the only downsides with printing the housing unit would be designing the chassis in one piece. Since the requirement is to design it 1.5ft by 1.5ft by 1.5ft, it might have to be printed in multiple parts. This issue could easily be solved in the

design, however, by simply creating interlocking sections in the CAD files so that the chassis could snap together and effectively act as a single unit.

3.4 Sensing

To achieve the task of disabling a target the design must first be able to sense the target and ensure that it can attack once the target has entered the blast radius. To achieve this multiple sensors will be utilized to guarantee that the target will be located, and information of its specific whereabouts will be updated accurately and efficiently.

3.4.1 Target Sensing

The most crucial factor in ensuring mission success for the overall design is being able to properly identify and track the enemy target, an autonomous drone. It is very imperative that the design features a very accurate and consistent set of "eyes", or way of locating the object in space. There are many different types of sensors that are used to paint an image of a scene but determining which one is best for the application is a primary goal in this design process.

LIDAR
The first imaging technology that was discussed among team members was LIDAR. LIDAR is a technology that functions by the use of a laser and a photosensor in a receiver configuration. The laser is used to emit intermittent pulses of high-frequency light, usually near-infrared or actual infrared. This light then interacts with an object and is reflected back towards the photosensor which in turn paints a point at the location that the pulse landed. LIDAR works by utilizing many of these emissions and then using them in tandem to paint a scene. The imaging is not what one would usually expect to see from a camera but is instead a collection of these points imposed on a black background. These sensors are still very accurate, however, and are not prone to environmental interactions or other disturbances that might hinder the reliability of a camera.

LIDAR is great for imaging and would be fantastic in this application but obtaining a unit capable of generating a high enough point count capable of being processed by object detection algorithms would not be budget-friendly whatsoever. Considering this sensing technique is relatively new and the technology involved is rather advanced it is not cost-efficient to pursue this type of imaging.

Radar
A second imaging technique that was explored was Radar. Radar functions similarly to LIDAR in the fact that it emits a pulse and then records the intensity of the signal once it returns, but in contrast to LIDAR, radar uses radio waves to achieve this feat. Radio waves are generated and emitted by the radar module and then the response is recorded using an antenna and then stored for viewing. This type of imaging is generally used for surveying and generating scenes of large-

scale landscapes, so it is not exactly the perfect technology to use for this application. Also, as is with LIDAR, these types of imaging systems are not cheap and would definitely stress the budget afforded to us. Overall radar, while interesting in concept, is not applicable to this design [2]. Figure 2 shows are comparison of the two.

Lidar   High Resolution Radar
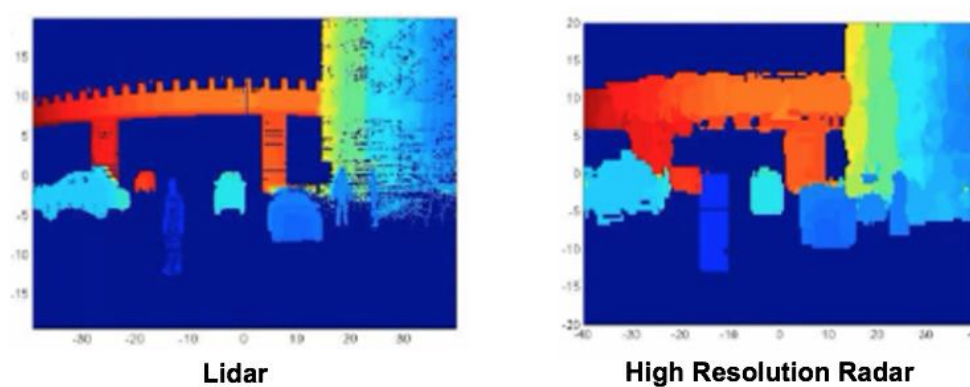
Figure 2: LIDAR Imaging vs. High-Resolution Radar

Camera
A third option is to employ a camera to perform all of the imaging and vision needs. Cameras work by allowing light to pass through a lens. When the light traverses the lens, it is focused onto a light-sensitive medium where the colors of the light entering are processed into specific pixels. Finally, as the image is created it is saved or stored for viewing. In a video camera, such as one that would be utilized in this system, this process happens very quickly and is repeated continuously, usually around an average of sixty images per second (or sixty frames per second). This type of imaging technology is very accurate and creates an almost perfect representation of the scene at hand.

On top of being a great technology for this application due to its image quality and frame rate abilities, it is also a technology that is very old and common, so it is possible to obtain a high-quality camera for very cheap. As this design will possibly require multiple camera units this is a huge positive as not much capital will be spent on each individual unit. Overall this type of sensor, when compared with the other imaging solutions, is the obvious go-to for this application.

The MS COCO dataset has images with a resolution of 640x480 and a bit precision of 8 i.e. pixel intensities range from 0 to 255. In order to provide a 360-degree field of regard, we want to start with a camera solution that can handle a wide field of view and still provide ranging past 11 feet (the maximum range of the intercept boundary). In order to achieve this, a custom stereo should be built, using commercial off the shelf raspberry pi cameras (see Figure 3) and implementing OpenCV functions to create a depth map [3]. In doing so, this provides the freedom to experiment with both different cameras and lenses. On the other hand, Intel sells

a powerful Depth sensing camera: the RealSense Depth Camera D415 for $150 that has onboard processing to handle the creation of a 3-D point cloud for ranging, and a powerful software developer kit that can be leveraged without additional setup (see Figure 4). Due to the 30-foot range of the D415, opting for developing with this established technology platform was made, before diving into custom solutions with cheaper cameras as shown in the figure below.
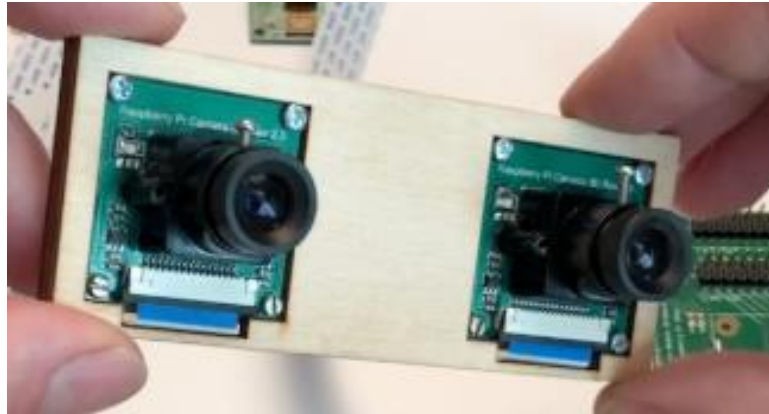
Figure 3: Raspberry Pi Cameras in Stereo Configuration Operable using OpenCV
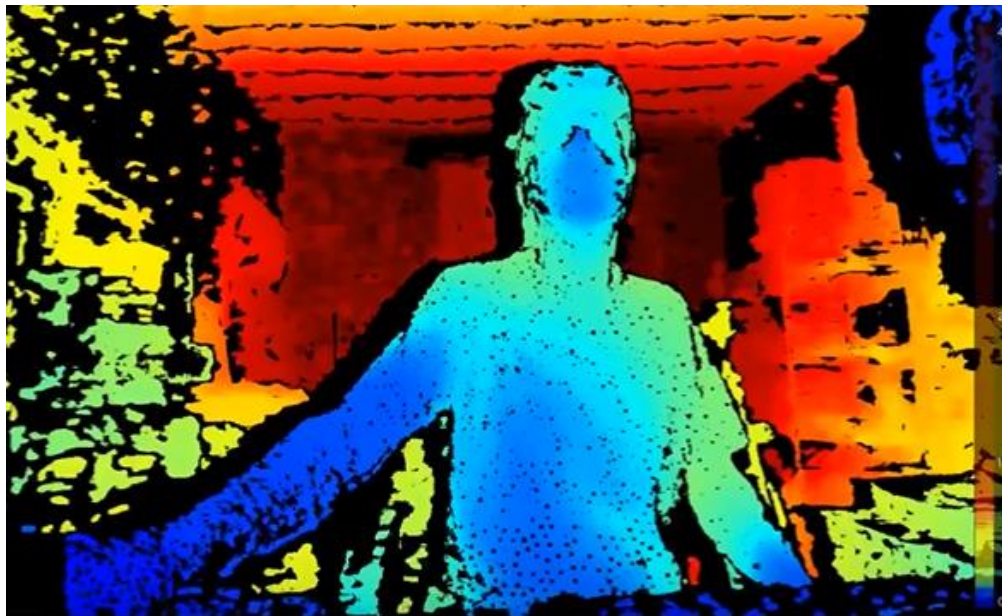
Figure 4: Example Depth Map Using Intel RealSense D415 with RealSense SDK

Multiple Camera Utilization
The first design concept that was utilizing multiple cameras, more specifically four, with one placed at every ninety-degree increment of the mine housing. This would have given the device a nearly three-hundred and sixty-degree (depending on

camera FOV) view at all times which was ideal in all aspects. It would have been possible, with this implementation, to locate a drone at any point that it was approaching the device. This option was heavily weighed as it was clearly ideal but began to notice the negatives that came with it as well, the main drawback being to process four separate camera feeds at once. The amount of image processing required of image detection algorithms is very large and multiplying that by four did not seem like a good idea in the fact that not only would it wane on the devices ability to function as a real-time system, but if a more powerful processor were used to counteract this then there would be a need to dig into the budget deeply most definitely. Not only would the more powerful processor have drained the budget significantly but having to purchase four cameras on its own would not have been a lucrative endeavor.

Single Camera Utilization
In contrast to using multiple cameras, the secondary design idea was to use only a single camera. This comes with the obvious drawback of only being able to see one view at any moment, the angle of which is determined by that specific cameras FOV, so ways to counteract this negative was looked into. One idea that was proposed was to have the camera mounted and rotate the housing of the device so that there would be three-hundred and sixty degrees of viewing for the unit. This has its drawbacks as well, such as that the target could appear in the devices blind spot before it was able to readjust to that particular location. At first, this appeared to be a fatal flaw of this concept, but upon further evaluation, we noted that since the firing range is so limited due to the constraints (3ft radius: 10ft height) the likelihood that the target approached this close without being spotted by the mine was slim. Most likely the target would fly within view of the rotating camera at some instance, and when that occurs the image detection software would detect it and begin tracking at that instance. This is not as ideal as having a three-hundred and sixty-degree view at all times, but it was believed it to be a more than an adequate method of scanning the environment for the target.

Conclusion
Deciding that the most important factor to consider when choosing which technology to use when design the DOMINANCE mine is cost. The cheapest alternative would be the camera. There is also the choice to buy multiple cameras that can target sense.

3.4.2 **Depth Sensing**

One factor that this design must be able to accurately determine is the distance at which the target is located. The constraint placed on the system is that it will only be able to engage the target when it is in its "blast radius", which is defined by being a radius of three feet around the unit with its height extending to eleven feet. This is a tight window and knowing the moment the target enters the blast radius will give the mine the highest probability of success when attempting to disable the said target.

LIDAR

LIDAR, as well as being a great method of imaging, is also a great tool for determining distance. As previously mentioned, LIDAR functions by using lasers to emit an array of near-infrared pulses that paint the view in question. These points are emitted and the time at which they are emitted is archived as time 't' equals zero. Once the points land on an object they are reflected back towards the LIDAR unit, which houses a photodetector driven receiver, and the time, 't' equals one, is recorded. Now, knowing the emit and return times of the laser point in question, the module can now perform a simple calculation utilizing the speed of light in order to determine the distance at which the object was located. Figure 5 shows an illustration of how this transmission and sensing is done. This technology is very similar in functionality to infrared distance sensors but is much more reliable and less likely to be corrupted by light or any other outside factors. The main drawback of LIDAR, in this project specifically, is that it is not budget-friendly. Having a tight, sharply defined budget such as the team does means that, even though this might be the most accurate technology for the job, it might not be beneficial for this specific application.
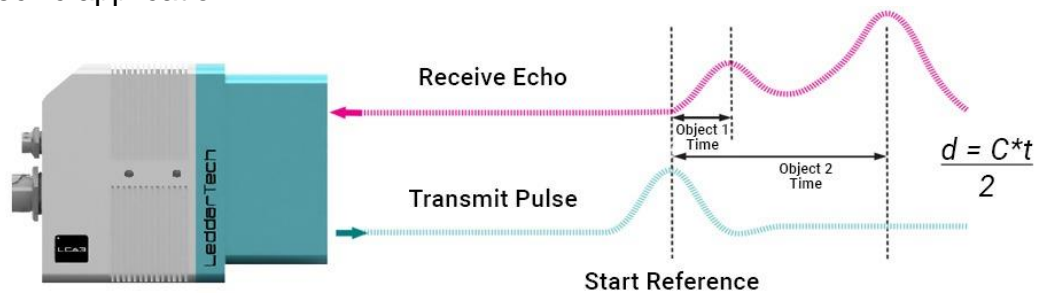
Figure 5: LIDAR Transmission and Sensing Illustration

Ultrasonic

An ultrasonic sensor functions similarly to LIDAR and infrared sensors except in the fact that it utilizes sound waves instead of light waves to accomplish its task. Figure **6** shows an illustration of how a ultrasonic sensor works. A single transducer is used to generate an ultrasonic sound that vibrates at a frequency the human ear cannot detect, and at this moment the initial time is then recorded. That same transducer then stands dormant until that sound is reflected off of an object and is eventually returned to the sensor, at which point the time is then again recorded. Then, using an equation ($D = 1/2 \times T \times C$) which utilizes the speed of sound, the distance is then calculated and sent to the controller. Ultrasonic sensors are quite reliable but might not be the best for this application. It is one fear that, since the target is a drone, the high-pitched tones of the driving motors may be interpreted as the transduced signal returning to the sensor and cause false readings. This would be the worst-case scenario assuredly, but it is still a possibility that hinders the possible effectiveness of this sensor in this specific design.
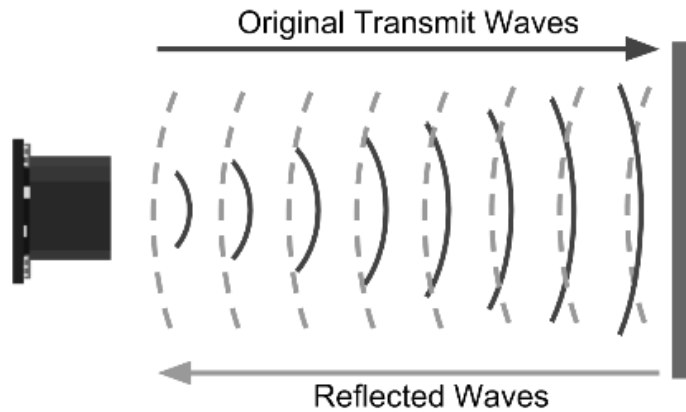
Figure 6: Ultrasonic Sensing Illustration

Stereo Camera Configuration

A third option for sensing distance in the design would be to use two cameras in a stereo configuration. This consists of using two cameras of the same specifications and placing them on the same plane at a certain distance apart. Once the cameras are configuring a frame is then captured of the same scene by each and then they are rectified, and the images are then compared. Depending on the disparity in location of a specific object in the frame a distance can then be calculated by using the difference in location of a point relative to the scene. This can easily be visualized by imagining that, if the object is very close to the camera configuration, that the object will appear in a vastly different location (x,y) in each camera. If the object is far away, however, the disparity between the object's location in each image will be quite small and will require the pixel level calculation to determine the actual distance. Figure **7** shows the stereo camer output with rectified image.

This method for determining distance is actually quite reliable as was found in the paper "Distance Measurement with a Stereo Camera" which was published in the International Journal of Innovative Research in Advanced Engineering (IJIRAE) where the error was measured to be around four percent, on average [4]. For this application, this would be considered an acceptable error, and the fact that the design is already utilizing at least a single camera means this would not require any extra sensor management or costs.

Figure 7: Stereo Camera Output w/ Rectified Image

Conclusion

Due to coherence and budgeting, a decision to continue using a camera was made. Stereo cameras can get a sense of depth while being one of the cheapest alternatives. Although stereo cameras are one of the more expensive cameras, it is still one of the best options for this application.

3.5 **Computer Vision**

In order to meet the computer vision requirements, conducting trade studies on different object detection, classification, and tracking methods are necessary. Compared to traditional computer vision approaches, this system opted for an intelligent algorithm by testing Convolutional Neural Networks with different architectures suited for pure classification like Resnet18 or MobileNet-v2, object detection with a Single Shot Detector using different Convolutional Neural Network back-ends for classification, and a stretch goal is to test semantic segmentation networks like SegNet. It has been shown that deep learning networks can in-fact be better at image classification than humans.

The Jetson Nano has already been validated by Nvidia for the performance of certain networks shown below in Figure 8 and Figure 9. In order to run in real-time, Single Shot Detectors will be validated standalone, while traditional object detectors, like the OpenCV function "Good Features to Track" will be paired with standalone Convolutional Neural Network classifiers like Vgg16 or AlexNet to maintain inference times below 33ms and provide real-time classification capabilities at around 20 frames per second. Figure 8 compares frame rates of inferencing with different network architectures. Figure 9 compares more references for inference timings specifically for the Jetson Nano. These reports from Nvidia will serve as the baselines for training and evaluation performance of the networks come run time, and also give us direction towards what is viable for real-time performance, specifically looking at SSD MobileNetV2, and SSD Resnet18 for integrated detection and classification tasks, or standalone MobileNetV2 and Resnet18 as pure classifiers. In order to classify correctly, we'll implement a 5 second time of arrival count down timer. The Algorithm must detect the drone for 5 seconds continuously, and the center must be within 15% of the center pixels in both height and width in order to fire. Our main function will be written in matlab and run on our remote laptop. It will make remote calls to run code on the nano for motor control, solenoid firing, and streaming frames.

Model	Application	Framework	NVIDIA Jetson Nano	Raspberry Pi 3	Raspberry Pi 3 + Intel Neural Compute Stick 2	Google Edge TPU Dev Board
ResNet-50 (224×224)	Classification	TensorFlow	36 FPS	1.4 FPS	16 FPS	DNR
MobileNet-v2 (300×300)	Classification	TensorFlow	64 FPS	2.5 FPS	30 FPS	130 FPS
SSD ResNet-18 (960×544)	Object Detection	TensorFlow	5 FPS	DNR	DNR	DNR
SSD ResNet-18 (480×272)	Object Detection	TensorFlow	16 FPS	DNR	DNR	DNR
SSD ResNet-18 (300×300)	Object Detection	TensorFlow	18 FPS	DNR	DNR	DNR
SSD Mobilenet-V2 (960×544)	Object Detection	TensorFlow	8 FPS	DNR	1.8 FPS	DNR
SSD Mobilenet-V2 (480×272)	Object Detection	TensorFlow	27 FPS	DNR	7 FPS	DNR
SSD Mobilenet-V2 (300×300)	Object Detection	TensorFlow	39 FPS	1 FPS	11 FPS	48 FPS

Figure 8: Nvidia's Comparison of Different Classification and Detection Neural Network Performances (Image Pending Approval)
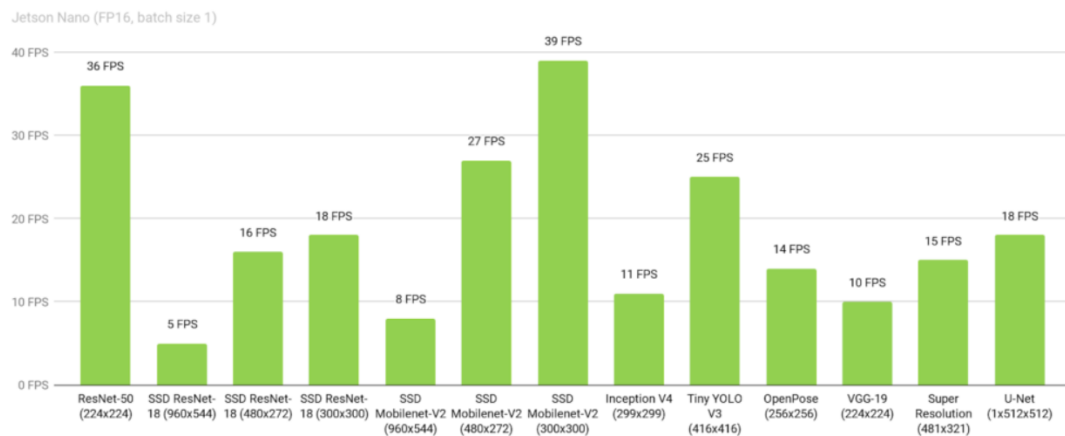
Figure 9: Deep Learning Inference Performance on Jetson Nano. Reported by Nvidia (Image Pending Approval)

3.5.1 Data Pre-Processing

An Unmanned Aerial Vehicle Drone Dataset curated by Mehdi Özel on Kaggle [5] along with more images from the web and data we collect ourselves at the competition location, home, and out in similar environments to the final competition location in order to train and test the algorithms. At training time, we will implement random crops, translations, flipping, rotations, and lighting changes that will all be used to augment the image data we use to train the network on to recognize a Drone class. This helps regularize the network and generalize its classification and detection ability. We plan to simulate flying a drone in order to capture and characterize the spectral phenomenon like lighting conditions, distance from target, resolutions, saturation, and obscurations that may affect the network's performance come test time. A drone class is uncommon in mainstream deep

learning algorithm training regimens, although pre-trained COCO networks have an airplane class that has presented good localization and classification of airborne drones (see Figure 10 below).

Zero-Center normalization is a best practice for helping a network converge quickly. Before the network starts training, an average image of the entire training dataset will be computed. This is then subtracted from individual images that are passed through the network, so the network will really only be cueing on variances in the training data i.e. differences from the mean for the sake of a quick convergence. This helps regularize the network to variations that it might see during runtime.

At runtime, we will normalize the camera's input data to have a bit precision of 8 based on the speed of the final algorithms. By reducing the dynamic range of the input sensors, we reduce processing complexity. An optimization library like TensorRT or cuDNN can be used to further boost performance come runtime and lower bit precision results in far less inferencing time. Pure inference ability can be quickly calculated using the trtexec function that comes with the Jetson Nano.

Dataset
In order to train a network to recognize a custom 'Drone' class that is not available in any large public online datasets, we created a two-class dataset of over 6,600 images of commercial drones and over 11,700 images of background 'Clutter' images. Clutter refers to background image chips that are likely to be around the target. This clutter class is used to reject any image chip that is not a Drone.
Software Discussion

In order to build a dataset and train preliminary networks, we used MATLAB, specifically the deep learning toolbox. MATLAB provides a general platform to parse out the ground truth in the Kaggle dataset, which contains PNG images and XML files with bounding box data. Using the Video Labeler tool provides a way to create custom labeled data shown in Figure 10. When the first data collection at Lockheed Martin on November 8, 2019. We combined both datasets in a single image datastore and used the imageAugmenter function to incorporate random rotations and translations into the input images in the networks' training process. The MATLAB Deep Learning Toolbox provides readily available functions for loading in convolutional neural networks that were pre-trained on 1000 classes from the ImageNet database. We can transfer learn the new classes in Matlab and score the results via confusion matrices. We can also take the classification network and integrate it into an RCNN, Fast-RCNN, or Faster-RCNN object detection architecture.

Figure 10: Example of Hand Labelled Data from Data Collection

Development Hardware

For training the networks and testing code, we used a Dell XPS 15 9570 with 32 GB of RAM and an Intel Core i9-8950HK CPU clocked at 2.9 GHz. Most importantly, this machine has an Nvidia GeForce GTX 1050 Ti with Max-Q Design GPU. The 4GB of GPU memory allows training on larger mini-batch sizes (passing multiple images through the network in parallel) which can change how and where the network converges. It also allows us to evaluate the network's performance much more quickly than purely using the CPU for processing.

For deployment on the Jetson Nano, we use Jetpack 4.2.2 to flash the System on Chip. This includes a full build of a Linux operating system – Ubuntu 18.04, as well as necessary software libraries like CUDA, OpenCV, and TensorRT. CUDA is used for hardware acceleration when using Nvidia's GPUs, OpenCV provides a standard interface for connecting to external cameras, and TensorRT provides deep neural network acceleration by optimizing neural networks matrix calculations to work on Nvidia's GPUs. Using the Simple DirectMedia Layer (SDL) library we can interface with our camera easily, and generate our GUIs on the target hardware. The Video4Linux library also allows for simple streaming of cam era video through an ssh connection, and there are readily aviailible functions in matlab to call both the camera and display object, whether you'd like to generate a gpucoder executable on the nano, or call and display cameras on a remote host. This works well for our wireless datalink solution.

Software Algorithm Development Platforms

Anaconda is a free and open-source development platform for creating and managing python scripts. We use Anaconda to manage common python packages like NumPy, time, os, OpenCV, TensorFlow and ImageAI in separable environments. These packages run high-level functions for rapid development and prototyping. It can be installed cross-platform as well, which means we'll be able to run the same environments for development on the Windows laptops with GPUs for training the deep learning solutions, then migrate the same environments,

24

without having to repeat the tedious installation process of each package to the Linux distribution on the Jetson Nano.

The Intel RealSense SDK provides an integrated platform for leveraging Intel's RealSense camera and depth-sensing modules along with prebuilt functions to handle their proprietary hardware.

Tensorflow is a framework created by Google for deep and machine learning in python. This is the industry standard for doing novel neural network development and has implementations of all the latest convolutional neural network object detectors and classifiers. It can also be used as a backend for handling neural network computations on a GPU.

ImageAI is a python package that encapsulates all TensorFlow operations for object detection and recognition into simple functions that we used to test and execute RetinaNet and compare single-shot detection methods with the R-CNNs in MATLAB.

MATLAB was used as a platform to develop convolutional neural networks with their Deep Learning Toolbox and add on support packages for MobileNet-v2, ResNet18, and AlexNet. These add-ons contain the network models along with pre-converged weights that were trained on the ImageNet dataset on 1000 different classes. In the end, matlab was able to host and run all the code we needed. The gpucoder toolbox and related add-ons allow us to call cameras remotely through an ssh client and stream video directly onto our host laptop. We can also make system calls to run our python and c++ scripts for motor controls.

3.5.2 Object Detection

Speed vs accuracy trade-off. A higher mAP and a lower GPU Time is optimal.
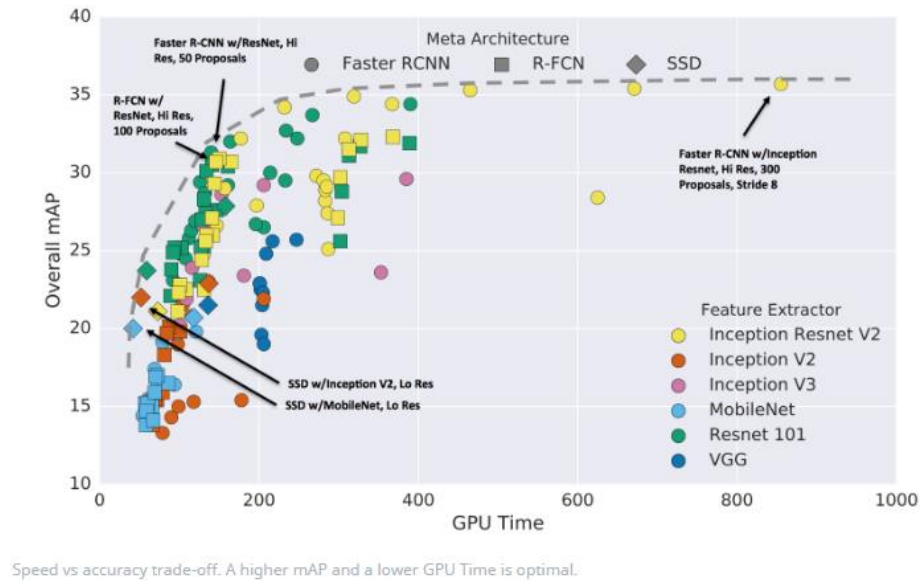
Figure 11: Speed vs Accuracy Trade-offs for Different Neural Network-Based Classifiers (Approved for Use)

As seen in Figure 11 above, there is a multitude of different neural network architectures to choose from, each with the possibility of using a different convolutional neural network architecture for feature extraction and classification. Based on the speed vs accuracy trade-off, we will be evaluating networks along the lowest end of GPU Time in order to maintain consistent frame rates and inferencing times. Mid-tier mAP (mean average precision) scores are acceptable since we will be transfer-learning fewer classes that require less distinct features in the network. Single Shot Detectors will be evaluated for their speed, while Faster R-CNNs will be evaluated for their accuracy [6].

There are many object detection methods based on traditional computer vision approaches from Sobel edge detection to advanced techniques like Scale-Invariant Feature Transform (SIFT). We will look at traditional computer vision object detection ensembles like the OpenCV function. However, recent advancements in graphical processing units (GPUs) have allowed for the deployment of neural network architectures that contain millions of parameters and can learn how to localize objects within an image automatically.

In order to achieve state of the art results in object detection, an approach would be to implement a Single Shot Detector (SSD) with a Resnet50 backend, pre-trained on the Common Objects in Context (COCO) dataset. Pre-training the multi-million parameter network on a bank of 80,000 images allows transfer learning, the process of changing the outputs to new or more specific classes, to quickly converge to an optimal model.

26

Frame Differences
In order to provide a cheap object detection strategy, the mine can leverage the fact that it can be a stationary platform looking for a moving target (see Figure 12). This gives an edge one could subtract frames to look specifically for blobs of movement when the cameras are static. Then, one can calculate centroids of the difference blobs, and crop out a fixed size image chip centered on that point to feed into a convolutional neural network classifier. This would provide a quick and dumb detector that is computationally cheap. The tracking algorithm would take over to follow the target from there.
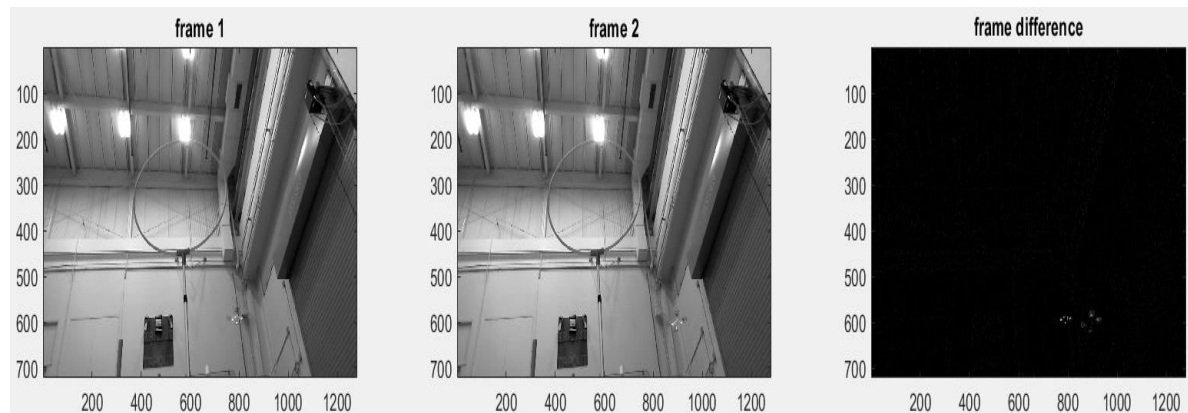
Figure 12: Example Output of Frame Differences from a Stationary Camera

Good Features to Track
Classic features to cue on in image processing are typically based on image gradients, i.e. changes in pixel intensities over space. Concatenating gradients in both the horizontal and vertical directions yield a method to detect corners, which has been shown as a strong and robust feature to track objects with. Using the Shi-Tomasi modification of traditional Harris Corners (see outputs in Figure 13), this traditional computer vision technique is easily realizable in python using the OpenCV function 'GoodFeaturesToTrack()'. This technique takes in a grayscale image, which already reduces the complexity involved with processing 3-channel color images and returns coordinates for confident corners within an image. From here, we can attempt clustering creating centroids for object detection. Once a drone is detected and classified, then we can use the same corners to track that object over time. The perk of this methodology is that it is computationally cheap, as it only tracks sparse features [7].
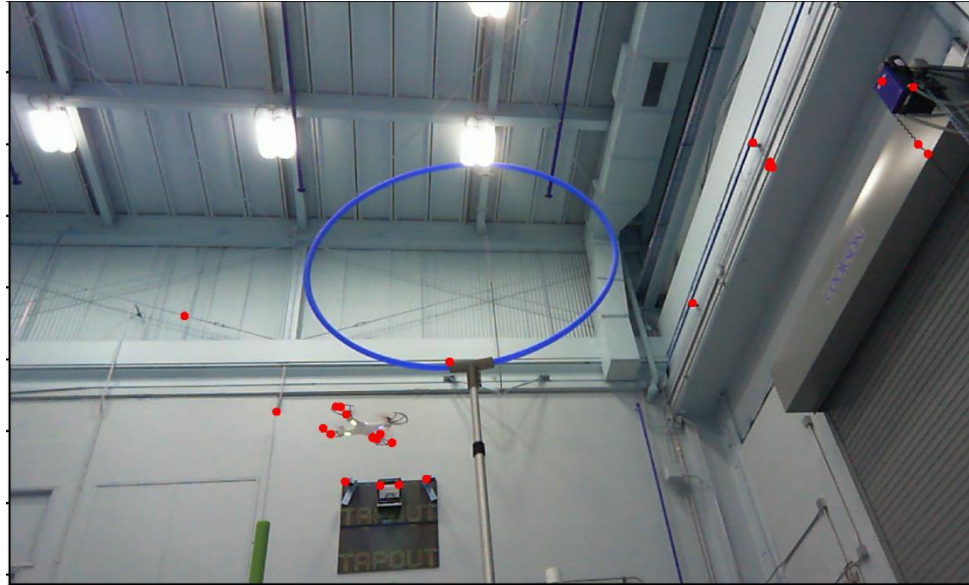
Figure 13: Example Output of Good Features to Track Object Detection Method.

CNN Object Detector Comparison

RetinaNet

RetinaNet does both object detection and classification in a single pass through the network. In traditional methods, we would threshold the number of detections returned by an object detector algorithm from some number of declarations. The single-shot detector simplifies this process by both suggesting bounding boxes and associating classes with them. The network (see Figure 14) looks a lot like AlexNet or Vgg16 and is based on the architecture with one big change. Layers are added at the end of the network that suggests bounding box positions through priors or anchors [8] [9].
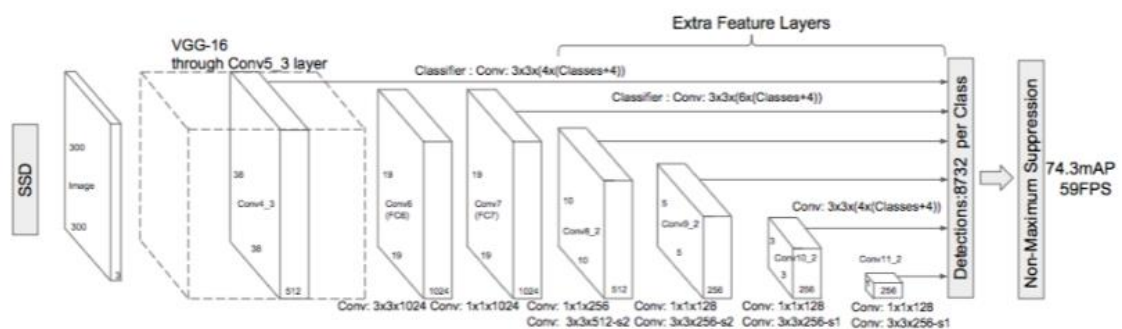
Figure 14: Architecture of a Single Shot Multi-Box Detector (Pending Approval)
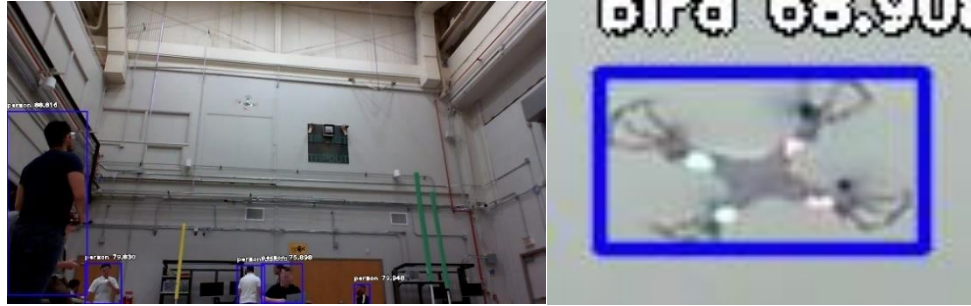
Figure 15: Example Classification Using a Pre-trained RetinaNet on Drones

These are suggestions for bounding box placement, and then a location loss is computed, and the boxes are regressed closer to the location of the true location using the training data. Instead of single class decisions with confidence values, the end of the network is morphed into a 2-D array at the size of the input image. There are two cost functions needed to optimize a detector and classifier like this: A *Confidence Loss* that measures how much a region looks like an object, then computes a bounding box typically achieved with a *Categorical Cross-Entropy* function that is used to compute the per class loss. And a *Location Loss* that measures how far away the network's predicted bounding boxes are from ground truth in the training set. Here the function *L2-Norm* is used. Although the algorithm achieves above-average classification and detection accuracy, the network is computationally expensive and larger than necessary. The network trained on the MS COCO dataset was still able to find drones in test imagery with a tight bounding box showing promising results for the detector choice (see Figure 15) [10].

R-CNN

R-CNN is a novel architecture proposed by Ross Girshick et al. that utilized a selective search methodology to minimize the number of detection windows needed to find an object within an image. This is done by generating many candidate regions, then using a greedy algorithm to combine smaller regions into larger ones. These larger regions are then run through the convolutional neural network backend to compute features and then classify said regions (see Figure 16). The automatic feature extraction and bounding box proposals are incredibly useful. Some of the drawbacks are the long processing times, and there is no learning in the bounding box proposals. By using Matlab's deep learning toolbox, an R-CNN was implemented. Initial qualitative results were positive, but the bounding box regression was often poor having a low IoU score (shown in Figure 17 below).
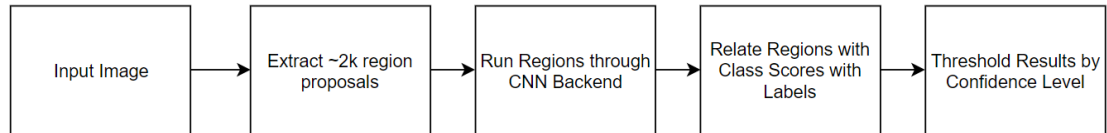
Figure 16: R-CNN Architecture
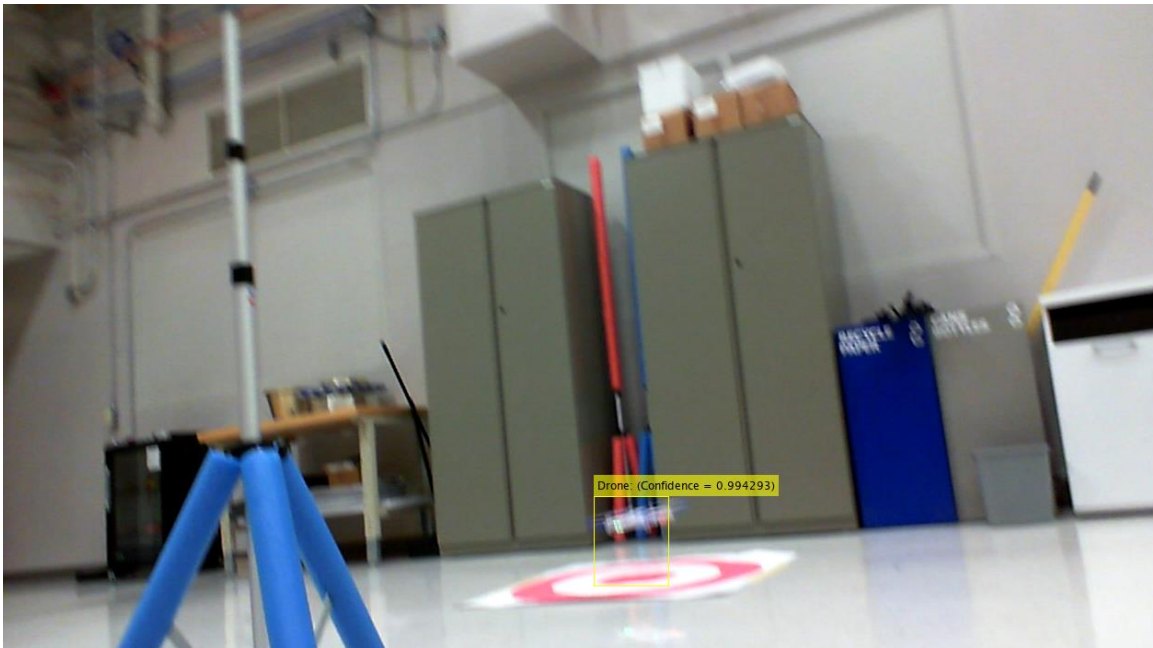
Figure 17: R-CNN Implementation in Matlab

Faster R-CNN

Shaoquin Ren et al. expanded on R-CNN with Faster R-CNN. Instead of the selective search algorithm, the network itself learns how to create region proposals with a network separate from the convolutional feature extractor. The two networks are then concatenated with a region of interest (RoI) pooling layer that outputs the final decision back in the same dimensions as the input of the network (see Figure 18).
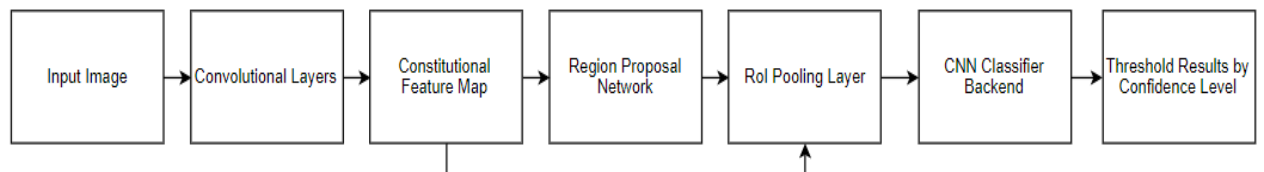
Figure 18: Faster R-CNN Architecture

Final Object Detection Algorithm Selection

Based on the intelligent bounding box selection and runtime speed of Faster R-CNN, we opt to use this object detection algorithm as the baseline deep neural network object detector. This simplifies the computer vision pipeline by combining region proposal and classification in a single network.

Scoring and Evaluation Procedure

In order to score and validate results, IOU, precision, recall, F1 score, and Receiver Operator Curves will be used to quantify detector performance on the datasets. These metrics can be computed for both dumb and intelligent detectors. And simply provide metrics to validate 1. How close was the bounding box to the actual location (IOU) as seen in Figure 19 below. How well it did on images it has seen before and how much of each class was predicted correctly (precision, recall, and F1 scores), and 3. How many detections should we have the object detector nominate to find the targets [6].

In order to evaluate the network runtime, we used the TensorRT function trtexec in order to test inferencing speeds directly on the Nano. This was done by exporting a trained convolutional neural network classifier from MATLAB into the ONNX file format which is an acceptable input to trtexec. We average the inferencing time over 10,000 runs on random input data for benchmarking. We also gather power consumption, and thermal data directly from the Nano tegrastats application.

Figure 19: Figure of Scoring Detector Bounding Boxes Using IoU

Classifiers

The power of CNNs is the ability to leverage automatic feature extraction from a training dataset. In order to meet the given detection requirements, and safety considerations, we will transfer learn a pre-trained convolutional neural network to

handle new outputs. Transfer learning is the process of slightly adjusting the weights from a pre-trained model and changing input and output definitions to suit a new task e.g. taking a classifier that has 100 output classes and relearning just 10 that the network has never seen before. To meet Lockheed Martin's DOMINANCE design requirements, we opt for a binary classifier that classifies either 'Drone' or a rejection/clutter class. We'll be taking networks pre-trained on the ImageNet dataset of 1000 classes and transfer learning just two output classifications. Most classifiers are trained on a large dataset of over a million images like the ImageNet or COCO databases and output 100-1000 classes, meaning their learned features are very general and already highly optimized for classifying objects. We will be taking pre-trained networks and relearning a new drone class with the possibility of increasing the number of output classes as the dataset develops through data collections with the customer.

Hyperparameter Trade Studies
In order to achieve reasonable accuracy with convolutional neural network classifiers, trade studies are conducted in three key areas: network architecture, cost-functions, and regularization techniques. Stochastic Gradient Descent with Momentum (SGDM) has been the default optimization algorithm of neural networks for years, and however, Adam, another solver, has been shown to converge more quickly to better optima from academia. When close to optima, SGDM can overstep the exact location of the optima and never converge to the most optimal point computed by the cost function. Adam can help address this problem. Adam was derived from adaptive moment estimation and uses parameters with added momentum terms i.e. an elementwise moving average of both gradients and their square values (see Figure 21 for optimization procedure). Adam introduces three hyperparameters to adjust: The Gradient Decay Factor, Squared Gradient Decay Factor, and an Epsilon term. It performs well compared to other modern optimizers, reducing cost more quickly than other modern optimizers (see Figure 20 below) [11] [12].
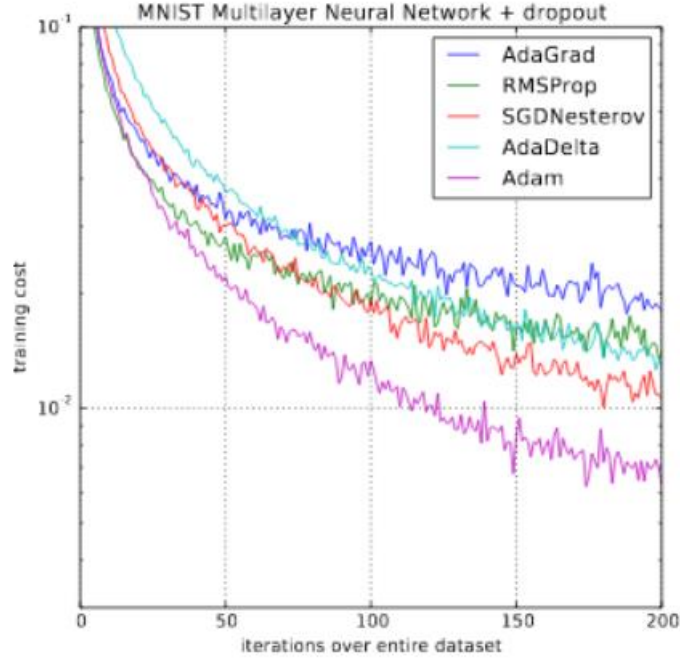
Figure 20: Comparison of Optimizers Using Standard MNIST Handwritten Digits Dataset (Pending Approval)

$$m_\ell = \beta_1 m_{\ell-1} + (1 - \beta_1)\nabla E(\theta_\ell) \qquad \theta_{\ell+1} = \theta_\ell - \frac{\alpha m_l}{\sqrt{v_l} + \epsilon}$$

$$v_\ell = \beta_2 v_{\ell-1} + (1 - \beta_2)[\nabla E(\theta_\ell)]^2$$

Figure 21: Optimization Procedure of Adam

Addressing regularization is a challenge when building large neural network models with millions of parameters. It has been shown that adding a regularization term to your loss function can reduce overfitting [13]. In the case of L2 regularization, also known as Ridge Regression, we add a squared magnitude of the weights. We can adjust the effect of this penalty term with the adjustable parameter lambda (see Figure 22).

$$E_R(\theta) = E(\theta) + \lambda\Omega(w), \qquad \Omega(w) = \frac{1}{2}w^T w.$$

Figure 22: Adding a Penalty Term to the Solver's Function Allows for Regularization

In order to find the optimal number of times to show the network the same data, i.e. how many epochs to run, implementing a learning rate scheduler with

33

validation validation patience is a best practice. The learning rate scheduler slowly decreases the learning rate over multiple epochs, slowing learning to avoid overfitting. Then, a global watchdog of sorts: validation patience is used to find the perfect cut off point. Since the network is only shown training data, we can simultaneously evaluate the network on a separate set, the validation data, to see how the network is performing on unseen data at the same time as training. When the accuracy of that validation set stop increasing, we know that the model is beginning to overfit to the training set and training is stopped and the network is saved off [14].

Best practices dictate forking available data into three sets: a training dataset with the majority of images at 80%, a validation dataset that will be used to evaluate and iterate through hyper-parameters at 10% (like the initial learning rate of the solver, regularization terms as either L2 or L1 regularization terms, number of epochs, etc.) and a final testing set to evaluate the trained Model's results at 10% [15]. Hyper-parameters will be automatically optimized using a grid search, testing each possibility and returning the best result. Results from the trained solutions resulted in the chosen hyperparameters that are highlighted in Table 6 in green below [15].

Solver	Initial Learning Rates	L2 Regularization	Gradient Decay Factor (Adam)	Mini Batch Size
SGDM	1E-3	0	0.95	32
	1E-4	1E-4	0.90	64
Adam	1E-5	5E-5	0.85	128
	1E-6	1E-6	0.80	Maximum Value set by GPU Memory Capacity

Table 6: Hyperparameters Tested via Grid Search

Classifier Scoring
Confusion Matrices will be used to validate classifier performance across four classes (see Table 7 below). We compute per class accuracies and can then compute an overall percent correct classification of the network based on the sum of all correct classifications over the total number of images classified.

Precision and recall can also be calculated to quantify how well each class is being classified. Precision The number of true positives compared to all positives, which equates to how many of the selected classifications are relevant e.g. Drone classifications. Recall measures the percentage of a class that is identified, comparing true positives to false negatives and true positives. F1 Score combines

both metrics and yields another value close to the overall percent correct classification that mathematically yields the harmonic mean of precision and recall.

	Human Class	Drone Class	Unidentified Aerial Object	Clutter / Rejection Class
Human Class	Correct Classifications	Misclassified	Misclassified	Misclassified
Drone Class	Misclassified	Correct Classifications	Misclassified	Misclassified
Unidentified Aerial Objects	Misclassified	Misclassified	Correct Classifications	Misclassified
Obstacles	Misclassified	Misclassified	Misclassified	Correct Classifications

Table 7: Sample Confusion Matrix for Scoring Classifiers, Truth on y-axis vs Declared on the x-axis

Convolutional Neural Network Architectures

Due to their location on the Pareto frontier in Figure 23, attaining maximum efficiency in both overall accuracy and speed for the ImageNet challenge, we chose to evaluate the MobileNet-v2, Resnet-18, and AlexNet convolutional neural network architectures for maximum classification accuracy vs computational expense at runtime.
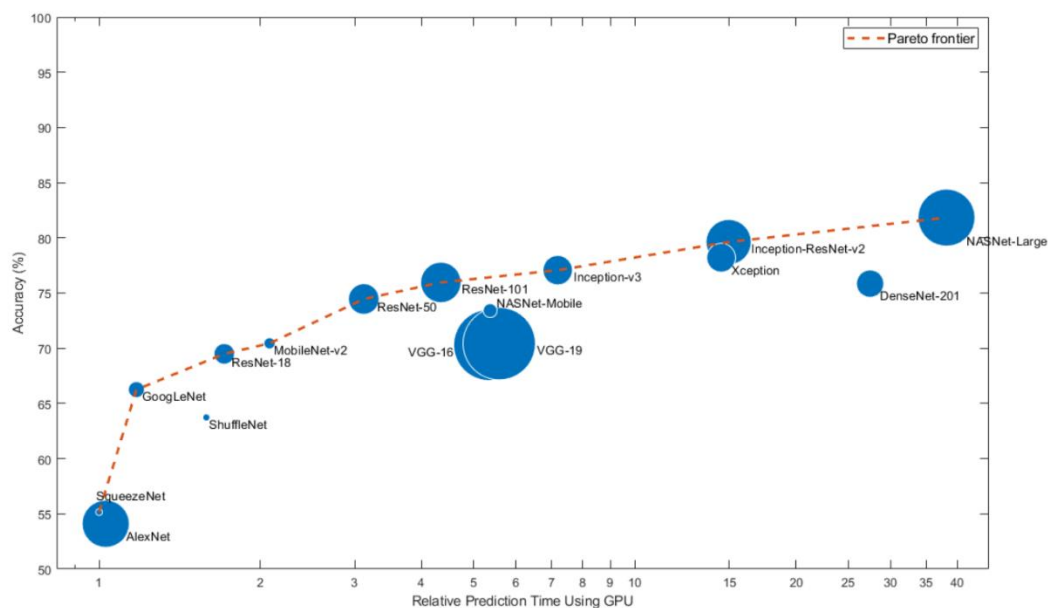
Figure 23: Pareto Frontier for CNN Classifiers in MATLAB

In order to meet the memory constraints of the mine's processing platform, the Nvidia Jetson Nano, architectural changes need to be made to mainstream neural network architectures. Older architectures, like AlexNet use fully connected layers and a process known as Dropout in order to regularize the connectivity between feature extractions done in earlier convolutional layers to final classification neurons that yield output class confidence values. This is memory intensive, adding 8,192 neurons to the network that need to process along with an activation function (ReLU). In order to address regularization, batch normalization layers are added in-between each convolutional layer in order to regularize and normalize the distributions of data being passed into the network at training time from convolutional layer to convolutional layer. The main architectural considerations amount to three neural network architectures for comparison: AlexNet, Resnet18, and MobileNetV2.

AlexNet

AlexNet broke ground in 2012 by beating out classical computer vision classification methodologies in the ImageNet challenge. The revolution came from sparse connections compared to fully connected neural networks. Sparse connections were used along with 3x3 matrices of filters to automatically learn features from given training images. The network is shallow, but still holds great generalization ability due to internal regularization in the fully connected layers at the end of the network (see Figure 24 below). In the results shown in Figure 25, AlexNet performed well on both the entire dataset (left) and the unseen sequestered testing set (right). The shallow architecture also allows AlexNet to be run in Realtime easily.

Modified AlexNet

By removing the dropout regularization, we can further increase inferencing speed. By adding batch normalization throughout and modifying the network to be more 'ResNet-like' we can remove computationally expensive fully connected layers at the end of the network (see Figure 24 below) without sacrificing accuracy.
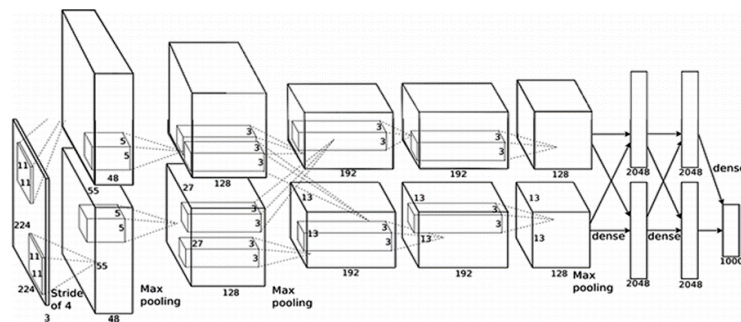
Figure 24: AlexNet Architecture (Image Approved)
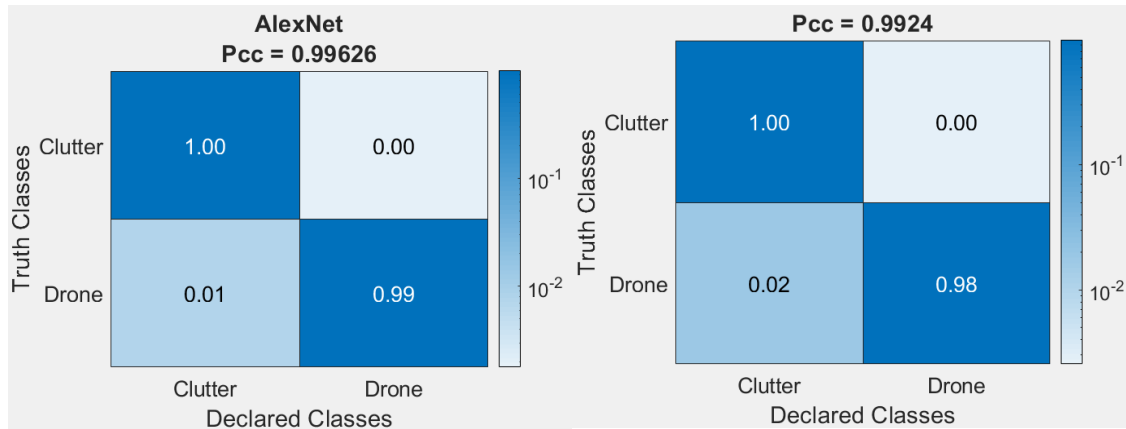
Figure 25: AlexNet Results

ResNet18

The Residual Network architecture (ResNet) introduced the concept of the 'residual block': A set of CNN layers that allow information to flow smoothly throughout the network while maintaining feature extraction and regularization (see Figure 26 below). Skip connections are added between blocks of convolutional layers in order to allow for a more robust network that accounts for *elimination singularities*, where parameters in the network are pushed to zero and are therefore no longer useful to the network, *overlap singularities,* where different network pathways connect into each other instead of fully propagating to the end of the network, and *linear dependence singularities*, where parameters become linearly independent. These singularities have been shown to significantly reduce learning and including skip connections has been shown to help mitigate these effects. We also replace the final max pooling layer with a global pooling layer, compressing the activations of a filter into a single value. This helps the network's classification ability to become spatially invariant i.e. it matters which filters are activated early in the network, not specific weights in those filters that correspond to certain spatial locations in the input image [16].

Evaluating on the dataset, ResNet18 had the best classification scores in both the full dataset and the unseen testing set (see Figure 27). It is, however, too computationally expensive to run on the Jetson Nano in the ONNX file format.
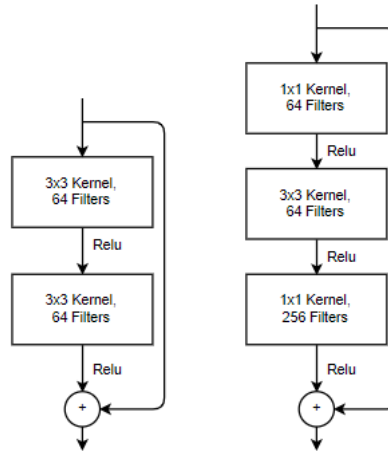
Figure 26: Residual Block
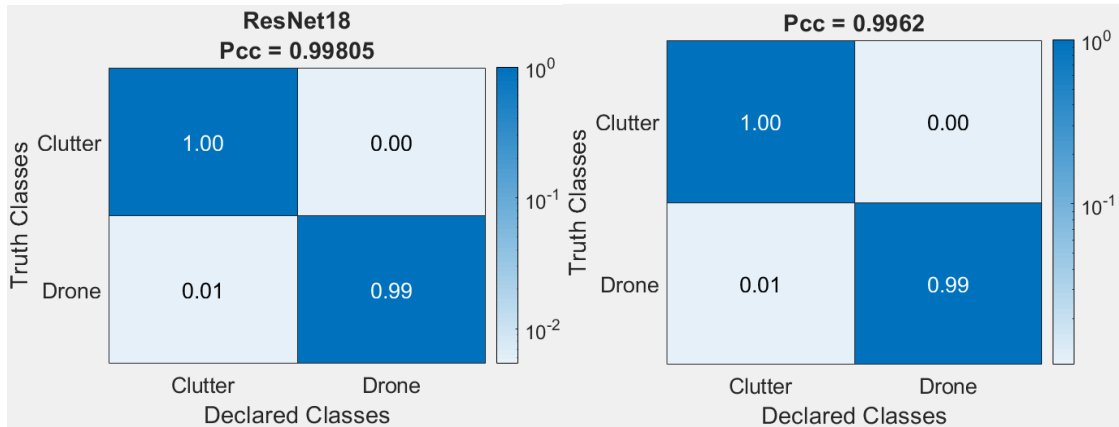
Figure 27: Resnet18 Results

MobileNetV2

MobileNetV2 was produced by Google for the purpose of creating a classification network optimized for mobile devices. This is done by introducing new layers and convolutional blocks that simplify typical CNN mathematical operations e.g. convolution is broken down into depth-wise separable convolution calculations. It also utilizes the skip connections from Residual Network architectures. It also introduces linear bottlenecks (see figure) through 1x1 GroupWise convolutions that reduce network complexity by preventing the non-linearities (ReLu) from destroying information as it propagates through the network (see Figure 28). From the experimental results, we found that mobileNetV2 preformed second to Resnet (see Figure 29), but with a much faster runtime.
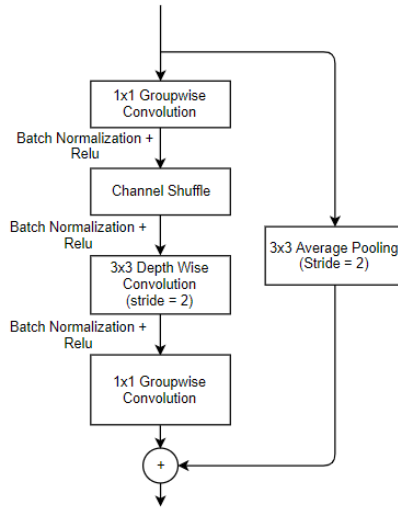
Figure 28: MobileNet-v2 Linear Bottlenecks
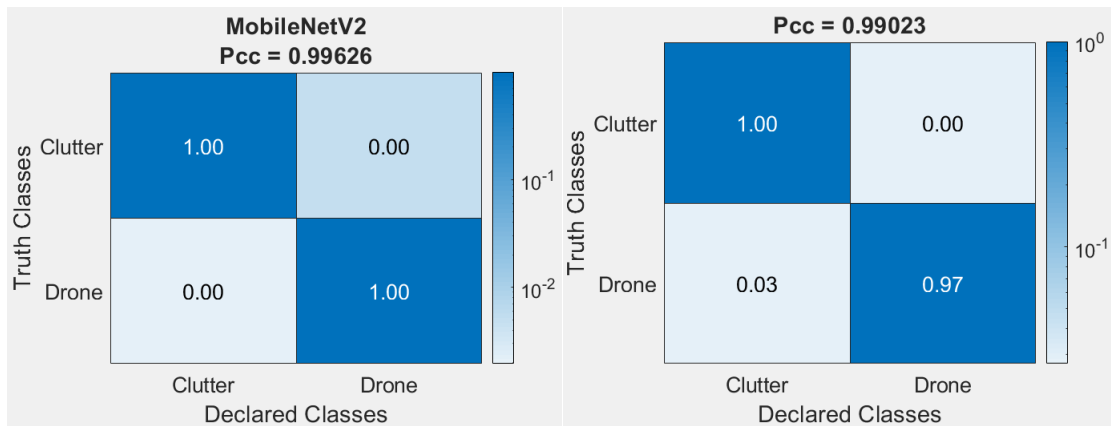
Figure 29: MobileNet-v2 Results

Final Classifier Selection

After Training MobileNet-v2 for a single epoch on the training data, we can immediately see the power of transfer learning from pre-converged ImageNet weights in Figure 30. Within 10 iterations of 32 image batches, the network was correctly calling each new input image Drone or Clutter over 90% of the time. The final classification results are over 99% accurate as well. The quantitative classification results coupled with the inference speed as benchmarked on the Jetson Nano of 13.9881 milliseconds per inference lead us to choose MobileNet-v2 as the principle CNN classifier. The results are tabulated in Table 8 below.
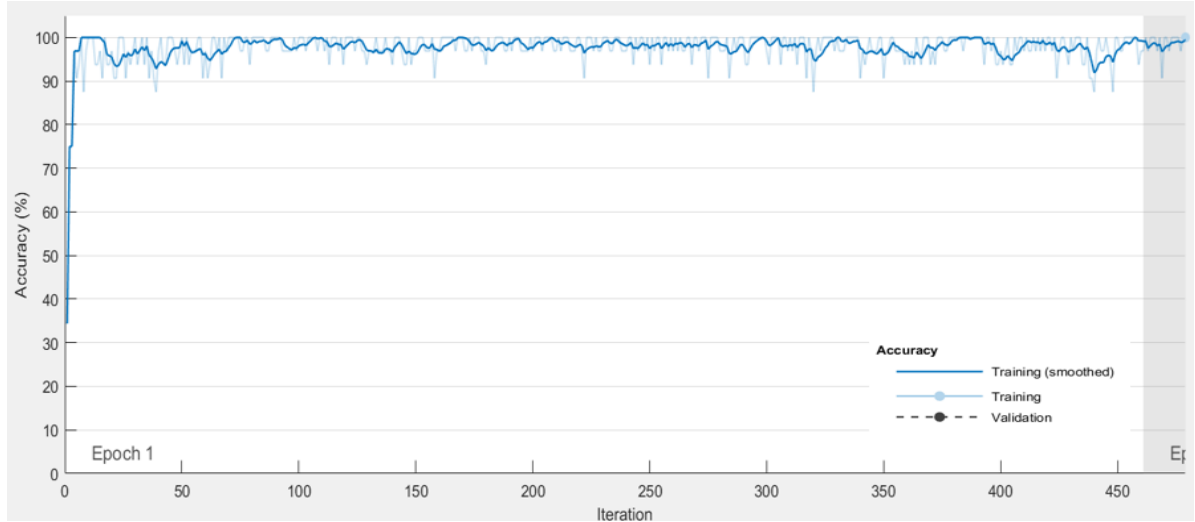
Figure 30: MobileNet-v2 Training Plot

	Overall Classification Accuracy on Custom Dataset	Inference Time on Nano in milliseconds	Number of Layers
MobileNetV2	0.99023	13.9881	155
Resnet18	0.9962	Would Not Run	72
AlexNet	0.9924	46.0165	25
Modified AlexNet	TBD	TBD	TBD

Table 8: Comparison of Different Convolutional Neural Networks for Classification

Tracking Methods

After establishing a single frame detection, using a tracking algorithm will help us maintain accurate detection and classification of a target over time and space. This will also help remove false alarms thrown by the detector and classifier, effectively smoothing out temporal and spatial anomalies. The approaches that we considered are the KCF tracker and both sparse and dense Optical Flow using the Lucas-Kanade algorithm [56] [17].

KCF Tracker

For the KCF tracker, we can use readily available OpenCV object detection, which functions, and also yields other similar detectors to trade. The KCF tracker works by looking for correlation between an original nominated image patch from the object detection method, and then looking for that image patch in the next frame with a representation of the image patch's appearance, then regression training

fits the bounding box from the last frame to a correct position in the next frame (see Figure 31). This leads to an updated model, which is then used to return maximum x and y coordinates of the correlation between frames. This is repeated frame after frame and can be validated by continuously running the detector and or classifiers. We can empirically determine a certain number of frames to declare a valid track [57]. In other words, if the detector and or classifiers are validating the tracking position, we continue to use the tracking positions for the following n number of frames. This helps ensure a smooth track, even in frames that the detector and classifiers may misclassify or not detect at all [18]
.
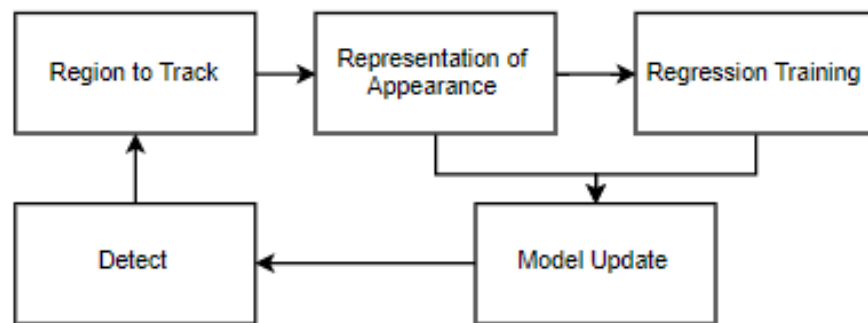
Figure 31: KCF Tracker Block Diagram.

Optical Flow

To understand sparse optical flow, reference object detection method: goodFeaturesToTrack(), specifically the corner detection using the Shi-Tomasi algorithm. Again, leveraging the functionality of OpenCV, use the calcOpticalFlowPyrLK() function to follow Shi-Tomasi corners through time and space. This is one method to track sparse features aka some number of corners in an image. The Lucas-Kanade algorithm assumes that the change in pixel location is small, which may hinder the tracking of a fast-moving drone and a moving camera [19].

A better, but more computationally expensive, approach is to do a dense Optical Flow. In this case, the system looks at all the differences between image frames. Although the algorithm weights two key factors heavily in its tracking calculations. The Lucas-Kanade algorithm assumes small displacements in small time increments. This may not work well for fast-moving drones. Also, the image is assumed to be 'textured' with different intensity levels changing slowly over time. These effects, however, can be mitigated by the precision of the depth map produced from the stereo solution.

Final Tracker Selection

By using the KCF tracker, reliably track any movement within the camera frame and provide a regressive approach to refining bounding boxes produced from the object detector that can be made.

Alternatively, Optical Flow can be implemented in certain situations e.g. when the camera is static. This method guarantees speed and direction is recorded for every pixel for tracking detections even if some sparse features are lost. This method also means that, when new objects are detected, the algorithm solution already has an estimation of where the object will be in the next frame. This is not guaranteed by sparse tracking methods like sparse Optical Flow or the KCF tracker.

3.6 Strategic Disruption Tactics

The primary system for the mines disruption device was chosen after many other considerations. Due to the customers strict design constraints, the options were very limited to what would fit within the defined space for the mine while regarding the other restrictions. The disruption devices within consideration included systems to disrupt the sensors of the target, systems to capture the target, systems to disguise the mine from the target, as well as systems to attract the target to enter the defined blast radius for the mine. All of these methods were discussed at length before dedicating the time into research as many ideas led to a customer constraint that would void the idea entirely. By incorporating as many of the following tactics as possible to all work simultaneously while the targets mission is underway, the chances of successfully disabling the target increase significantly.

3.6.1 Sensor Disruption

A strong method for disabling the target involves disrupting the sensors used on the enemy target; obscuring the control systems used to navigate the target through the course. A large portion of the research for sensor disruption was based on learning about the common sensors used for autonomous flight navigating as well as flight controllers that are used on a wide variety of simple drone hobby kits similar to the ones suggested for the target UAV teams. Dedicating time and research into the targets main system components allows further definition of the types of disruption devices needed to disable the primary controllers used within the targets control systems.

Figure 32: Suggested Quadcopter Hobby Starter Kit

It was strongly defined in the customers' requirements that radio frequency jamming could not be implemented within the design of the mine. Radio frequency jamming, or RF Jamming, works by a transmitter being set to produce the same frequency as the targets' receiving equipment and with a strong enough signal can override any signal at the receiver of the target. RF jamming is commonly used on commercial drone defense systems utilized by military, airports, and even businesses and housing. Using RF jamming would be a very simple solution to disabling the target drone as it would limit or fully eliminate the enemy control signal used to transmit data from the targets transmitter such as the TS5828 shown in Figure 32 above. Disrupting the enemy signal could cause the loss of control, termination of video live feed, as well as disabling live data collection used for properly navigating the obstacle course. This is not allowed due to the danger this could cause for nearby bystanders as well as the hardware used for both the target and the mine. If the control feed is completely disabled and the UAV loses control, the ability to shut down the target remotely or send an auto-land command is also inaccessible. For the pure sake of safety to the spectators, RF jamming is strongly forbidden.

Another common sensor that will be utilized on the target UAV is a microphone array. The target will have an array on their device for the ability to listen for the signal transmitted by the acoustic waypoint located on the obstacle course of which the target is required to navigate to, automatically land, and automatically take flight again. Similar to the RF jamming, it is not permitted for the mine to emit acoustic signals to interfere with the microphone array on the target. If this disruption was allowed, the mine could simply transmit an acoustic signal which would lead to the target to sense and process the sound into thinking that the mine is the acoustic waypoint. If the target is designed to standards, the UAV would autonomously navigate to the mine and descend; placing the drone within the blast

43

radius for further attacking methods. Since this is prohibited, various other luring techniques have been considered and are further discussed in section 3.6.4.

Since there are strict limitations defined by the customer for how the mine is allowed to interact with the target, the previously discussed methods for sensor interference limit the types of sensors that can be targeted. Another known constraint for the target is that the UAV must operate autonomously with no global positioning system (GPS). This results in having to incorporate a vision-based sensor. Vision based sensors were heavily discussed and compared in regard to performance based on various environments and properties as seen in Table 9. In regard to this project, the sensors used for comparison were in the range of $200 to stay within a practical budget. While this same topic was at large for deciding what would work best for the mine's vision sensor as well, there was one specific objective required for the target to perform that determined what type of sensor would be guaranteed to be on the UAV for navigation.

	Radar	LIDAR	Stereo Camera
Range	~50m	~3m	~10m
Field of View	30°	360°	120°
Color/Contrast	x	x	☐
Works in Dark	☐	☐	x
Works in Bright	☐	☐	☐
Works in Acclimate Weather	☐	x	x

Table 9: Vision Sensor Comparisons

One of the targets primary goals is to not only navigate the course, but to perform a variety of tasks that are dependent of the obstacle the target encounters. While some obstacles vary in shapes and sizes, of which could be detected from each compared sensor, there are also a few tasks that are dependent on the color of the obstacle. From Table 9, it can be observed that neither radar nor LIDAR can differentiate color therefore it can be anticipated that the UAV will be equipped with a camera as one of the navigation and/or identification sensors. This allowed for the first element for disruption to be targeted [20].

3.6.2 Target Capturing

Another tactic for disabling the target is to physically capture the device. Since high-velocity projectiles are prohibited per the customer's constraints, the method for capturing had to be meticulously discussed with the customer to further define what could and could not be implemented on the mine. The conclusion resulted in the capturing system being a CO_2 powered net launcher. There are many net launchers available online for purchase, however none of these solutions fit within

the given budget. It was decided amongst the team that designing a net launcher from scratch was the only possibility of having a capturing system incorporated on the mine without exceeding the budget, size constraints, and customer's definition of a high-velocity projectile.

Net launchers similar to the one shown in Figure 33 are powered using a 16 gram, non-threaded, disposable CO2 cartridge triggered by an electronic solenoid valve. When the user presses the button to fire the launcher, the solenoid valve opens; releasing the pressurized gas to four separate chambers containing weights tied to four corners of the net. These four weights accelerate out of the chambers at opposing outward angles to fully expand the net as it opens and drags behind. These handheld net launchers are a single shot use and require the head containing the net and weights to be replaced after each use. While implementing one of the available net launchers within the mine would be an easy solution for a capturing device, the MSRP for a basic starter kit ranges around $800-$1000. Given a generous budget of $700 from the customer for the mine, this is not an option. However, it was determined that a very similar concept could be implemented for a mere fraction of the cost.

Figure 33: Commercial Handheld Net Gun Courtesy of TheNetGunStore.com

After deciding that a net capturing device would be utilized on the mine as the primary form attack, the goal was to try to replicate this readily available system to fit the specified design constraints. To power the net launcher, CO2 would be utilized as it contains a large amount of pressure in a very small amount of space. CO2 canisters are a mixture of liquid and gas at equilibrium. As long as there is liquid CO2 present, the cartridge will automatically maintain pressure by boiling off the liquid as the gas form is released. A typical 12g CO2 cartridge has an internal volume of 14 cubic centimeters with a pressure of around 850-1000psi, or 56 bar at room temperature [21]. This is far more pressure than what is needed to deploy the net for the given requirement. Pressure regulation can be used by incorporating a regulator at the output of the CO2 canister, however since these are single use cartridges with no threading, that solution requires more parts which also adds to the budget. Another way to reduce this pressure is to add extra volume for the CO2 to expand to. Increasing the volume of the space that the pressurized gas is stored in before being released can regulate the amount of pressure contained. Once the volume has exceeded a certain amount, all of the liquid CO2 boils off leaving only

a gas. Then the ideal gas law can be applied of which increasing the volume further will result in reducing the pressure. At 70°F, the following approximation (derived from the Ideal Gas Law) results in the pressure of a given chamber when filled with a 12g CO2 cartridge:

$$Pressure\ (psi) = \frac{5910}{Volume\ (in^3)}$$

This approximation will be further used to design the chamber to regulate the pressure for optimal settings to deploy the net safely and successfully.

To release the pressurized air, an electronic solenoid valve will be used; controlled by a signal from the microcontroller when the mine detects the target within the blast radius with a confidence over 95%. Once all of the criteria are met to assure the target is within range for the system to engage, the controller will send a 12V pulse signal to the normally closed solenoid to open the valve just long enough to deploy the weights and shoot the net. This solenoid must be rated to withstand the pressure from the 12g CO2 cartridge to ensure it can operate smoothly without failure. Using the equation above, once the volume of the depressurization chamber is determined, the pressure applied to the solenoid will be known. This will limit the available options for solenoids to be used within the system.

The net capsule will need to contain four separate barrels as well as room to load the net. The net will have a 1" mesh and be approximately 6ft x 6ft. This size is to ensure that once deployed, the net will have the area needed to fully occupy the blast radius if fired directly up. The larger the net used, the higher the probability is of successfully capturing the target with less accuracy needed. However, if the net is too large, this requires more pressure needed to fire the net as more drag is created from the added weight and surface area. There are multiple nets available for purchase that have been designed for the commercial net guns like the ones shown in Figure 33 above. While mesh net is sold in bulk from various hardware stores online as well as locally, it is difficult to find similar net as to what is produced for the existing net gun products for a price that is drastically cheaper than the one made for the readily available weapons.

The capturing system will be dual purpose and also serve as a defense mechanism for the mine. Since there were no constraints introduced by the customer regarding the target being able to attack back, it is crucial to prepare for the worst-case scenario of the target disabling the mine before the mine is able to attack. This tactic involved thinking from the target's perspective of the options for counter attacking the mine and determining all possible ways that this could be achieved. One way that seemed easily achievable is for the target to detect the mine and disrupt the vision sensors so the mine cannot sense the UAV. This could be accomplished by the target deploying a cover, such as a sheet or net, overtop of the mine. While the mines primary attacking systems should be triggered before the UAV would have a chance to maneuver over the mine to deploy a cover-up over the mine, in the scenario that the target counter attacks first the mine will be programed to trigger the net launcher to increase the chances of deflecting the

cover-up. Since the launcher only has one net shot before having to be reloaded, this would significantly reduce the chances of capturing the target. However, the large sized net would still have a chance of capturing both the sheet and the target in one blast. This is the most optimal outcome for this counterattack scenario and while it may not be achieved, the probability of capturing both the target and the counterattack is significantly higher than capturing anything with the mine's sensors being disabled entirely.

3.6.3 **Camouflaging**

While majority of the focus of the mine was dedicated towards attacking the target, there was a fair amount of thought put into defensive mechanisms as well. Research into the common types of systems used for navigation of autonomous vehicles was crucial in development of the mines systems that can disable or disorient the targets navigation. Since the mines goal is to detect and destroy the target, the target carries a similar interest in detecting and avoiding the mine. By camouflaging the mine, the chances of completing the mission greatly improve as the plan of attack is backed up by the art of surprise.

Camouflaging is typically thought of as disguising the physical appearance of something however that is not always the most practical solution. While the mine will be designed to blend in with its surroundings as much as possible to reduce the chances of being detected by a camera on the UAV, this will not phase being seen by various other sensors that could possibly be incorporated. Infrared Sensors (IR Sensors) are used to detect objects based on the infrared radiation emitted from the object; typically, in the form of heat. Infrared radiation wavelengths range between 700 nanometers to 1,000,000 nanometers. The spectrum typically used for heat sensing is condensed to 700 nanometers to 14,000 nanometers The infrared sensor works by measuring the infrared energy emitted from an object and converting the energy into an electrical signal. This electrical signal is directly proportional to the energy emitted from the object of which is also directly proportional to the temperature of the object [22]. Using an IR sensor on the UAV would allow it to sense the mine simply by measuring the change in temperature due to the electronics on the mine compared to its surroundings. Since this could be an enemy tactic for detecting and avoiding the mine, temperature regulation for the systems incorporated on the mine would need to be regulated to reduce the chances of being detected.

Proper heat dissipation as well as heat regulation is necessary and ties together with choosing the components that control the systems on the mine. One crucial factor that will determine the amount of heat that is emitted from the mine is the processing power. If the processing of the data collected from the sensors of the mine is forcing the microchip to run at a higher frequency, this will increase the power used by the chip; creating more heat. Having an abundance of processing power allowed the algorithm to run more fluidly and keep these frequencies reduced. Picking a CPU with multiple cores expands the processing power and increases efficiency significantly. A 'core' is part of the processor that receives

instruction and performs computations or actions based on the instruction. The CPU's speed, or clock rate, is a measure of how many clocks cycles the CPU can perform in a second. This parameter is generally referred to as the frequency of the CPU and is measured in Hertz. The number of cores and the clock rate are two of the main specifications for a CPU that are generally found within the first sentence of a description for the component. It can be noted that two cores running at half speed require less power than a single core running at full speed. This is why deciding on a multi-core CPU is a fairly general but practical solution to reducing the heat emitted from the mine.

Since the main processing unit for the mine is the NVIDIA Jetson Nano, plenty of processing power is available to perform the intended tasks. The Nano boasts a 4-Core CPU running at 1.43GHz as well at 128 CUDA Cores that are capable of delivering roughly 472 GFLOPs of FP16 computations. This impressive amount of processing power is achievable while operating on as little as 5 Watts of power. Since the processing unit is defined, techniques to lower the operating temperatures of the Nano will be utilized by incorporating a cooling system to lower the temperature of the processor while running under the performing load. The Jetson Nano developer kit being used on the mine already has a heat sink attached to the board to regulate the temperature. The fins on the heat sink increase the surface area in which the heat is transferred from the chips significantly to allow better cooling. If the Nano reaches critical temperatures, the processing power will decrease to ensure no damage is inflicted to the components on the board. If maximum processing power while maintaining efficiency is desired, adding cooling to the Jetson Nano is a must.
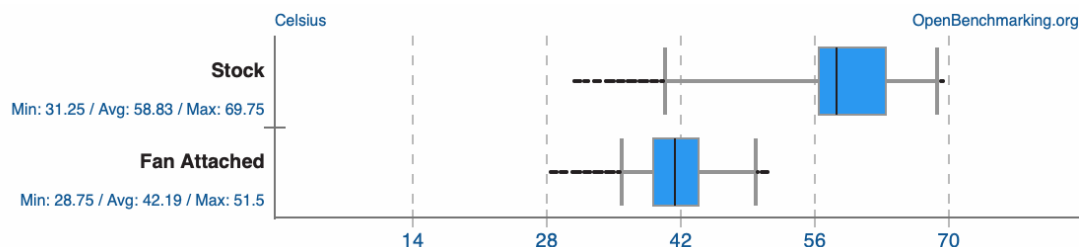
Figure 34: Average Temperature of Jetson Nano Undergoing Various Benchmarks

Cooling systems are commonly added to computers as they become more powerful and contained in smaller areas as the extra processing power generates more heat. There are two main types of cooling systems typically utilized for electronics: water cooling and air cooling (via fan). Water cooling is traditionally used on larger systems ranging from entire server rooms to household consumer computers. Water cooling works by circulating liquid through tubes of which feed through a water block that is directly in contact with the chip; similar to a heatsink. This process uses properties of thermodynamics to cool the hot water dispersed from the chip passing through a radiator in junction with fans before recirculating. For the application being implemented on the mine, this method would be overkill

and difficult to incorporate on such a small device. Instead, traditional fan cooling will be utilized to ensure temperatures remain low; decreasing the chances of being detected by the target. As seen in Figure 34, benchmarking tests were run on the Jetson Nano with and without the presence of a fan there was a significant increase in temperature. By adding a fan, the average temperatures dropped 16.64 degrees Celsius which is a 28% decrease in temperature under the same loads as the Jetson Nano without a fan [23]. Incorporating a fan into the final design for the mine will help to keep the clock speeds optimal on the Jetson Nano while also providing further camouflage to the system.

Fans For Jetson Nano	Size (Length x Width x Thick)	Operating Voltage	Airflow	Cost
NF-A4x20 5V PWM	(40 x 40 x 20)mm	5V	9.4 m^3/h	$14.95
NF-A4x10 5V PWM	(40 x 40 x 10)mm	5V	8.2 m^3/h	$13.95
NF-A4x20 PWM	(40 x 40 x 20)mm	12V	9.4 m^3/h	$14.95

Table 10: Cooling Fan Comparisons

Since the Jetson Nano is fully compatible with a dedicated 4-pin connection terminal for an external fan, options for the four-pin cooling solutions were explored and shown in Table 10. The four pins for the external fan are for ground, power, tachometer, and pulse width modulation (PWM). While the power and ground pins are self-explanatory, the tachometer pin is used to display the speed that the fan is rotating and the PWM pin is used to control this speed. The tachometer is useful in determining the speed the fan will run which can be adjusted do to cooling power as well as the noise emitted from the fan. The PWM pin is used to control the speed, or RPM, the fan is rotating at by acting as a switch to toggle the power on and off by varying how long the pulse sent from the controller to the fan. Since these options are readily available from the Jetson Nano, it is in the best interest to utilize them to their full ability.

Conclusion
From Table 10 it can be seen that the fan options were narrowed down to three choices, all of which are compatible with the 4 dedicated pins from the Jetson Nano. While some appear very similar, there are crucial differences that determined which one to implement on the design. The voltage supplied from the pin of the Nano for the dedicated fan is designed for 5V. This eliminated the third option, the Noctura NF-A4x20 PWM, as this fan requires 12V to operate nominally. The first two options mainly differ by size, in which also impacts the amount of airflow provided by the fan. The Noctura NF-A4x20 5V PWM fan will be utilized for cooling the main processor for the mine as this fan provides a 14.6% increase in airflow over the smaller NF-A4x10 [24]. It was concluded that while it is bigger and slightly more expensive, the tradeoffs were worth the extra cooling since this was

a critical component for camouflaging. This fan is also popularly used by developers all over the world for similar applications as the fan only requires 0.5W to operate; drawing 100mA and 5V max from the Jetson Nano. Incorporating this fan will greatly diminish the temperatures of the processor which in return reduces the chances of throttling the processing power as well as being detected by the target.

3.6.4 Target Luring

The majority of the strategies discussed thus far require the target to be within the blast radius of the mine or revolve around the mine not being detected by the sensors commonly used on autonomously navigated vehicles. A tactic that is generally hard to detect, hence its name, is luring. Various methods of luring the target to the mine were considered when researching systems to incorporate in the device. The UAVs primary goal is to navigate the obstacle course; with the secondary goal being to detect and avoid the mine. As previously mentioned in section 5.4.1, the use of producing acoustical signals to confuse the target into mistaking the mine for the acoustic waypoint on the obstacle course was prohibited. This resulted in the idea of incorporating a system within the mine to replicate one of the other obstacles on the course. If the UAV mistakes the luring system as one of the objectives on the obstacle course, the target will autonomously navigate towards the mine allowing the primary method for the attack to engage.

Figure 35: Defined Obstacles on the Targets Flight Path

Since there are three main obstacles on the course as shown above in Figure 35, the luring system would need to resemble one or more of these obstacles with the intent of the target mistaking the system for one of the objectives. The three main obstacles on the course are a hoop supported by a tripod, a pylon constructed out of a typical foam pool noodle, and the acoustical waypoint. With the acoustic waypoint not being a possibility of replication, the time was dedicated to developing a system to resemble the vertical pool noodle pylon or a hoop. The biggest challenge with this task came due to the size limitations of the mine. A typical hula hoop ranges in diameter of 40-44" which is far larger than the mines 18"x18"x18" size constraint specified by the customer. This meant that to lure the target using

a hoop imitation, the lure would either have to expand after deployment or the imitation would need to rely on the targets vision algorithm to not be able to correctly determine the scale of the decoy.

A couple solutions to make the imitation decoy expand to roughly 2.5 times the initial size after deployment were a spring-loaded mechanism similar to a sun shield used for the windshield of a car or the use of pressurized air to fill an obstacle-like reservoir. Both of these solutions were plausible but still difficult to design in a way that does not interfere with the main components of the mine that are required to make the primary launcher method function properly. Another idea for a solution is to use a loop of string spinning at a high rate of speed to form a circle, much like a lasso. While difficult to achieve, these ideas were not entirely disregarded and are anticipated for prototyping.

The other method for obstacle imitation is to simply incorporate a hoop like symbol on the faces of the mine. When the target is searching for an obstacle, it is sensing for a hoop or a pylon from an unknown distance. This means that from a further distance, the objects will appear smaller from the perspective of the vision sensor incorporated on the target. With a weak algorithm, the target will mistake the small symbol of a hoop for an actual hoop obstacle that is just placed at a further location. If this were to happen, the target would begin to travel towards the detected symbol of which would lead the target directly into the blast radius of the mine. Once the target enters the mine's blast radius, the primary disruption system takes over to fully disable the target.

3.6.5 **Multiple Mines**

The idea of incorporating more than one mine was heavily considered as this would increase the probability of disrupting and disabling the target significantly. Adding more mines strategically around the obstacle course would allow more than one chance at attempting to disable the target as the primary capturing system only allows for one shot. While the chances of disruption increase, so do the cost for components as more than one system needs to be purchased to allow each mine to sense, process, and attack the target. Various options were considered of which allowed multiple mines to be achieved to work simultaneously with one another with budgeting remaining a critical factor for determining which method would serve as the most practical solution.

Multiple Mines Operating Independently
The first theory explored was developing multiple mines that all functioned as separate entities. Incorporating multiple entities into the obstacle course would convert the single mine structure into a 'minefield', and would likely raise the probability of successfully completing the objective. Each of the multiple units would incorporate the developed object detection algorithms and attempt to disrupt the flight of the target. Originally, this approach seemed like an obvious strategy to implement, but when looking at the situation realistically it was apparent that this method of operation would actually be detrimental to team success.

The fact that the probability of capturing a target with multiple units would rise was obvious, but the sacrifices that would be made in terms of the time, money, and reliability of each unit made this approach unusable. Developing multiple mines of the same architecture would mean that the overall budget for prototyping as well as final design would need to be divided amongst repeated systems. This would result in the budget being stretched tightly as buying multiple controllers and the costs of fabrication would have added up rather quickly. Another drawback of this consideration was the fact that time is of the essence. There is a very limited amount of time specified from the customer to develop and test the design so adding multiple units needing to be fabricated and tested would have added much more stress overall for the team as a whole. If multiple mines that are poorly developed is all that can be delivered due to the lack of time provided, the overall result would be worse than dedicating the same time and efforts to perfect a single mine. Overall this approach, while ideal in a perfect world, quickly began to bear its weaknesses and was discarded for more realistic designs.

Multiple Mines Operating Cohesively
Once the conclusion was made that multiple mines operating independently were not a realistic solution, the concept then arose of using multiple disruption devices controlled by a single central 'master' unit. This would have aided the budget issue due to the heavy image processing algorithms only running on the master unit so that the central unit would be the only device required to have a powerful processor. The other units could have simply been driven by much cheaper hobbyists MCUs such as an Arduino and would receive a signal to fire when the target was in the capture zone as sensed by the central unit. Also, since the only operation of the secondary units were to fire, the parts necessary to function properly would be a chassis, an MCU for the actual launching process, and the launcher or another disruption device. Again, this seemed like a positive solution to increase the probability of a successful mission, but the negatives quickly began to outweigh the positives as the team delved deeper into design concepts.

A major flaw in this design is the lack of complexity contained within the secondary mines. When the secondary units would receive the trigger from the master unit, the reliability of capturing a target would be decreased significantly as there would be a fixed trajectory that the firing would happen. Secondary units that would fire straight up were discussed to further simplify the components needed within the systems, however, this presented issues as shooting a projectile directly upwards is typically the least beneficial angle of attack. In designing the singular mine, a mechanism that turns the mine in a turret-like motion is incorporated which greatly increases the angle of attacks possible and the likelihood of actually interacting with a target. All of this complexity would be lost in this secondary mine design and the probability of an induvial secondary unit disrupting the target would drop dramatically.

The second flaw in this design was again overshooting the given budget. The team is developing this design with limited funds in mind in which are very strict so any extra amount of materials, even if it is a cheap item such as an Arduino, will add up quickly. Having fewer funds available means having less opportunity to acquire components that might aid drastically in mission success. Due to these shortcomings a decision to stick with a singular mine design that was well optimized and fully capable of the task at hand.

Multiple 'Dummy' Mines
As mentioned previously when discussing camouflaging techniques to make the mine less detectable by the target, incorporating decoy obstacles within the design of the mines is a powerful tactic to disrupt the sensors and algorithms on the enemy target. A very affordable and simplistic way of incorporating decoy obstacles is to develop additional mines in which their only purpose serves to disrupt the sensors on the target. This idea ranges from having a mechanical system in which the mine expands to replicate an obstacle with the goal of distracting the target from the real objectives to make the UAV travel off course to attempting to lure the target towards the mine. Since minimal to no electronics are needed for these dummy mines, the design would be very simple to incorporate while also being relatively cheap. If the target is searching to detect and avoid the mine, developing fake mines that look similar to the real mine can distract the target in which would reduce the chances of the target sensing the primary mine. Dummy mines could also be used to attract the target to the primary mine. If the target incorporates an avoidance algorithm to detect and divert away from the mine, making visually bold mines could be strategically placed in a funnel-like fashion to lead the target directly towards the blast radius for the primary mine to engage. While dummy mines may not be the most technical approach to disrupt the target, it is the cheapest and easiest tactic listed thus far.

3.7   Mine Movement

Due to the fact that the DOMINANCE mine will function using a turret-like motion, it is imperative that this motion is easily controllable and quite precise. There are multiple types of technologies to imbue motion in a system, but the two most common involve the use of servo and stepper motors.

Servo Motors
The first type of technology commonly used to supply motion to a system is a servo motor. A servo motor is a rotary actuator that is used to achieve precise control of angular position, acceleration, and velocity. These motors are always part of a closed-loop system which includes the motor itself, an encoder that is able to send feedback to a controller, and a driver (amplifier) that allows the motor to be driven efficiently. This closed-loop makes the motor very precise, but also adds to the complexity of components and the control involved.

Another fact to note when it comes to servo motors is the torque to rpm (rotations per minute) curve. This curve for a normal servo motor models a horizontal line, which means that torque is approximately constant across increasing rpm. This implies that servo motors excel in high speed applications. This is not only due to the torque to rpm curve, but is generated by the low number of poles and feedback system that allows for the driving of the motor in this consistent torque fashion.

Stepper Motors
The second most commonly used device to create precise motion is a stepper motor. These motor functions quite differently than servo motors, and this is due to the fact that they contain many poles, almost always more than 50. Motion is controlled by the systematic energizing of the poles which push the stator and therefore pushes the motor's output shaft. Each of these poles is positioned in an evenly distributed manner, which means each step corresponds to an approximate change in angular position. Each stepper motor has a documented number of steps, and the angle in which each step will move the motor is easily found by dividing 360 by the number of steps. Also, because the motor is controlled by the energizing of these poles, stepper motors do not require the feedback loop that a servo motor would and function as an open-loop system. This cuts down on the complexity of utilizing this type of motor in a system drastically.

Stepper motors are still very accurate, but as the rpm of the motor is pushed higher steps might begin to be skipped, meaning that the end location might not be what the user had expected. That is not the only issue with these motors, though, as problems begin to arise when the torque to rpm graph is examined. Stepper motors have a very high stationary and low-velocity torque. As the rpm begins to increase, however, the amount of torque the motor is able to supply begins to decrease. This can be problematic for certain applications, and most definitely means that stepper motors do not represent a reliable source of motion in high-speed applications.
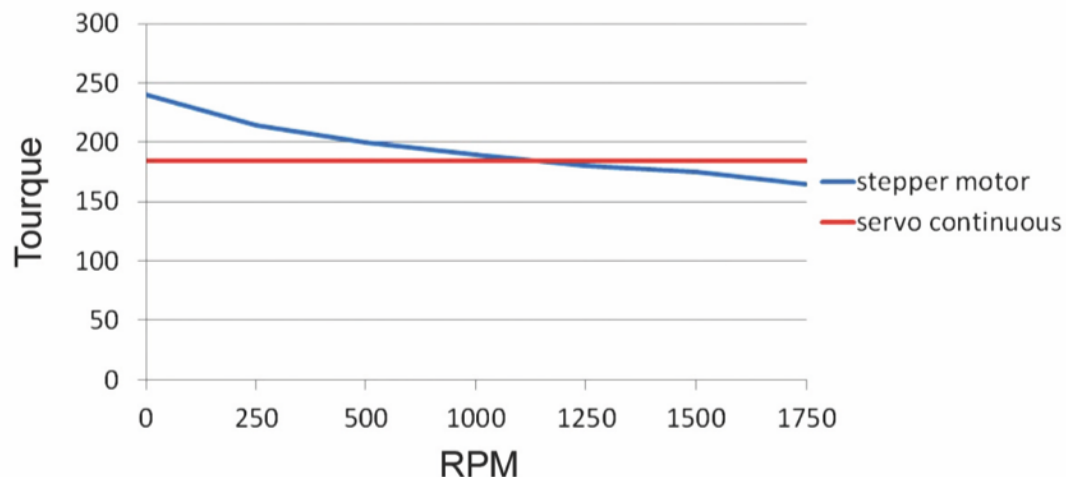
Figure 36: Torque of Stepper Motor vs. Servo Motor

Conclusion

In this application, because the velocity of movement does not need to approach high speeds, it is believed that the stepper motor would be the best solution. Figure 36 provides the torque an rpm comparison on the stepper motor and servo motor. This will still supply high torque at the speed in which it is operated, while also allowing the system to utilize an open-loop system that eliminates the need for extraneous feedback circuitry and components. The precision of this type of motor will also allow accurate targeting of a target once it is located via the object detection algorithms.

3.8   Communication

The DOMINANCE mine must be fully autonomous when disrupting the drones on the obstacle course, but metadata must be captured and sent to a local laptop. In order to send the data, a communication modulator will be used. This section will analyze Bluetooth communication and WIFI communication.

3.8.1 Bluetooth Module

Bluetooth technology is a high-speed low powered wireless technology link that is designed to connect two devices together. IEEE (802.15.1) specifies for the use of low power radio communications to link phones, computers and other network devices over short distances without a wired connection. Bluetooth covers a wireless signal transmission over short distances, typically up to 30 feet. Bluetooth communicates on the 2.45 GHz frequency and can support up to 721 KBps along with three voice channels. This frequency band is set aside by international agreement for the use of industrial, scientific devices. It is an unlicensed ISM frequency band Bluetooth can connect up to "eight devices" simultaneously and each device has a unique 48-bit address from the IEEE 802 standard with the connections being made a point to point or multipoint. This is usually presented in the form of a 12-digit hexadecimal value. The first 24-bits (most-significant half) of the address is an organization unique identifier (OUI), which is used to identify the manufacturer. The lower 24-bits is a unique part of the address.

The Bluetooth Network is a Personal Area Network that contains a minimum of 2 to a maximum of 8 devices. It is typically a single master and up to 7 slaves. The master is the device that initiates communication with other devices. The master device is in charge of governing the communication link and traffic between the slave devices connected and itself. The slave device is the device that responds to the master device. They are required to synchronize their transmission/receiving time with the master. The frequency hopping sequence is defined by the Bluetooth device address (BD_ADDR) of the master device. The master device sends a radio signal, first, asking for a response from the specific slave devices that it is trying to connect to within the range of addresses. The slave device responds by sending a response and synchronizes its hop frequency as well as the clock with the master device [25].

Connection Process

Creating a Bluetooth Connection between two devices is a multi-step process involving three progressive states. Figure 37 diagrams the Bluetooth procedure. Listed below are the typical steps for this process [26]:

1. **Inquiry:** If two Bluetooth devices don't know anything about each other, one device must run an inquiry to try and discover the other device. One device sends out the inquiry request, and any other device listening will respond with its address.

2. **Paging (Connecting)**: After inquiry, the two Bluetooth devices must connect with each other. Both devices must know the address of the other device.

3. **Connection:** These are the four different statuses that the devices can be in after paging.

   a. Active Mode: This is when the device is actively transmitting or receiving data, aka the regular connected mode.
   b. Sniff Mode: This is the power saving mode, where the device is less active. It will only listen to transmissions at a set interval while sleeping.
   c. Hold Mode: This is a temporary power-saving mode. The master can command a slave device to hold. The device will sleep for a defined period. Once the period has passed the device will return back to active mode.
   d. Park Mode: This mode sets a slave device to sleep until the master wakes it back up.
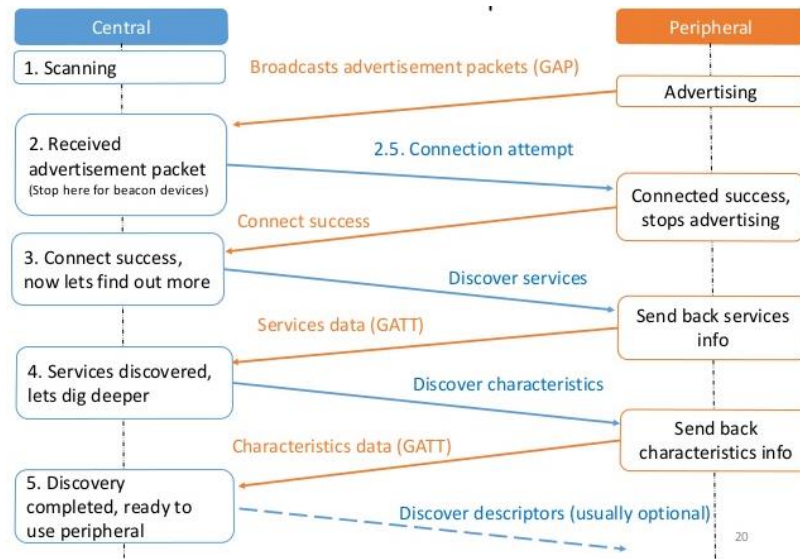
Figure 37: Bluetooth Connection Procedure (Pending Approval)

3.8.2 Wi-Fi Module

Wi-Fi, short for "wireless fidelity" and technically known as IEEE 802.11, is a wireless network communication similar to Bluetooth. It uses radio transmission that is built on a set of standards that allow high speed and secure communications between a wide variety of digital devices. It allows Wi-Fi-capable devices to access the internet without being wired. Wi-Fi can operate over short and long distances, typically ranging from 150 feet (indoors) to 300 feet (outdoors). Wi-Fi devices typically communicate on a frequency band of 2.4 GHz or 5 GHz. Wi-Fi devices have the ability to be secured or open and free.

Wi-Fi is used to connect a router or internet access point to another device in a wireless manner. The wireless network works as two-way traffic. The data received from the internet will also pass through the router. Once it passes through it is coded into a radio signal that can be received by the wireless adapter. Wi-Fi connection uses a low-power radio that transmits and receives. It also provides access to a local network on connected devices. This is known as a Wireless Local Area Network (WLAN). Wi-Fi-capable devices within a network's range can detect the network and attempt to connect to it. Ethernet (IEEE 802.3) is an international standard that governs the network setup [27].

Connection Process

Wi-Fi connection established between multiple devices requires a specific protocol. Figure 38 outlines the Wi-Fi connection procedure. Listed below is a description of each step [28]:

1. <u>Beacons</u>: A beacon frame is sent periodically from an access point announcing its presence and relaying information required to connect to the wireless network.
2. <u>Probe Request</u>: Probe requests are sent from a station to discover other networks within a range. Probe requests are sending the station data rate and 802.11 capabilities.
3. <u>Probe Response</u>: A probe response is sent when the access point receiving a probe request has at least a common supported data rate with the station. The probe responses by sending the service set identifier (SSID), supported data rate, encryption type, and other capabilities of the access point.
4. <u>Authentication Request</u>: The station makes a choice on SSID/network from the probe response it receives. It checks the compatibility of encryption types. Once the network determines compatibility, the station will attempt a low level 802.11 authentication with the compatible access point. The low-level authentication is sent to the access point. This sets the authentication to open and the sequence to 0x0001.
5. <u>Authentication Response:</u> The access point receives the authentication frames and the authentication frameset to open indicating a sequence. If an access point receives an authentication frame that is different it will respond with a de-authentication frame. This will leave the station into an unauthenticated and unassociated state.
6. <u>Association Request</u>: The association request contains chosen encryption types and other compatible 802.11 capabilities.
7. Association Response: If the association request matches the capabilities of the access point, it will create an association ID. It will then respond with a success message allowing network access to the station.
8. <u>Data:</u> After the connection is established with successful authentication and association, it is ready for the transfer of data.
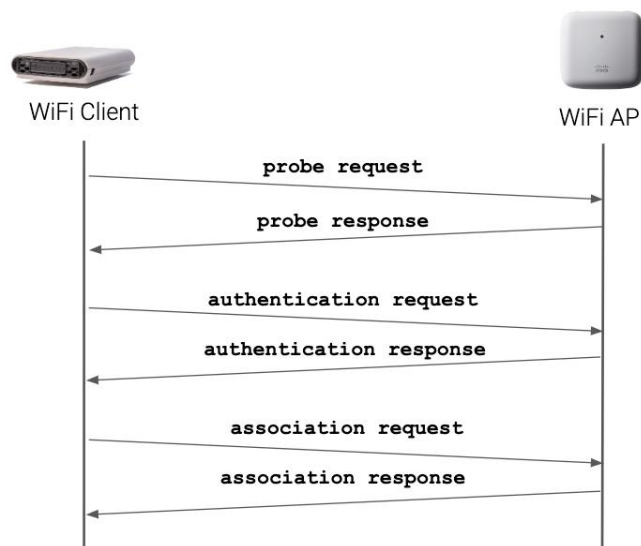
Figure 38: Wi-Fi Connection Diagram (Pending Approval)

3.8.3 **Which Communication to Use?**

This section analysis which form of communication works best in each criterion: range, bandwidth, cost, security, power efficiency, and design effort. A conclusion on which form of communication will be made.

Range

Wi-Fi technology was built to replace Ethernet technology in local area networks. It offers a superior range compared to Bluetooth. Wi-Fi can typically access over 100 meters. Bluetooth is intended to exchanged data over short distances, usually between personal devices. Since the obstacle course is an open room 30 feet x 40 feet (9.144 meters x 12.192) it is not necessary to use Wi-Fi technology. Bluetooth has the capability to connect within the room [29].

Bandwidth

Wi-Fi technology was built with the expectation to deliver connectivity at multi-gigabit speeds. This makes it ideal if you are passing large amounts of data (like video). Wi-Fi is also a great choice for a multiple-user environment. Wi-Fi typically has a bitrate of 250 Mpbs. Bluetooth was designed to be simple, to connect two devices with minimal power consumption. This, however, makes Bluetooth much slower and offers less bandwidth than Wi-Fi. Bluetooth is better suited for audio applications rather than the massive bandwidth of streaming video. Bluetooth typically has a bitrate of 3 Mpbs. The goal is to search for a form of communication that can pass metadata (confidence, range to target, time of arrival) and live video feedback to home base (a laptop). Wi-Fi communication is an ideal network for live video feed [29].

Cost

The cost of Wi-Fi and Bluetooth modulators are very similar. The typical price of both modulators can range for 5 dollars to 20 dollars depending on the specific requirement. These criteria is a tie since both modules are similar in price. The other key features will continue to play a large role in deciding with the communication network to use in the design. [29].

Security

Wi-Fi can accommodate a wide range of security of protocols. Security protocols are inherent to the 802.11 standard. Wi-Fi also has network-based encryption techniques (virtual private networks, VPN). In order to gain a security protocol to Bluetooth, specific protocols must be implemented in order for devices to establish a secure connection. This may include the user acknowledgment of connecting devices (pairing procedure). It is not necessary to have a secure network between the mine and the land station. Bluetooth would be a better option since there is not a need to establish a secure connection [29].

Power Efficiency

Wi-Fi can be very power consuming. This can be a big issue for mobile applications. It was originally built to connect office devices, which are not battery operated. Bluetooth was developed with low-power consumption in mind. This allows Bluetooth devices to have a much longer battery life. This can typically be 10 to 100 times longer than similar devices that use Wi-Fi. Bluetooth would definitely be better for the mine if power consumption was considered in thee design. Since the design is not battery operated, both options can be considered [29].

Design Effort
Wi-Fi has traditionally been complex and required significant efforts to set up, both hardware and firmware development. With the advance in technology and an increase focus on IoT devices. Wi-Fi technology has evolved to be easier to set up and at a lower cost. From a purely hardware perspective, Bluetooth is not as complex as Wi-Fi. The firmware communication stack, however, requires more knowledge of the Bluetooth stack to setup. Since Bluetooth is fairly simple to use and switch between devices Bluetooth is a more viable option that Wi-Fi from a design standpoint [29].

Standard	BLE	Wi-Fi
IEEE Specs	802.15.1	802.11 b/g/n
Frequency Spectrum	2.4 GHz	2.5 GHz, 5 GHz
Topology	Star, point to point	Start, point to point
Network Size	Not defined	32
Data Rate (Mbsps)	2	11/54/600
System Resources	TBD	1 MB+
Range(m)	< 50	< 100
Number of Channels	40	11-14 (3 orthogonal)
Security	128-AES	SSID
Relative Power Consumption	Low	High
Latency	200 ms	150 ms
Modulation Techniques	Gaussian Frequency Shift Keying (GFSK)	Orthogonal Frequency Division Multiplexing (OFDM) and Quadrature Amplitude Modulation (QAM)

Table 11: BLE and Wi-Fi Comparison [30].

Conclusion

In conclusion, Bluetooth and Wi-Fi technology are very similar forms of network communications. In order to help streamline the decision. Table 11 evaluates the pros and cons of each form of communication.

Both the Bluetooth and Wi-Fi network can connect can use the frequency band of 2.4 GHz. They both have relatively similar latency times, and both use point-to-point topology. The cost is very similar depending on what requirements. Since these key points are similar in both networks. They will not play a role in design decision making. Bluetooth network has considerably low power consumption. It is relatively easy to set up between two devices and allows a large number of channels. The key takeaway from Bluetooth technology is lower power consumption. This, however, will not play a major role in this design due to the ability to have the DOMINANCE mine powered by the wall outlet. Wi-Fi network has a better data rate than Bluetooth technology. This will allow for the processing of live video feed. Wi-Fi technology also has a larger connectivity range. This will allow us to deploy the mine at further ranges from the test station. Other key takeaways are security protocols. The security protocol is more flexible and allows for various security methods. Since power is not an issue, large power consumption is not a large factor. To summarize, the data rate will be very beneficial when trying to connect live video feed from the camera to the test station.

With the key points determine, Wi-Fi technology was used. This is primarily due to the ease of design. The ability to setup the Wi-Fi module with the NVIDA Jetson Nano with ease was a major factor. A major plus side is the capability of having a larger bandwidth between devices. This will allow a more stable live video feed between devices. Wi-Fi also has the capability to connect multiple mines at once. This can be beneficial when developing multiple mines [31].

3.9   Router vs Switch vs Hub

The goal is to connect the land station (computer) and DOMINANCE mine on a local area network. The mine will send live video feed as well as metadata back to the land station. The Lockheed Martin Test Facility will not provide any internet connection, so figuring out how to pass data packets back and forth without an internet connection is necessary.

Router

A router is a hardware device that is designed to pass information between two or more packet-switched computer networks. The intended purpose of a router is to connect multiple networks together. It can receive, analyze, and move incoming packets to another network. Routers can direct traffic on the Internet by performing various functions. A router connects two or more data lines using internet protocols (IP) addresses. IP address are unique ad come in either IPv4 or IPv6. A data packet is sent from the internet and the router reads the network address information from the packet header and determines the destination. The router has

information where the packet should go. This is called the routing table. This table lists the ideal routes between two network devices on the interconnected network. A router organizes its network on two separate planes, control plane and forward plane. The control plane contains the routing table, like previous mentioned, contains a list of ideal routes that a data packet should be forwarded. It has internal preconfigured directives called static routes. Depending on the routing protocol, routes can be learned. This is called dynamic routing. The forward plane simply forwards the packet with the given information. [32]

Switch
A switch is a hardware device that connects devices on a network. The switch is designed to use packet switch, to receive incoming data, and then forward that data to a specific destination. Switches forward data to the specific data, unlike the network hub. Multiple data lines (typically ethernet cables) are plugged into a switch. This allows network communication between multiple devices. The network switch has the ability to organize the flow of data. The switch manages who to send the data packet to. It identifies the network address for each packet glowing through and determines the correct destination. Each device that is connected to the port can communicate with each other at any time without transmission interference [32].

Hub
A hub is a hardware device that connects multiple Ethernet devices together. The connected devices become one network segment. A network hub is the most basic networking device and has largely been replaced by the network switch. A hub has no routing table; therefore, it does not know where to send incoming data packets. A hub will broadcast data to all the network devices connected to the hub. This causes security risks and bottlenecking [32].

Conclusion
With an analysis done on three network devices, router, switch, and hub. We came to the conclusion that a router would be the best option. A router has the ability to connect multiple networks if we want to, and it has the ability to act as a switch. Since we are still determining how we want to set up the LAN, it is best to have hardware that allows options. The easiest method is to use an Ethernet cable and connect the mine and land station together, using the router as a switch. The second method is to set up a personal LAN and have the router send data packets between the two devices, wirelessly.

3.10 **Printed Circuit Board (PCB) Fabrication**

One of the main objectives of the project is to incorporate a custom printed circuit board (PCB) within the design. PCBs are common within the majority of modern electronics due to reliability, small size, and mass production ability. A PCB is a board that is composed of layers of conductive and insulating materials that allow a point of contact to external components to be easily connected to one another

via internal circuitry within the board. Figure 39 provides a figure of a 2-layer PCB with the thickness indicated in a table to the right. Having connections between the components being within these layers adds protection to the circuitry, reduces the footprint of the device due to less wired connections being needed, as well as creates a component that appears professional and sturdy. PCBs are manufactured as a tool utilized for mass produced components to ensure consistency, simplicity, and unique compatibility. As technology advances, PCBs are becoming widely available for consumers to produce themselves via electronic modeling software and PCB manufacturing websites. This is the method that will be used to accomplish the task of designing and producing a custom PCB to fit the need for the given project task.

Layer Stack For 2-Layer, 1.6mm PCB

Layer	Thickness (mm)
Top Solder Mask	0.01
Top Later Copper	0.07
Substrate	1.50
Bottom Layer Copper	0.07
Bottom Solder Mask	0.01

Figure 39: A 2-Layer Printed Circuit Board.

Single layer printed circuit boards are commonly used within simple electronic devices as they are easy to understand since all the connections, known as traces, are externally visible through the solder mask. Multi-layer PCBs contain two or more layers of a conductive material, typically copper due to its extremely high conductivity, separated by a dielectric material for insulating these copper layers from one another [33]. The substrate contains this dielectric material as well as a core that has the sole purpose of adding rigidity to the board. A protective layer known as a solder mask is applied on top of the conductive metal layer to prevent common electrical problems such as short-circuiting, corrosion, and oxidation. Soldermask is what gives the circuit board its unique color and depending on where the board is purchased, the colors can vary from red to blue, with green being the most commonly recognized. The solder mask is applied directly over the traces only leaving the connection points for the components exposed. These connection points can be exposed on the flat surface of the PCB as well as through a drilled hole that goes completely through the circuit board to allow components to be easily and sturdily mounted to the board via solder. The top layer of the circuit board also contains a thin silk screen. The silkscreen is more used as a tool for the user rather than a crucial component to manufacture PCBs as its sole purpose is to display numbers or letters on the board to annotate what components are supposed to be placed on the board as well as their locations. All of these layers work together to form a printed circuit board and can be layered tens of times to fabricate multilayer PCBs [34]. For the application needed for this project, a two-layer PCB will be utilized as this will simplify the design process to ensure the time

provided before the final delivery to the customer is not at risk of being unachievable.

3.10.1   Supply Power Solutions

To begin designing a custom printed circuit board, all of the features needing to be incorporated on the board must be defined. For the design being used for the DOMINANCE Mine, it is well known that power distribution is going to be needed to provide reliable power to each electrical component utilized on the mine. This is going to serve as the main purpose of the PCB. Choosing the method of wall power discussed previously in section 3.2 over a battery solution limits the portability of the mine, however, it saves money within the budget while also adding flexibility for the components used to make the mine operate with minimal power constraints. The PCB system will incorporate all of the hardware necessary to accept incoming power from a standard wall US outlet at 120V AC and step down, convert, and distribute this reduced DC power to allow the device to function properly.

Creating Usable Power via Transformer
A transformer is a component used to increase or decrease AC signals using magnetic flux and electromotive forces which is all part of Faraday's Law. For this application, a transformer is used to reduce the power from the wall down to a voltage that can be regulated using IC voltage regulators. The amount in which the input is reduced by the transformer is dependent on the specifications for the chosen component. For this design, a transformer to reduce the 120V AC wall power to 12V AC power will be utilized. While this power is closer to the output desired, it is still in the form of alternating current which produces a sinusoidal signal. AC power is typically only used for motors as well as incandescent light bulbs however this AC signal can be converted into a steady DC signal with the use of diodes.
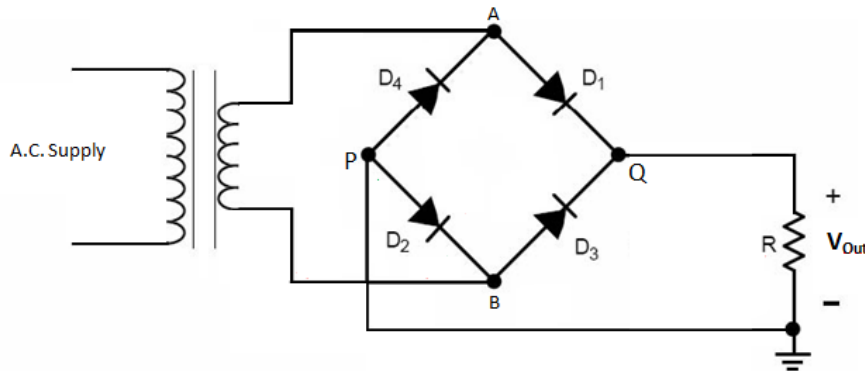
Figure 40: Full Bridge Rectifier Circuit.

Diodes are used to convert or rectify, AC power into DC power by controlling the flow of current throughout the circuit. By adding a diode to the positive and negative

leads of the AC source, when the sinusoidal signal is greater than zero volts, the output follows the input signal, however, when the input waveform is less than zero volts, the diode restricts current from flowing, resulting in an output of zero volts. This is known as half-wave rectification since only half of the input signal is passed through to the output. If two more diodes are introduced to the circuit, a full-wave rectifier can be designed. A full-wave rectifier works by allowing current to flow from the positive lead from the input source through the diodes when the input is greater than zero volts; sending this input signal to the positive lead out of the rectifier. When the input voltage is less than zero, the current flows from the negative lead from the input source through the diodes to and out to the positive leads of the output of the rectifier. This inverts all of the negative areas of the input signal to produce a positive waveform. The input before rectification, during rectification, and after full wave rectification can be seen in Figure 41 below. This output is still AC, however how it remains positive instead of varying from positive to negative. To help achieve a more stable output waveform from the circuit, a capacitor is added in parallel with the load resistor R in Figure 40. A capacitor is an electrical component that charges up and stores energy in which can be discharged very quickly if needed. Adding a capacitor into the circuit introduces time into the equation as the amount of energy stored within a capacitor is not constant and varies with time. The capacitor and resistor work together to control how fast the capacitor charges and discharges. Using a capacitor within the circuit, the output from the rectifier begins to become steady; making the conversion from AC to DC voltage become noticeable when measured at the output.
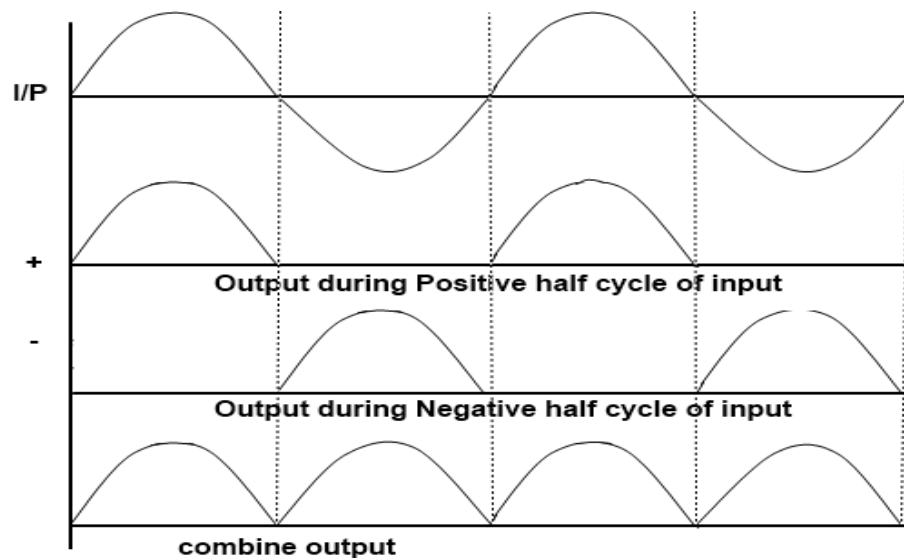
Figure 41: Outputs After Full-Wave Rectification

The capacitor is added to the circuit to smooth out the changes in voltage seen in the combined output in Figure 41 above. When the output voltage increases up to its maximum value, the capacitor begins to charge until eventually storing the peak output from the input. Once the output voltage begins to decrease, this capacitor retains the charge and rather slowly discharges until the output begins to increase

again; meeting the capacitor voltage along the way. This quickly recharges the capacitor and this process repeats over time until the input supply is turned off; making the capacitor discharge fully. From the perspective of the output voltage across the resistor, this voltage appears more stable as the output pulses from the rectifier keep the capacitor charged. Increasing this capacitance or the resistance changes the RC time constant, in which in return reduces this change in voltage from when the output peaks to where the capacitor begins to recharge. This is known as the ripple voltage. If the load resistance used is too small, the output voltage begins to decrease as well as the ripple voltage becomes high. Finding optimal values for the resistance and the capacitance as well as relying on a full-wave rectifier over a half-wave rectifier is crucial when building an efficient AC to DC converter.

While incorporating the rectification within the PCB would be possible, there is a much simpler solution as this method would involve adding many more components within the circuit and further complicate the designing process. Also, since many of the components only require 5-12V to operate, stepping down the 120VAC wall power can be a dangerous process if done incorrectly.

Using an External Power Supply
Another method for power delivery for the mine is achieved using an external power supply. With this, power delivery can be achieved very easily using a standard wall power supply module that can be purchased for relatively cheap; in which performs all of the voltage regulation and stepping-down the 120VAC power into a more usable signal. This method also allows the PCB to be smaller since all the AC to DC transformation takes place externally which in return reduces cost and fabrication time when soldering the components to the board.

There are many considerations to make when choosing a power supply as there are countless variations to provide different voltages and current combinations dependent on the amount of power that is needed within the system. To determine the power supply needed to power the entire mine system, all of the operating currents and voltages are used to calculate the power dissipated by each component. Power consumption is calculated by multiplying the current drawn by the component by the voltage needed to be supplied in order for the component to operate, or *P=IV*. All of this data can be found for each component on their respected datasheets along with many other useful parameters that are considered when designing circuits. Once all of the power requirements for the individual components are determined, they are summed together to calculate the total power draw from the system; allowing a proper power supply to be chosen.

Conclusion
To simplify the design process and reduce the number of components required on the PCB, an external power supply will be utilized to power the mine. This power supply will use the 120VAC 60Hz wall power and convert this to a DC voltage with a known current draw limit. This eliminates the need for incorporating more

components for rectifying and converting the incoming signal from the wall onto the PCB, allowing cheaper manufacturing as well all easier component implementation on the finished board. Also, by using an external supply, this greatly improves the safety of the team as wall power can cause serious harm if not controlled properly or a design error occurs during testing of the PCB prototype.

3.10.2 **Power Distribution**

Using the now converted and regulated power from the wall to drive the mines systems requires many sources of individual power internally. As these individual components require different operating voltages and currents, proper means of power distribution need to be considered. Given that the power from the wall is now DC voltage, DC to DC converters are needed to step down this higher voltage into a more usable source for each controller through the means of voltage regulators.

There are two main types of voltage regulators: Linear Voltage Regulators and Switching Voltage Regulators. Both voltage regulators can accept various ranges of inputs and be able to regulate them as a steady DC output. Linear regulators are used in low power applications where the input is not dramatically larger than the desired output. These regulators are easy to find as they are very common, however there is a downfall to this type of regulator as the stepping down of voltage is dissipated via heat. Switching regulators tend to be much more efficient as they do as the name suggests and toggle on and off at a very high rate. This increases the efficiency significantly as there is very little to no power dissipated during regulation as the component is either fully conducting or off entirely. While the switching regulator may sound like an obvious choice for voltage regulation, with this comes noise which can distort the DC signal.

This is a crucial component as it allows larger voltage from the power supply to be divided to provide multiple stable outputs to power the microcontrollers, motors, cameras, and solenoid all without worrying about an unstable input frying an expensive component. Typical voltage regulators range between 15V to 3.3V outputs as these are the most common voltages needed for powering majority of hobbyist hardware. The LM7805 is one of the most widely used regulators for hobbyist and students as it is very simple to use as well as very cheap to purchase. The PCB will have various embedded voltage regulators to provide stable power to the on-board IC as well as the external Jetson Nano and other peripherals via GPIO pins.

The Jetson Nano Developer Kit has three methods of power input: micro USB, GPIO Pins, and a barrel jack for use of a power supply. All three methods can safely deliver the power needed for the Nano to function properly however each method has its tradeoffs. The micro USB input to the Jetson Nano supplies 5V at 2A of power to the board. This is enough for most computation however to fully maximize the processing potential, the Jetson Nano can be pushed to 5V at 4A to allow higher clock speeds and even overclocking without being underpowered.

This can be achieved using the barrel jack or the GPIO pins on the developer board. Since an external power supply is already being used to power the PCB, rather than using another external supply for the Jetson Nano the PCB will have an output power hub dedicated for driving the Jetson Nano. This hub will supply the Nano with 5 volts at 4A to allow the Nano to operate to its full potential without starving the processor of power.

3.10.3   **PCB Schematic Design and Fabrication Software**

After designing a schematic of what components should be incorporated on the PCB, the design in implemented within the chosen software to virtually develop the schematic for production. Simulation software will be utilized to test virtual circuits for prototyping before modeling a PCB and submitting an order online. National Instruments Multisim live is a powerful and widely popular simulation software that majority of electrical engineering students are familiar with as it is commonly used in circuit development labs. Another widely used circuit simulation software is LT Spice, of which is also free. LT Spice is a very powerful software as it is fairly simple to find majority of the components available for purchase correctly modeled online and available for download to be used for modeling. This simplifies the simulating process dramatically as all of the components have the proper parameters already input for each component rather than having to custom model each one that will be implemented in the design. Once the general circuit has been designed and tested, the design is drafted using Electronic Design Automation (EDA) software [35].

PCB Design Software
There are many readily available tools to design printed circuit boards. Software such as PROTEL, EAGLE, ORcad, DesignSpark PCB, Kicad, and many others are available for download online; most requiring a license or subscription to be purchased before use. This software allows for schematic development, PCB design, 3D modeling of PCBs, as well the ability to export projects to send to PCB manufacturers to turn the concept into a physical component. A similar approach will be used for the software as well; taking advantage of free design software to virtually fabricate the PCB design before being manufactured. A few of the more popular PCB drafting softwares are compared in Table 12 below based on their cost as well as constraints.

PCB Drafting Software	Constraints	Maximum Layers	Cost
Eagle Standard	160cm^2	Unlimited	$100/yr
DipTrace Standard	1000 Pins/4 Signal Layers	Unlimited	$395.00
ORCAD Lite	100 Pins/2 Signal Layers	Unlimited	$0.00
Eagle Free	80cm^2	16	$0.00
DipTrace Lite	500 Pins/2 Signal Layers	Unlimited	$0.00

Table 12: Comparison of PCB Drafting Softwares.

Autodesk Eagle Free will be used to design the schematic as well as the PCB. This selection is primarily due to cost and the available resources for learning how to draft and design via this software. Although this software is limited for the free version, none of the constraints will impact the outcome of the final PCB due to its simplicity and fairly small size. The software turns the designing process into three easy steps: designing the schematic, organizing the components on a virtual PCB board, and routing the traces to have a final design that is functional and professional. While limited, Eagle Free is a very advanced and powerful software containing all of the components needing to be incorporated within the design already pre-modeled or available for download to allow the schematic as well as the final Gerber files to be created smoothly and efficiently.

PCB Prototype Manufacturers
Similar to the design software, there are an abundance of online PCB manufacturers to select from to fabricate the board based off of the design submitted through the ordering process. Many of these manufacturers offer samples for free or at a very low cost for the first few prototypes. PCBs tend to be cheaper when purchased in bulk which can be a nuisance when only needing one board for a design. Therefore, to keep cost at a minimum, one of these websites that allow for free or cheap sample boards at a lower quantity will be utilized for ordering the custom PCB boards for prototyping, testing, and the finalized product.

*Pricing is for 150x150mm, 2 Layer, 5qty.	**ALLPCB**	**PCBWay**	**NextPCB**
Cost Per Unit	$4.20	$10.40	$5.68
Shipping Cost	$4.00	$28.00	$27.00
Total Cost	$25.00	$70.00	$55.40
Build Time	24Hr	24Hr	24-48Hr
Fastest Shipping Time	1-2 Days	3-5 Days	2-3 Days

Table 13: Comparison of PCB Manufacturers.

From Table 13, the cost analysis, fabrication times, and shipping times of three major online PCB manufacturers were compared with one another. Each quote is based upon a 2-layer PCB with a minimum order of 5 units and dimensions being 150mm x 150mm. From this table, it can be seen that ALLPCB is far cheaper and has a quicker turn-around time from order to final product delivery. For this reason, ALLPCB will be used for all iterations of the PCB including prototyping as well as the final board used within the completed mine.

3.10.4   PCB Constraints

When designing a PCB, there are various parameters to take into consideration that affect the performance, reliability, and complexity of the board as well as the overall manufacturing cost. To ensure that the PCB performs optimally and guarantees longevity, constraints such as the copper thickness and width used in the traces, partitioning the differing components, decoupling the power used within the circuit, and grounding must be strategically designed.

Trace Constraints
As previously mentions, a trace is what connects the components on a PCB, basically serving the same purpose as a wire for most electrical components. The major difference comes with size limitations. Traces are typically made up of copper as copper is highly conductive. The sectional area of the trace can limit things such as the PCB size as well as the amount of current that can flow through it. As current flows through the traces on the board, heat is dissipated from these traces due to the resistance of the foil. This heat can cause damage to the board as well as nearby components if the trace dimensions are not designed properly. The thickness of the copper layers is measured by weight, typically 1oz of copper per square foot. This is the thickness that will be utilized in the PCB design for the mine as this is cheap and should be more than adequate for the design. With this chosen thickness, the other main concern comes with the width of the traces [36].

The width of the trace will determine how much current can flow without causing damage to the board. To calculate the width needed, IPC-2221 standards are used along with the temperature change, amount of current needed to flow, and the thickness and resistivity of the copper foil. First, the area is calculated by:

$$Area = \frac{Current}{(0.024 * (TempRise)^{0.44})^{1/0.725}}$$

This area is then used to calculate the width of the trace by plugging it into the equation:

$$Width = \frac{Area}{Thickness * 1.378}$$

Using these equations, the trace width needed to deliver a certain amount of current can be determined.

Changing the width of the trace also changes the resistance created within the trace; dissipating more or less power in the form of heat. If the trace is too narrow,

the current will have more resistance to flow against and create too much heat which can result in burning out components or the PCB as a whole. Space on the PCB is a big determining factor of how wide the traces can be; however, these trace widths cannot be neglected when designing precise PCB circuits.

Partitioning
Partitioning, or separating, traces and components that deal with analog and digital signals is a very important design aspect when dealing with PCBs. If digital traces become too close to analog traces, interference can occur on the analog signals due to electro-magnetic compatibility (EMC). Two fundamental principles of EMC are: 1. The circuit loop area should be minimized and 2. Only a single grounding plane can be applied in a system. Grouping similar signals in different areas of the board along with keeping traces as short as possible helps to reduce electromagnetic radiation from one trace to the next. Since the PCB on the mine will contain analog and digital traces, keeping the voltage regulation and distribution on one side of the PCB and the analog signals from the GPIO rail to the controller onboard on the opposite side is crucial [37].

3.11 Technology Comparison

This section provides various parts for the specific application we want to apply to the DOMINANCE mine. We will do a full comparison for each part as well as weigh out the pros and cons of why the component would and would not be implemented in the design. This section will be later referenced in 3.12 in order to make a final decision on which part we want to use.

3.11.1   Image Processor Comparison

Due to this fact, we knew that we would not be able to use a basic hobbyist MCU such an ATMEL ATMega328 or Texas Instruments MSP430G2x53 but would have to investigate identifying a more powerful system; most likely a small-scale computer that is more than capable of these calculations. Coming to this realization we began to investigate possibilities for this component and weigh the pros and cons of each.

NVIDIA Jetson Nano Developer Kit
The Jetson Nano is a very realistic option for the "brains" of the system as it was built with support for computer vision and deep learning algorithms in mind. This board is very powerful, featuring a 128-core Maxwell GPU and a quad-core ARM A57 CPU with 4GB of LPDDR4 RAM. This, in combination with its 472 GFLOPS of GPU processing power, means that it should easily be able to handle multiple camera inputs and the data manipulation associated with image processing algorithms that will be used to locate and track a drone in space. The power input is also very low at 5VDC, so the power consumption from this chip should present no apparent issues [38]. Figure 42 shows an image of the Jetson Nano Developer Kit.

Figure 42: Jetson Nano Developer Kit w/ Jetson Nano Computing Module

One drawback of the Jetson Nano is that it has been released very recently. This means that there is not much information readily available on the internet and not many projects have been completed using this hardware yet. This is not a deal-breaker whatsoever but will propose a challenge in that all of the implementations must be developed from the ground up.

Raspberry Pi 4 w/ Intel Neural Compute Stick
In contrast to the brand-new Jetson Nano, the Raspberry Pi has been in the hobbyist market for many years and the hardware has experienced multiple iterations to this point. The most common firmware, Raspbian, is well documented and has been used in many projects, so multiple examples related to the application are most located online. This board is powered by a low 5VDC input and is capable of drawing slightly more power than the Nano, up to 15W. It features a 1.5GHz quad-core ARM CPU as well and also utilizes high-speed LPDDR4 RAM. These specs are comparable to the Nano, but the downside becomes apparent in the lackluster capabilities of the GPU [39]. Because of this, it would be most beneficial to pair this development board with an Intel Neural Compute Stick, a USB-bound VPU (Vision Processing Unit) capable of handling the heavy math-related computations associated with image processing and neural networks [40]. This would drive up the price, though, to being nearly equivalent or slightly greater than the Jetson Nano, which is a fully contained board.

Google Coral Development Board
Similar to the Jetson Nano, the Google Coral is a new board that has just exited beta stages. The Coral also features a 1.5GHz clock frequency which, in conjunction with the onboard 32 GFLOP GPU and VPU, should be able to handle the level of image processing we are requiring of it. The three options we have evaluated here are all up to the challenge that we need them for, which makes Google Coral seem like a valid option, but it comes in at 1.5x the price of the Jetson Nano and still much more expensive than the Pi / Intel Compute Stick combination. With a strict, non-lenient budget this price difference definitely weighs in heavy on the decision [41].

Summary
Table 14 shows a technology comparison of the NVIDIA Jetson Nano Developer Kit, Raspberry Pi 4 w/ Intel Neural Compute Stick, and the Google Coral Development Board as the primary controller. We decided that the NVIDIA Jetson Nano Developer Kit was the best option.

	NVIDIA Jetson Nano Developer Kit	Raspberry Pi 4 w/ Intel Neural Compute Stick	Google Coral Development Board
Operating Voltage	5VDC	5VDC	5VDC
Max CPU Clock Frequency	1.43 GHZ	1.5 GHZ	1.5 GHZ
GPU / VPU	128-core NVIDIA Maxwell GPU / H.265@4K & H.264@1080P	VideoCore VI 3D Graphics / Intel® Movidius™ Myriad™ X VPU	Vivante GC7000Lite / H.265@4K & H.264@4K
Temperature Range	25℃ - 97℃	0℃ - 40℃	0℃ - 50℃
GPIO Pin Count	17	28	40
Max Power Consumption	10W	15W	15W
Unit Price	~ $99	~ $114	~ $149

Table 14: Image Processing Controller Decision Matrix

3.11.2   **Secondary Control Comparison**

ATMEL ATMega328
This is one of the most user-friendly microcontrollers on the market and has been used by hobbyists for some time, so information on the use and integration of this chip onto a PCB is quite readily available. The wealth of information for this chip does not stop there, though, as there are also tutorials on how to flash this chip so that it runs as it would directly from an Arduino. This would simplify the software development for this board tenfold as the team is well experienced with the Arduino development environment and developing applications on the platform in general.

The 8-bit ATMega328 runs off an input of 2.7-5.5VDC, which would be readily available considering the power source. Also, running the chip between 4.5-5.5VDC allows it to be operated at a speed of 16MHz which would more than satisfy the processing needs. Finally, this chip features 23 fully programmable I/O lines including SPI and I2C configurations, so setting this chip up to be a slave would present no issues whatsoever [42].

Texas Instrumentations MSP430G2553
A second option is to use an MCU from the MSP430G2x53 family of Texas Instrument products. The amount of information on the use of these chips and development on them is also very broad which would drastically cut down on the

amount of custom development required of us. This is also the chipset that was used when programming in the Digital and Embedded Systems courses which all members of the group were required to take, so we are all familiar with it to some extent.

This chip is can be powered by a voltage within the range of 1.8-3.6VDC, which again would be readily available given the power source. This chip also runs at 16MHz and, very similarly to the ATMega328, features 24 fully configurable I/O lines with some being specialized to handle SPI or I2C communications [43].

NVIDIA Jetson Nano (Use Only One Control)
A third viable option would be to have a Jetson Nano also control all of these secondary functions as well. Because of the large amount of processing power readily available this would most certainly be possible but integrating this chipset into the PCB design may prove difficult as it is interfaced with a 260 pin SO-DIMM connector. Leaving the Jetson Nano plugged into the development board may prove to be ideal as it would definitely simplify the amount of datasheet mining, we would have to do on the front end, but integrating it into the PCB design would simplify the control scheme overall as it would eliminate the need to include a second controller in the system.

Summary
Table 15 shows a technology comparison of the ATMEL ATMEGA328 and the MSP430G2553 as the secondary controller. We decided that the ATMEGA328 was the best option.

	ATMEL ATMega328	MSP430G2553
Operating Voltage	2.7 - 5VDC	1.8 – 3.6VDC
Max CPU Clock Frequency	16 MHz	16 MHz
Bit Count	8-bit	16-bit
Analog I/O	Input Only / PWM Output	Accepts Both
Temperature Range	-40℃ - 125℃	−55℃ - 150℃
GPIO Pin Count	23	24
Unit Price	~ $2	~ $12

Table 15: Secondary Controller Decision Matrix.

3.11.3   Chassis Material Comparison

Table 16 contains a table detailing the different types of 3D printing filaments. Printing filaments are used to form structures by feeding a spool of filament into the printer, melting down the filament within the nozzle, and dispersing the hot

filament while the printer moves along an x, y, z-axis system. This filament then cools; eventually stacking upon itself to form a solid structure. Different filament carry different properties such as rigidity, the melting point during printing, and overall composition. Figure 43: Filament Comparison contains an overall comparison of each filament. This will be a great resource when deciding how we want to print out chassis.

Filament	Description
PLA	PLA is the easiest polymer to print and provides good visual. It is very rigid and strong, but also quite brittle. Pros: Biodegradable, Odorless, can be post-processed with sanding paper and painted with acrylics, good UV resistance. Cons: Low humidity resistance, can't be glued easily
ABS	ABS is usually picked when higher temperatures resistance and higher toughness is required. Pros: Can be post-processed with acetone vapors for a glossy finish, can be post-processed with sanding paper and painted with acrylics, acetone can also be used as a strong glue, good abrasion resistance Cons: UV sensitive, odor when printing, potentially high fume emissions
PET	Softer Polymer that is well rounded and possesses interesting additional properties with few major drawbacks. Pros: Can come in contact with foods, high humidity resistance, high chemical resistance, recyclable, good abrasion resistance, can be post-processed with sanding paper and painted with acrylics. Cons: Heavier than PLA and ABS
Nylon	Nylon posses' great mechanical properties. It is the best for impact resistance for a non-flexible filament. Pros: Chemical resistance, high strength Cons: Absorbs moisture, potential high fume emissions
TPU	It is primarily used for flexible applications. It has a large range of uses. Pros: Abrasion Resistance, Resistance to oil and grease Cons: Difficult to post-process, can't be glued easily

PC	PC is one of the strongest materials. It has three main features: optical clarity, resistance to heat, and incredible toughness. Pros: Can be sterilized, can be post-processed with sanding paper and painted with acrylics Cons: UV sensitive

Table 16: Filament Description and Pros/Cons [44]
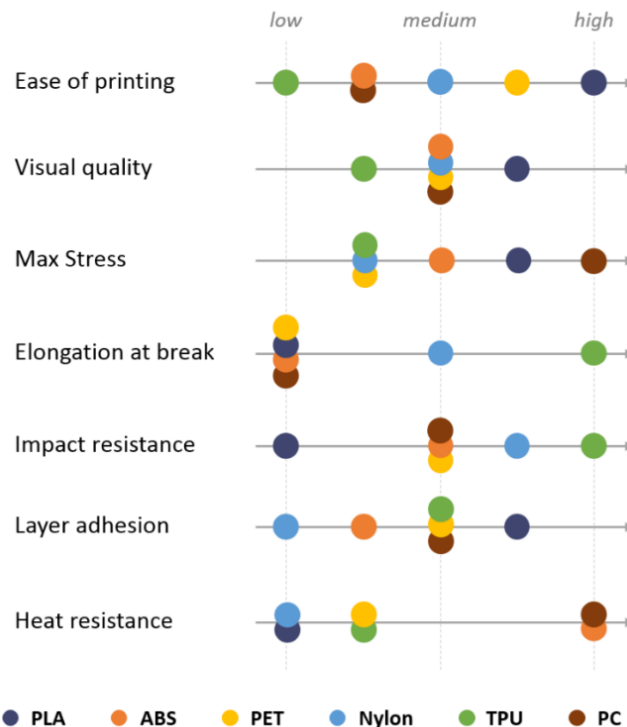
Figure 43: Filament Comparison (Approved by 3dhubs)

3.11.4 Camera Module Comparison

We adopt the standard Full HD resolution of 1920 x 1080 pixels captured at 30 frames per second. This standard is a compromise between video quality and necessary frame rates for real-time applications. This fidelity is acceptable in terms of the image processing workload since the ImageNet database we are leveraging can handle variable resolution imagery. Another aspect to consider was that, since the design requires a stereo configuration for the depth-sensing solution, either multiple cameras or a stereo configuration shipped as is was required for this application. Because of this fact, we explored an option for using inexpensive standalone cameras configured with a custom stereo vision algorithm to calculate a range map and a standalone stereo solution, pre-configured to support depth sensing.

Raspberry Pi Camera Module v2
The initial camera considered was that of the Raspberry Pi Camera Module v2, shown in Figure 44 [45]. This is a widely used camera in homemade projects and is very well-documented online. Also, being the second version of the popular camera, it has been upgraded to 8 megapixels, which would provide much better image quality than the original module which shipped with a still resolution of 5 megapixels in single-shot photography. This can always be leveraged when the object detection pipeline is failing at lower resolutions. This maximum resolution allows the sensor to support up to 3280 x 2464 pixels. Typical video streaming is supported at 1080p at 30 frames per second. The Jetson Nano supports one native MIPI connector allowing for directly connecting to the module. Peripherals would be required to either include another camera feed or multiplex more cameras for stereo vision or an expanded field of view [46].

The downside with this camera, however, is that the stereo capability contained within the design would require two of these modules. This would not only drive up the price but would also require an accurate mounting method to ensure the cameras were adequately aligned and securely held. This extra requirement would require either a store-bought mount specialized for this application method or would require a custom 3D printed mount. The 3D printed mount would be the cheaper option of the two most definitely but would require extra design and prototyping time; especially if the mount was built into the outer chassis itself.
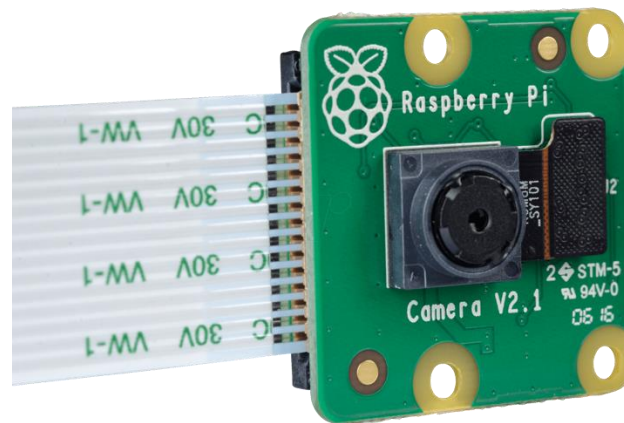
Figure 44: Raspberry Pi Camera

Intel RealSense Depth Camera D435
The second camera module considered was the Intel RealSense Depth Camera. This module is quite advanced and has many features included that the Raspberry Pi camera does not, and even cannot support. This module comes complete with two cameras in a stereo configuration, an IR projector, and an RGB module. Being that the camera ships with multiple cameras, it is already configured to measure depth straight out of the box; up to 10m depending on the scene and sensor

calibration. This means that no extra design will be required to mount the cameras in the stereo configuration, and also that no extra measurements or algorithms will be required to discern distance from an object in the scene. This will increase convenience and means the only mounting design required will be that of the two M3 thread mounting points required to attach it to the chassis.

The camera is also quite user-friendly, as it ships with Intel's RealSense SDK 2.0, which offers a variety of wrappers that support multiple programming languages and platforms; of which includes Python and OpenCV. This fact is very important as the image processing algorithms the design is planned to be developed in Python and will utilize multiple functions from the OpenCV libraries.

Intel RealSense Depth Camera D415
The Intel RealSense D415 provides nearly the same utility as the D435 with a smaller field of view and a lower price. The smaller field of view is better for the image processing applications as it reduces the size of the object detection window, thus lowering the object detection runtime [47].

Final Camera Selection
We selected the Intel RealSense D415 as the camera of choice. Leveraging the pre-built RealSense SDK for depth mapping, a narrow field of view, and a low price point made this option stand out. The relevant characteristics are summarized in Table 17.

	Raspberry Pi NoIR Camera Module v2 x2	Dorhea Raspberry Pi Camera x2	Intel RealSense Depth Camera D415	Intel RealSense Depth Camera D435
Horizontal FOV	62.2°	72°	69.4°	87±3°
Vertical FOV	48.8°	72°	42.5°	58°±1°
Color Camera Focal Length	3.04 mm	3.6 mm	1.93 mm	1.93 mm
Depth Technology	N / A	N / A	Active IR / Stereo	Active IR / Stereo
Minimum Depth Sensing Range	N / A	N / A	0.16 m	0.105 m
Maximum Depth Sensing Range	N / A	N / A	10 m	10 m
Solution Price	$54	$43	$150	$175

Table 17: Camera Sensor Decision Matrix

3.11.5   Capturing Device Comparison

We analyze three different possible capturing devices at three different prices points. The CO_2 Net Launcher is the cheapest option then the Spider Net Gun,

lastly the CODA All-Purpose Net Gun. We will do a full analysis on which devices is the best for the mine design.

CO2 Net Launcher Design
Our net launch will be personally built and designed in order to tailor to the systems needs. Table 34 shows a part list of the design. The net launcher will be powered by a 12-gram CO_2 cartridge. It will have an effective range of 10 feet and a short span of 6 feet. The overall price is predicted to be $121.22.

Spider Net Gun
The Spider Net Gun is a light and compact net capturing device. The gun is powered by 12-gram CO_2 cartridges, similar to the approach that will be taken for the CO2 design discussed in the previous section. The effective range is 30+ feet featuring a net in which can span about 5 feet. The net is also weighted at each end. The net gun fires one net at a time. It is shaped like a flashlight, so it is easy to handle and transport. The overall price is $793 [48].

CODA All-Purpose Net Gun
CODA All-Purpose Net Gun is a powerful net gun that can capture almost anything. It is powered by a blank 308 military cartridge. Classified as a "tool" by the Alcohol, Tobacco and Firearms of the U.S. Justice Department, its main intention is to capture birds to elk. The net gun fires one net and blanks at a time. The net, when fired, can span about 10 feet apart (horizontal and vertical direction). Its effective range is about 15 feet. The net gun is also weighted at each end. The CODA is fairly large and fired from a standing or crouching position (like a rifle). The standalone price is $5700 [49].

Summary
Listed below is Table 18, it contains a basic summary of each Wi-Fi modulator. We will use this later to conclude out part selection.

	CO2 Design	**Spider**	**CODA**
Price	$121.22	$793	$5700
Range	10 feet	30+ feet	15 feet
Net Span	6 feet	5 feet	10 feet
Propulsion	12-gram CO2	12-gram CO2	Blank 308 military

Table 18: Capture Device Part Comparison

3.11.6   Stepper Motor Comparison

As was discussed in Section 3.7, the best approach to obtaining the turret-like motion utilized in this design is to employ a stepper motor. There are, however, an exorbitant amount of these motors on the market. Narrowing down the best motor for this application is imperative to mission success.

Nema 17 Bipolar 1.8deg 26Ncm (36.8oz.in) 0.4A 12V

The first option that was explored was that of using two Nema 17 bipolar motors, one for controlling the horizontal motion of the launching system and another for controlling the vertical angular position. This motor features 200 steps with a step angle of 1.8 degrees, meaning that it is able to be very precise in its targeting capabilities given that it is being controlled by a reliable algorithm. It also features a current draw of 0.4A per phase, meaning it will only draw 0.8A in total. This is an important fact as it means there will be a large number of options available when a motor driver is selected. Because this is such a low power motor, however, the torque available is quite low. This could cause complications when it comes to rotating the launching assembly in a high-enough velocity manner due to the drop of the torque to RPM curve [50].

Wantai 42BYGHM809 Bipolar Stepper Motor

The second motor examined was that of a Wantai bipolar stepper motor. This motor has double the steps as the Nema 17 motor, coming in at 400, which implies that this device will be much more precise in terms of targeting a drone. This motor also features a higher torque than the previous motor, but this does come at a cost in terms of power consumption. The Wantai motor draws approximately 1.7A per phase, which means that during operation it will be drawing 3.4A. This could prove to be problematic during operation due to the constant current draw from the power supply and also due to power waste in the form of heat [51].

Summary

Listed below is Table 19, it contains a basic summary of the Nema 17 and Wantai Bipolar stepper motor. We will use this later to conclude out part selection.

	Nema 17 Bipolar Stepper Motor	**Wantai Bipolar Stepper Motor**
Amps Per Phase	0.4 Amps	1.7 Amps
Holding Torque	.26 Nm	.48 Nm
Number of Steps	200	400
Step Angle	1.8°	.9°
Motor Weight	280 g	340 g
Unit Price	$7.63	$17.95

Table 19: Stepper Motor Comparison

3.11.7   **Motor Driver Comparison**

Since this design is intended to use a stepper motor, it is imperative that an adequate motor driver is selected. This component will not only assist in supplying power to the motor via an external power source but will also aid in controlling the motor itself.

Big Easy Driver

This motor driver is simple to use and utilizes 0-5V logic, which means that it will be compatible with control from an ATMEL ATMega328 chip. This driver is able to control 4-wire bipolar stepper motors, which is what will be used in this application. It can take an input voltage between 6-30V and supply a per-phase Amperage of 1.4-1.7A, which can be increased if an external heatsink is attached to the module. Overall, the only downside of this driver is that it can only control a single motor. This proves problematic considering this design consists of two stepper motors, but incorporating a second module would not be a difficult endeavor [52].

L298N DC Stepper Motor Drive Controller Board Module

This motor driver uses the popular L289 chip, which is used in many maker motor drivers. It is able to drive up to two 4-wire bipolar stepper motors, so the issue of having to incorporate multiple modules would not be an issue with this technology. This driver similarly takes an input of 5-30V and is able to output a max amperage if 2A for all phases. This low current output could prove problematic, as many of the stepper motors considered require a per-motor current of approximately 1.6A. It is said that this motor can be operated at slightly higher amperages, but this would definitely require the application of an external heat sink to operate efficiently [53].

Summary

Listed below is Table 20, it contains a basic summary of the Big Easy and L298N DC motor driver. We will use this later to conclude out part selection.

	Big Easy Driver	L298N DC Stepper Motor Drive Controller Board Module
Logic Control Voltage	5V	3.3-5V
Motor Supply Voltage	6-30V	5-30V
Amperage per Phase Rating	1.4-1.7A+	.5A+
Number of Motors Able to Control	1	2
Unit Price	$19.95	$10.50

Table 20: Motor Driver Comparison

3.11.8 Wi-Fi Module Comparison

Since we decided Wi-Fi would be the best method of communication between the land station and mine, we will do a part comparison between three different Wi-Fi modules, two of which are USB and one which is mounted or soldered on a PCB/micro-control.

Geekworm NVIDIA Jetson Nano Wi-Fi Adapter
The Geekworm NVIDIA Jetson Nano Wi-Fi Adapter is a dual-band 1200 Mbps Wi-Fi adapter for about 20 dollars. It is supported by the NVIDIA Jetson Developer kit using USB 3.0. The Wi-Fi adapter contains a Realtek RTL8812BU chipset and is easy to use, only requiring two steps: plugging in and installing the driver. The 1200 Mbps network card is compatible with Windows XP/Vista/7/8/10, Ubuntu, and Mac OS X. The Wi-Fi adapted uses a 5 dBi sma antenna. It can support wireless standards IEEE 802.11 a/b/g/n/ac on frequency bands 2.4 and 5 GHz. It can also support 64/128-bit WEP, WPA-PSK/WPA-PSK. It uses DBPSK, DQPSK, CCK, OFDM, 16-QAM, 65-QAM modulation technology. The Jetson Wi-Fi adapter transmits power less than 20 dBm. Table 21 outlines the signal rate of 2.4 and 5 GHz and Table 22 outlines the reception sensitivity [54].

	2.4 GHz		5 GHz
11n	300 Mbps	11ac	867 Mbps
11g	54 Mbps	11n	300 Mbps
11b	11 Mbps	11a	54 Mbps

Table 21: 2.4 GHz Signal Rate

	2.4 GHz		5 GHz
11b 1 Mbps	-99 dBM	11a 6 Mbps	-96 dBM
11b 11 Mbps	-93 dBM	11a 54 Mbps	-39 dBM
11g 6 Mbps	-94 dBM	11n HT20 MCS0	-94 dBM
11g 54 Mbps	-77 dBM	11n HT20 MCS7	-77 dBM
11n HT20 MCS0	-95 dBM	11n HT40 MCS0	-92 dBM
11n HT20 MCS7	-76 dBM	11n HT40 MCS7	-74 dBM
11n HT40 MCS0	-92 dBM	11n VHT80 MCS0	-89 dBM
11n HT40 MCS7	-73 dBM	11n VHT80 MCS9	-64 dBM

Table 22: Reception Sensitivity

COMFAST CF-WU810N
The COMFAST CF-WU810N is a mini USB wireless W-Fi adapter for 6 dollars. It contains an RTL 8188EUS chipset that supports IEEE standards 802.11g, 802.11b, and IEEE 802.11n. It uses USB 2.0 on a frequency band of 2.4 GHz. The CF-WU810N has 1 – 13 working channels that use CCL, DQPSK, DB PSK, OFDM (w/ PSK, BPSK, 16-QAM, 64-QAM) data modulation. It consumes a maximum of

20 dBm and an RF gain of 20 dbi internal smart antenna. The CF-WU810N uses 64/128/152-digit WEP, WPA/WPA-PSK, WPA2/WPA-PSK security encryption. It has a theoretical range of 50-100m indoors and 100 – 200m outdoors. Table 23 outlines the data rate of COMFAST CF-WU810N [55].

	2.4 GHz
11n	150 Mbps
11g	6/9/12/18/24/36/48/54 Mbps
11b	1/2/5.5/11 Mbps

Table 23: 2.5 GHz Signal Rate

ESP8266
The ESP8266 Wi-Fi module is a self-contained System on Chip (SOC) for 7 dollars. It allows PCB or microcontrollers access to the Wi-Fi network using an integrated TCP/IP protocol stack. The ESP8266 has the ability to host and application or offload all Wi-Fi networking functions from another application processor. The ESP8266 supports automatic power save delivery (APSD) for VoIP applications and Bluetooth co-existence interfaces. The ESP8266 contains a self-calibrated RF allowing it to work under all operating conditions and does not require any external RF parts. Table 24 provides a summary of the transmission power of the ESP8266. Table 25 provides the a summary of the receiving sensitivity og the ESP826.

The Wi-Fi module can support IEEE standards 802.11 b/g/n and has a data rate up to 72.2 Mbps using a frequency band of 2.4 GHz. The ESP8266 uses a PCB Trace antenna and a Tensilica L106 32-bit processor. It can use UART/ SDIO/ SPI/ I2C/ I2S/IR Remote Control and operate at 2.5 – 3.6 V at an average of 80 mA. The ESP8266 also supports WPA/WPA2 security with WEP/TKIP/AES encryption. Note: The ESP8266 Module is not capable of 5-3V logic shifting and requires an external Logic Level Converter [56].

	2.4 GHz
11n	+14 dBm
11g	+17 dBm
11b	+20 dBm

Table 24: Transmission Power

	2.4 GHz
11b 11 Mbps	-91 dBM
11b 54 Mbps	-75 dBM
11n MCS7	-72 dBM

Table 25: Receiving Sensitivity

Summary

Listed below is Table 26, it contains a basic summary of each Wi-Fi modulator. We will use this later to conclude out part selection.

	Geekworm	**CF-WU810N**	**ESP8266**
Price	$20	$6	$7
IEEE support	IEEE 802.11 a/b/g/n	IEEE 802.11 b/g/n	IEEE 802.11 b/g/n
Power Consumption	20 dBm	20 dBm	20 dBm
Frequency Range	2.4 and 5 GHz	2.4 GHz	2.4 GHz
Chip Set	RTL8812BU	RTL 8188EUS	Tensilica L106 32-bit processor
Security	WPA/WPA2	WPA/WPA2	WPA/WPA2
Encryption	64/128-bit WEP	64/128/152 WEP	WEP/TKIP/AES
Max Data Rate	300 Mbps	150 Mbps	72.2 Mbps
Interface	USB 3.0	USB 2.0	GPIO Pins

Table 26: Wi-Fi Comparison

3.11.9 Router Technology Comparison

Since we decided a router would be the best method for send data over a local area network, listed below is a part comparison between three different routers. We kept the price in consideration, so each router is under 25 dollars.

TP-Link N300

The TP-Link N300 is a 300 Mbps wireless router. It has two 5dbi antennas used for signal transmission and reception. The TP-Link N300 has one WAN port (used to connect to the internet) and 4 LAN ports which are used to connect ethernet port devices. The N300 complies with IEEE 802.11 n/g/b standards. Table 27 outlines the key features of the N300 [57].

Features Name	Feature Specification
Ethernet Ports	4 by 10/100 Mbps LAN 1 by 10/100 Mbps WAN
Antennas	2 Fixed Omni Directional Antennas (5dbi)
External Power Supply	9VDC/0.6A
Wireless Standards (Signal Rate)	IEEE 802.11n (300 Mbps) IEEE 802.11g (54 Mbps) IEEE 802.11b (11 Mbps)
Frequency	2.412~2.472 GHz
Wireless Security	WEP WPA/WPA2 WPA-PSK/WPA2-PSK
Price	$17.98

Table 27: TP-Link N300 Spec Sheet

TP-Link N450

The TP-Link N450 is a 450 Mbps wireless router. It has three 5dbi antennas used for signal transmission and reception. It uses 3 by 3 MIMO technology to strength Wi-Fi connection. The TP-Link N450 has one WAN port (used to connect to the internet) and 4 LAN ports which are used to connect ethernet port devices. The N450 complies with IEEE 802.11 n/g/b standards. Table 28 outlines key features of the N450 [58].

Features Name	Feature Specification
Ethernet Ports	4 by 10/100 Mbps LAN 1 by 10/100 Mbps WAN
Antennas	3 Fixed Omni Directional Antennas (5dbi)
External Power Supply	9VDC/0.6A
Wireless Standards (Signal Rate)	IEEE 802.11n (450 Mbps) IEEE 802.11g (54 Mbps) IEEE 802.11b (11 Mbps)
Frequency	2.4~2.4835 GHz
Wireless Security	WEP WPA/WPA2 WPA-PSK/WPA2-PSK
Price	$24.83

Table 28: TP-Link N450 Spec Sheet

Linksys E2500 (N600)

The Linksys E2500 is a dual-band Wi-Fi router. It can support N600 (300 + 300 Mbps) reliably. The Linksys E2500 can support 2.4 and 5 GHz frequency. The E2500 has one WAN port (used to connect to the internet) and 4 LAN ports which are used to connect ethernet port devices. The E2500 complies with IEEE 802.3 /

u/ab and IEEE 802.11 n/g/b/a standards. Table 29 outlines the key features of the E2500 [59].

Features Name	Feature Specification
Ethernet Ports	4 by 10/100 Mbps LAN 1 by 10/100 Mbps WAN
Antennas	4 internal antennas (3.5 dbi)
External Power Supply	9VDC/0.6A
Wireless Standards	IEEE 802.11n IEEE 802.11g IEEE 802.11b IEEE 802.11a
Frequency	2.4/ 5 GHz
Wireless Security	WEP WPA/WPA2
Price	$17.89

Table 29: Linksys E2500 Spec Sheet

Summary

After comparing the TP-Link N300, TP-Link N450, and Linksys E2500 we develop a useful table, Table 30, that will use to help decide which router we should use when connecting the DOMINANCE mine and land mine.

Features Name	TP-Link N300	TP-Link N450	Linksys E2500
Antennas	2 Fixed Omni Directional Antennas (5dbi)	3 Fixed Omni Directional Antennas (5dbi)	4 internal antennas (3.5 dbi)
External Power Supply	9VDC/0.6A	9VDC/0.6A	9VDC/0.6A
Wireless Standards	IEEE 802.11n (300 Mbps) IEEE 802.11g (54 Mbps) IEEE 802.11b (11 Mbps)	IEEE 802.11n (450 Mbps) IEEE 802.11g (54 Mbps) IEEE 802.11b (11 Mbps)	IEEE 802.11n IEEE 802.11g IEEE 802.11b IEEE 802.11a
Frequency	2.412~2.472 GHz	2.4~2.4835 GHz	2.4/ 5 GHz
Wireless Security	WEP WPA/WPA2 WPA-PSK/WPA2-PSK	WEP WPA/WPA2 WPA-PSK/WPA2-PSK	WEP WPA/WPA2
Price	$17.98	$24.83	$17.89

Table 30: Router Tech Comparison

3.12 Part Selection

This section provides an overview of each component and why we chose the corresponding part for them. This section will reference Section 3.11 due to the extensive research that was conducted on various parts. Major factors include but are not limited to cost, ease of use, and power consumption.

3.12.1   Image Processor

In conclusion, the team decided to choose the Jetson Nano for the image processing controller. At first, the Google Coral Development Board seemed like the proper selection as it was deemed the most powerful option, but upon further evaluations, it became evident that the price was much too steep and would have cut into the budget significantly more than the other options. The Jetson Nano was ultimately chosen because it had all of the specs that were required of it without being overly powerful, as well as a price that was 66% that of the Google Coral.

3.12.2   Secondary Control

The ATMEL ATMega328 was chosen as a secondary controller ultimately because of the wish to decrease the processing burden on the main controller, the Jetson Nano. The reason this MCU was chosen over the MSP43G2553 was that the price of the unit itself was basically negligible, meaning that it could be incorporated into the PCB design with virtually no hit to the budget. Also, on the topic of incorporating this chipset into the PCB design, this chip has been used by makers for years and there is much documentation on how to accomplish this goal. This means there will be fewer design considerations required of the team and will simplify integration into the system as a whole. The similarities in the boards were also so vast that price was another major deciding factor here.

3.12.3   Chassis Material

Out of the two possibilities, it would be a more viable option to use a 3D printed chassis. This is primarily due to cost and ease of use. 3D printing is a lot cheaper than getting it manufactured by a third-party vendor. If mistakes were made while developing the chassis it would be easy to edit or cad file and print it again. It would be a lot quicker too compared to send it out to a manufacturer. We also decided that it would best to use PLA filament because it is one of the cheapest and easiest to use. It is one of the most common filaments for 3D print which means there is large community support for it. Since we are not considering other factors besides cost this concludes the trade study for 3D printing with PLA filament.

Due to certain time constraints during our final build, wood was choosen as our primary chassis material. It allowed for a similarily cheap and easy alternative. The dense and heavy weight of the wood allows for a sturdy base upon firing the launcher.

3.12.4   Camera Module

The camera solution that fits this application best is the Intel RealSense Depth module. This module will not only provide the image quality, wide FOV, and frame rate that is required but will also measure depth without the need for any extra algorithm or hardware development. The price point is a major consideration, taking approximately 20% of the final design budget, but the added features and ease of configuration and usability ultimately make this the best and most reliable option for meeting the design requirements.

3.12.5   Capturing Device

After a thorough examination of different disruption tactics, we decided to design the main disruption device with target capturing in mind. We came to the conclusion that it would be the easiest to develop and had one of the highest effective kill confidences. We plan to design the mine with a one-shot one kill tactic. The mine would be placed on the obstacle course right underneath a scoring objective for the drone. We would detect and tract any drones about to fly over and make calculations when to fire the disruption device. This design would be heavily reliant on the software. Depending on the entire budgeting, we would consider a multiple mine option, but current funds have been allocated only for one mine. The kill confidence would increase if we could place multiple mines.

We plan on designing a homemade net launcher due to cost.This design is more affordable and has just the same effectiveness as the other two net guns. We have the ability to make modifications when integrating it with the mine. During the course of the design, we can make part modifications if things don't work.

3.12.6   Stepper Motor

After analysis of the motor options evaluated, the option selected was that of the Nema 17 bipolar stepper motor. This was selected due to the much lower current draw, which not only implies the amperage rating of the power supply can be much lower to be sufficient but also that the options in selecting a motor driver will be much faster. Another factor that strongly swayed this decision was also the weight, as, even though this motor features less torque than the other option, the decreased weight of this motor implies there will be less of a strain on said motor required to supply horizontal motion to the mine body.

3.12.7   Motor Driver

After analysis of the motor drivers in question, it became readily apparent that the Big Easy Driver was a much better option for this component. It is controllable by 5V logic and can take an input voltage that is well within the bounds of what the design requires. The aspect that makes this driver stand out from the rest, however, is the 1.4-1.7A+ Amperage rating per phase. This will allow for control of virtually any motor that we would select for this application. The fact that two of

these drivers will be required is not ideal, but the high amperage output possible with this component makes it the best option, even with this downfall.

3.12.8   **Wi-Fi Module**

After the analysis in section 3.11.6 and a concluded summary in Table 26. We decided that the best Wi-Fi modulator would be the COMFAST CF-WU810N. There are multiple reasons for the decision but the overall cost per technology and ease of use were the primary reasons. The CD-WU810 was the cheapest of the three but also had enough data transmission power for the DOMINANCE mine design. Since the three parts had very similar frequency bands, power consumption, frequency ranges, and security/encryption, this made it a lot easier to focus on the important factors for the design. It was unnecessary to have the best bandwidth since the minimum to set up a live video feed is about an upload speed of 6 Mbps. Security is not a major factor since we are only passing small amounts of metadata back to the land station for completion purposes. The NVIDIA Jetson Nano supports USB 3.0 and 2.0 which is a lot easier to "plug and play" than the ESP8266. It was also unnecessary to transmit in both the 2.4 and 5 GHz frequency band since we are only connecting to one device and there would not be much interference on the obstacle course.

3.12.9   **Router**

After the analysis in section 3.11.9 and a concluded summary in Table 30. We decided that the best router option would be the Linksys E2500. The three routers, overall, were very similar. The Linksys E2500 was the cheapest option and had one of the most features. The E2500 has a nice option if we want the highest bandwidth and more frequency options. It can support the most standards but that will not be necessary since we primarily use IEEE 802.11 n/g/b. Each router supports the same number of WAN and LAN ports. Each router also supports the same type of security.

Due to time constraints during the final build of the mine, the TL-WR940N was opted as our primary router. This router meets the necessary requirements to create a WLAN and support the bandwidth for the live datalink between mine and ground station. The TL-WR940N was currently the only router available at the time.

4.0   Related Standards and Design Constraints

Engineering standards are documents that specify characteristics and technical details that must be met the products, systems, and processes. The purpose of designing to standards is to ensure minimum performance, safety requirements, and consistency/ repeatability. The development of DOMINANCE mine, several standards are referenced to help with the design process.

4.1   Standards

Engineering standards can be found in several institutions. The Institution of Electrical and Electronics Engineering (IEEE), American Society for Testing and Material (ASTM International), and the American National Standards Institute (ANSI) are great sources for finding engineering standards.

4.1.1   IEEE 802.15.1 (Bluetooth)

IEEE 802.15.1, otherwise known as Bluetooth, is derived from the Bluetooth core, profiles, and testing specifications. The Bluetooth wireless technology is an industry specification specifically for small form factor devices that want a low-cost alternative to wireless communication. The standards were issued between 2002 and 2005. The clauses discussed in the document provide a general description of the standard and identifies the sources of each of the subsequent clauses.

The first five clauses contain standard IEEE introductory information. It provides an overview, reference citation, unique definitions, an acronym/ abbreviation. Clause 5 is generally used to provide guidance to the reader about the form and contents of 802.15.1. Clause 6 describes the inner workings and architecture of Bluetooth. It references the original design.

Clause 7 through clause 11 contains the in-depth details of the WPAN architecture overview. Clause 7 is the physical layer. This describes how the data is passed between devices. Clause 8 contains the baseband specifications. The frequency and data rate of Bluetooth are mentioned in this section. Clause 9 contains the link manager protocol. The link manager protocol details how devices connect (Probing, Authentication, etc.). Clause 10 is L2CAP. L2CAP is a packet-based protocol that can be configured with varying levels of reliability. This serves as the transport protocol. Clause 11 is about the host control interface (HCI). This section has undergone significant editorial modifications. The last clause is Service Access Points (SAPs). This cause was added by IEEE to describe how lower layers of Bluetooth would interact with the traditional IEEE logical link control (LLC). Figure 45 on the following page outlines the Bluetooth stack protocol in its entirety [60].
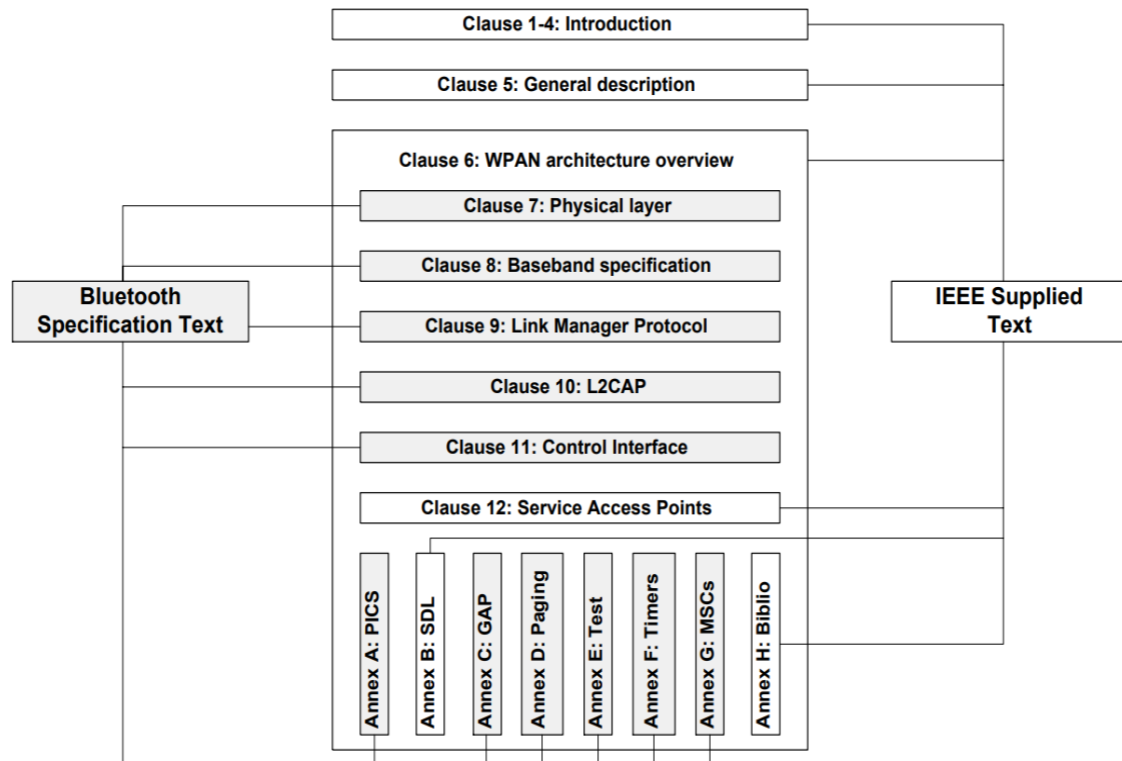
Figure 45: Bluetooth Stack Overview (Pending Approval)

4.1.2 **IEEE 802.11 (Wi-Fi)**

IEEE standard 802.11, also known as Wi-Fi, was first standardized in 1997. Standard 802.11 is a set of standards that define the protocol and compatible interconnection of data communication equipment via the "air". This would be passed in a local area network (LAN) using the carrier sense multiple access protocols with collision avoidance (CMSA/CA). The medium access control (MAC) supports operation under an access point as well as independent stations. The stack protocol contains authentication, association, and reassociation services. Encryption/ decryption, power management, and point coordination procedures are also optional. The standard also includes the definition of the management information base (MIB) using the Abstract Syntax Notation 1 (ASN.1). The infrared implementation supports a 1 Mbps data rate with an optional 2 Mbps extension. The radio implementation supports 1 Mbps data rate with an optional 2 Mbps extension for a frequency-hopping spread spectrum (FHSS) or direct sequence spectrum (DSSS), which supports both 1 and 2 Mbps data rates.

Similar to Bluetooth's standard, the first five clauses contain standard IEEE introductory information. It provides an overview, reference citation, unique definitions, an acronym/ abbreviation. Clause 5 is generally used to provide guidance to the reader about the form and contents of 802.15.1. Clause 6 describes the MAC service definitions. Clause 7 is the MAC frame format. This

describes how the data is framed and passed around. Clause 8 contains the Authentication and privacy specifications. How the devices authenticate each other is discussed in this section. Clause 9 contains the MAC architecture. This section describes how the MAC sublayer functions. Clause 10 is layer management. This gives a broad overview of the management model and the SAP interface. Clause 11 is the MAC sublayer management entity. This describes synchronization, power management, association/reassociation, and MIB definitions. Clause 12, Physical layer (PHY) service specification, explains the scope of PHY services and what functions they provide. Clause 14 is where the standards for Frequency-Hopping Spread Spectrum (FSSS) are discussed. A large overview of the functions is here. Clause 15 describes the direct sequence spread spectrum (DSSS). Similar to clause 14, this details the scope and functions of DSSS PHY. Clause 16, the last section, focuses on Infrared (IR) PHY specification. Once again, the scope and physical functions are detailed here [61].

4.1.3 Key 802.11 IEEE WLAN Standards

Since the development of the first IEEE 802.11 standard, new iterations and improvements have been accomplished throughout the years. This section outlines the name of the 802.11 standards and a brief description of what changes were made. Table 31 showcases the full outline.

Wi-Fi Standards	Standard
802.11	This standard applies to WLANs. It provides 1 or 2 Mbps transmission in the 2.4 GHz band. It can either use FHSS or DSSS.
802.11a	This standard is an extension to 802.11. It provides up to 54 Mbps in the 5 GHz band. It uses an orthogonal frequency division multiplexing encoding scheme rather than the original FHSS and DSSS.
802.11b	This standard is also referred to as 802.11 High Rate or Wi-Fi. It is also an extension to 802.11. It provides 11 Mbps transmission in the 2.4 GHz frequency band. This standard only uses DSSS. It allowed wireless functionality compared to the Ethernet.
802.11e	This standard defines the Quality of Service (QoS) support for LANs. This is an enhancement of 802.11a/b specifications. This standard adds QoS features and multimedia support while maintaining backward compatibility.
802.11g	This standard is used for short-distance transmission, allowing 54 Mbps in the 2.4 GHz band.
802.11n	This standard adds multiple-input multiple-output (MIMO). This allows for greater data throughput through spatial multiplexing. The range is increased by exploiting the spatial diversity through Alamouti coding. This standard allows a data rate of 100 Mbps.

Wi-Fi Standards	Standard
802.11ac	This standard delivers data at a rate of 433 Mbps per spatial stream or 1.3 Gbps in a three-antenna design (three steams). This standard operates only in the 5 GHz frequency range and supports for wider channels (80 MHz and 160 MHz).
802.11ac Wave 2	This standard is an update to the original 802.11ac. It uses MU-MIMO technology and other technologies to theoretically increase the maximum wireless speeds to 6.93 Gbps.
802.11ad	This standard allows the operation in the 60 GHz frequency band. It also, theoretically, allows a maximum data rate of up to 7 Gbps.
802.11ah	This standard, also known as Wi-Fi HaLow, is the first Wi-Fi specification to operate in frequency bands below 1 GHz. This standard has the capability of having ranges twice that of other Wi-Fi technologies. It has the ability to penetrate walls and other barriers.
802.11r	Also known as Fast Basic Service Set (BSS) Transition, is a standard that supports Vo Wi-Fi. It allows handoffs between access points to enable VoIP roaming on a Wi-Fi network with 802.1X authentication.
802.11X	This standard is for port-based Network Access Control. It allows network administrators to restrict LAN services in order to secure communication between authenticated and authorized devices.

Table 31: Wi-Fi Standards [62]

4.1.4 ISO/IEC 12207

ISO/IEC 12207, also known as "software life cycle processes", provides a common framework for developing and managing software. The document consists of clarifications, additions, and changes accepted by the IEEE and Electronic Industries Alliance (EIA). In summary, this standard provides a basis for software practices that would be useable for both national and international business. This standard is very useful for the DOMINANCE mine project since we are developing software that will later be integrated with hardware. It will require us to plan the entire life cycle of this application.

This International Standard establishes a common framework for software life cycle processes. It contains terminologies that are referenced in software industries. It contains processes that should be applied during the gain of a system that contains software, software services, development, operation, and/or maintenance of software products. ISO/IEC 12207 also includes a process that can help define, control, and improve software life cycle processes.

This document contains seven different clauses. Clause one through three gives a brief overview of the standard. Clause four goes into the terms that are used by software industries. They are simplified to make understanding easier. Clause five,

application of this international standard, summarizes the importance of this standard. It presents an overview of the software life cycle processes that can be employed to acquire, supply, develop, operate, maintain, and dispose of software products and services and describes the key concepts of software products and related systems/ services. It also provides an overview of different types of processes. Clause six, system life cycle processes, goes in-depth on each major process. Each process is unique and contains information that affects a system as a whole. Lastly, clause seven goes into software processes as a whole. Implementation, requirements, integration, qualification, verification, etc. are discussed [63].

The following figure, Figure 46, provides an overview of clause five through seven.
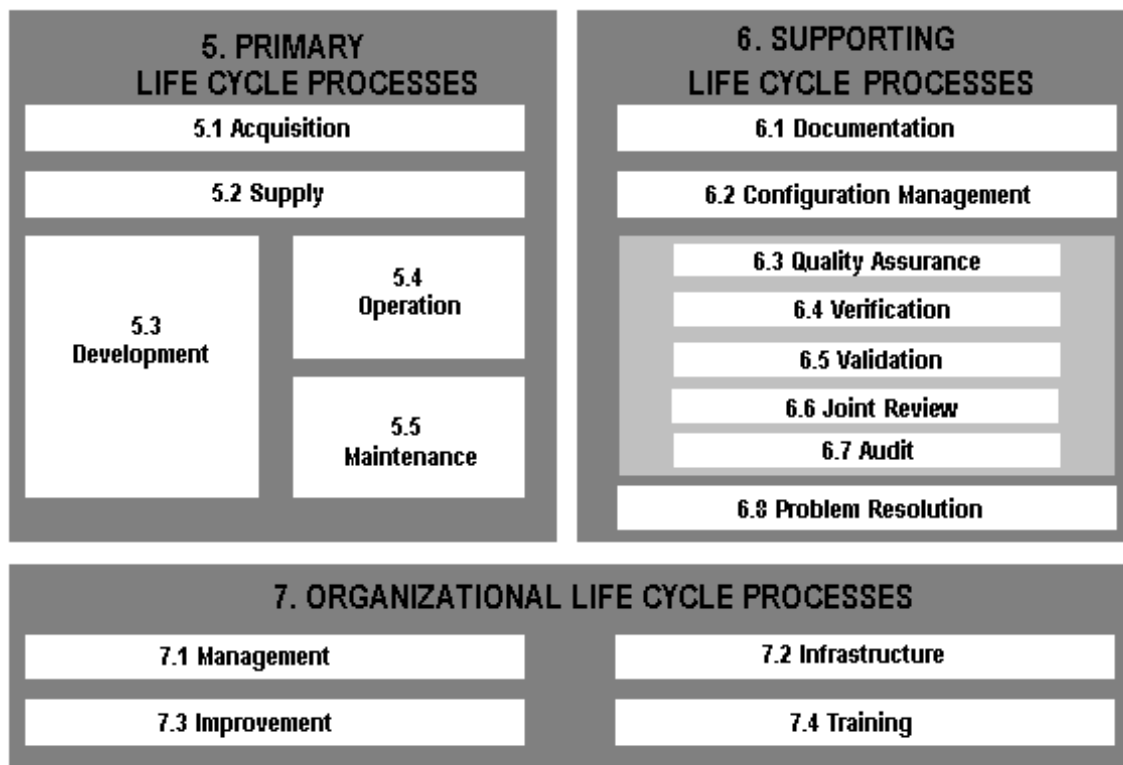
Figure 46: Software Life Cycle, Clause 5 - 7 (Pending Approval)

4.1.5 IPC Printed Circuit Board Standards

The Institute of Printed Circuits (IPC) standards are used to regulate designing, producing, and manufacturing PCBs as well as other electronics. These standards include but are not limited to the individual components implemented on PCBs, the software used to design the systems, the materials as well as size constraints for the materials, and the process of connecting the components correctly and safely. Following these standards ensure the longevity of the systems while also providing consistent products for the consumers. Figure 47 below gives a flow chart of all of the IPC standards that are put into consideration when designing, manufacturing, and assembling PCBs [64].
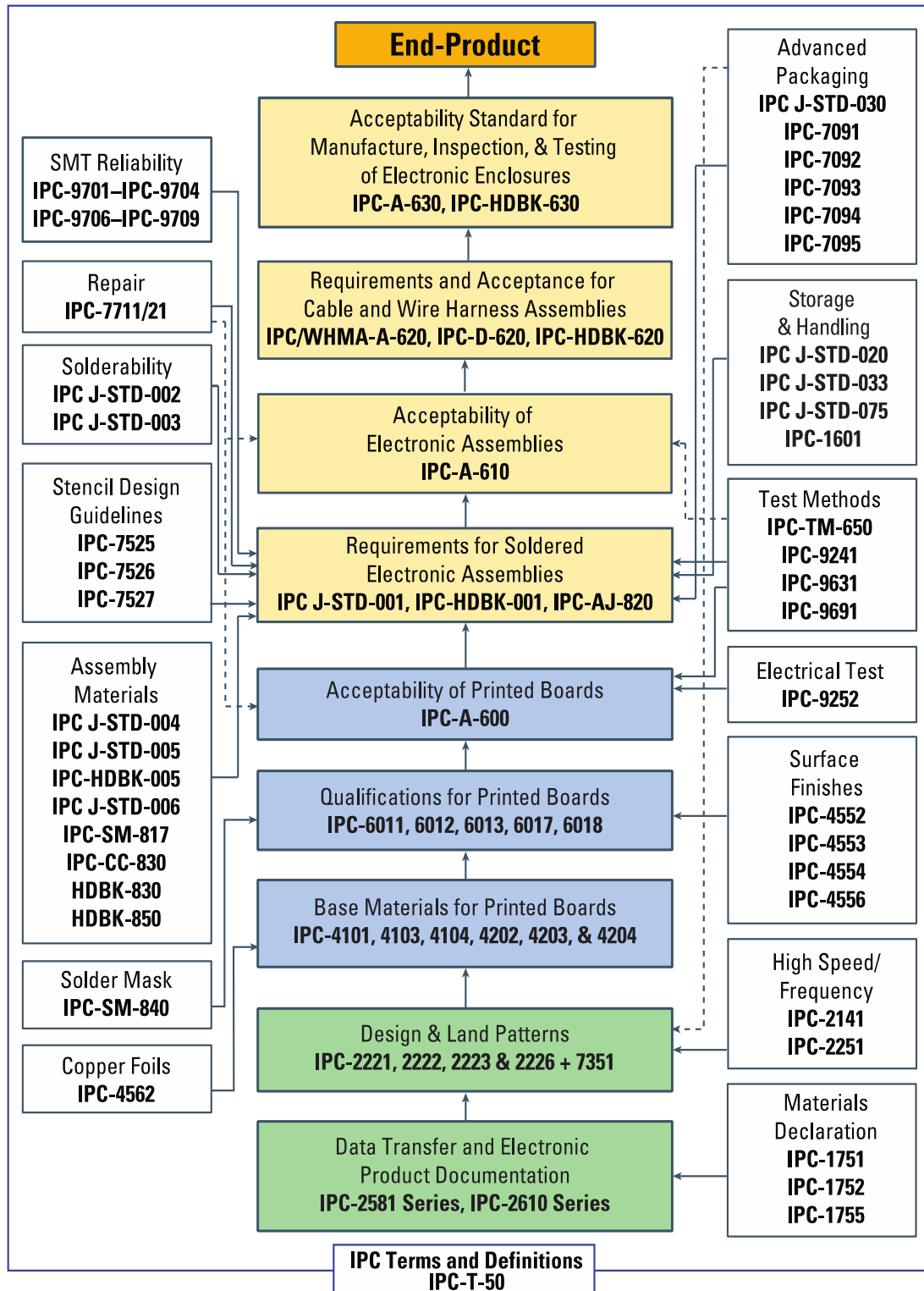
Figure 47: Chart of IPC Standards (Courtesy of www.ipc.org)

4.1.6 **IEC 61140:2016**

This electronics standard is particularly important in regards to protection against electrical shock. This standard is directed towards the applications and installations of electrical systems to ensure safety to any livestock that may be near or interact with the systems. This standard is particularly important for ensuring proper grounding techniques are exercised while also taking into consideration any added fault protection to the circuit.

4.1.7 **PEP 8 – Style Guide for Python Code**

PEP 8, Style Guide for Python Code, documents coding conventions for Python. This standard is import to us because we will be primarily writing in python code. It is important that we understand how we should format the python code for coherency. It will be a lot easier to read and understand each other's code. PEP 8 is broken into multiple sections. It begins with an introduction; this is where it provides a brief overview of the document. Next, the document goes over how consistency within a project is important. Afterward, it goes in-depth to analyze code lay-out, string quotes, whitespace, comments, etc. Table 32 provides a brief summary of PEP 8 python styling guide [65].

Topic	Description
Indentation	4 spaces per indentation level
Tabs or Spaces?	Spaces are preferred
Maximum Line Length	79 characters
Should a Line Break Before or After a Binary Operator?	Yes
Blank Lines	Surround top-level function and class definitions with two blank lines.
Source File Encoding	Code in the core Python distribution should always use UTF-8 (or ASCII in Python 2).
Imports	Imports should usually be on separate lines
Comments	Complete Sentences. English. Up to date.

Table 32: PEP8 – Python Styling Guide

4.1.8 **Power Supply Standards**

Power supply standards provides safety standards that protect against fire, electric shock, and injury. Different classes of equipment are allowed to be used for specific circuit classifications. Table 33 outlines common circuit definitions.

Circuit	Description
Hazardous Voltage	Any voltage exceeding 42.2 VAC peal or 60 VDC without a limited current circuit
Extra-Low Voltage (ELV)	Voltage in a secondary circuit cannot exceeding 42.4 VAC peal or 60 VDC, the circuit being separated from hazardous voltage by basic insulation.
Safety Extra-Low Voltage (SELV) Circuit	Secondary circuit cannot reach a hazardous voltage between any two accessible part or accessible part and protective earth under normal operation or experiencing a single fault. In the event of a single fault condition the voltage in accessible parts of SELV circuits shall not exceed 42.4 VAC peak or 60 VDC for longer than 200 ms. An absolute limit of 71 VAC peak or 120 VDC must not be exceeded.
Limited Current Circuit	These circuits may be accessible even though voltages are in excess of SELV requirements. A limited current circuit is designed to ensure that under a fault condition, the current that can be drawn is not hazardous. For frequencies < 1 kHz, the steady state current shall not exceed 0.7 mA peak AC or 2 mA DC. For frequencies > 1 kHz the limit of 0.7 mA is multiplied by frequency in kHz but shall not exceed 70 mA. For accessible parts not exceeding 450 VAC peak or 450 VDC, the maximum circuit capacitance allowed is 0.1 µF. For accessible parts not exceeding 1500 VAC peak or 1500 VDC the maximum stored charge allowed is 45 µC and the available energy shall not be above 350 mJ.
Limited Power Source (LPS)	The power sources are designed with prescribed output voltage, current, power and short circuit current limits. Specific methods can limit the capacity of the power source. The requirements for wiring and loads supplied by LPS power supplies are relaxed due to the reduced hazard of electric shock or fire caused by an LPS power supply.

Table 33: Circuit Definitions [66]

5.0 Design

This section provides an in-depth analysis of the hardware and software implementation that is going to be used for the development of the DOMINANCE mine. The mine will be designed to meet the requirements mentioned in Section 2.3.

5.1 Hardware

Section 5.1 outlines any hardware implementation within the final design. This section features specifics for the setup and implementation of each hardware component from the controller to the net launching mechanism. Also featured are the PCB design that will be utilized in this system and the specifics of it including the power distribution system and external connections. The integration of all these hardware components will be included in the next section, Section 6.0.

5.1.1 Hardware Flowchart
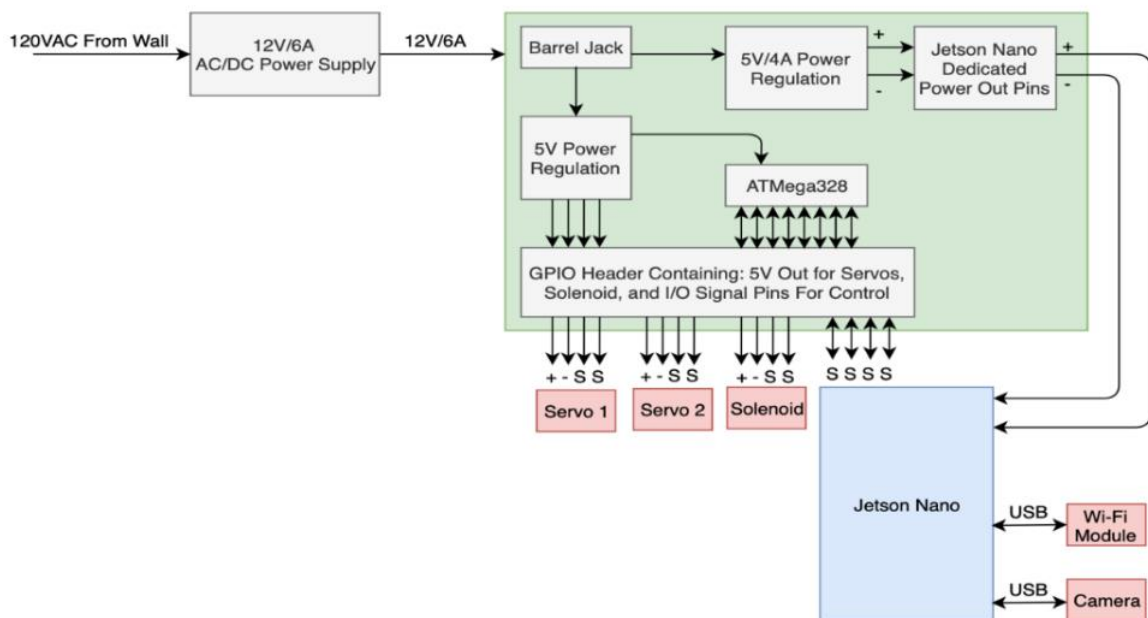
Figure 48: Hardware Flowchart

Figure 48 outlines the general hardware block diagram. We first pass 120VAC wall power into a 12V/6A AC/DC Power supply. This will convert AC to DC power and help create a steady 12V 6A that will later be used to power the PCB. On the PCB, we will use a Barrel Jack that takes connects to the power supply. On the PCB, there will be voltage regulation to step down the 12V input to 5V in order to power the Jetson Nano, ATMEGA328, and GPIO headers. The Jetson Nano and ATMEGA328 will use it dedicated power in/out pins to connect to the PCB. The GPIO headers will be used to connect the stepper motors, solenoid, and any other

98

input/output pins. The Jetson Nano will have the Wi-Fi module and camera peripherals connected to it to allow inputs for processing as well as wireless transmission abilities to the home base. When information to fire the drone will be passed from the Nano to the ATMEGA328 which will activate the stepper motors (to move the turret around) and solenoid (to activate the firing mechanism).

5.1.2 **Chassis Design**

Shown in
Figure 49 and Figure 50 is a rough CAD of the chassis design. The CO2 launcher will be mounted at the top of the chassis (marked in red) and the camera will be on the servo enabled mount. The camera will be able to move in the X, Y, and Z directions in order to help track any drones flying on the obstacle course. The Jetson Nano, PCB, and any other internal parts will be self-contained in the chassis. The chassis design will be made out of PLA filament and will meet the 1.5 by 1.5 by 1.5 feet requirement.

The figures below show where the processor will be housed in green, the point where the launching mechanism and camera will be mounted in red, and the positions of where the motors will be mounted for X, Y, Z controls. A housing sheath may also be incorporated further into development to help made the mine less discernable from its surroundings, but this addition was not included in the original design.
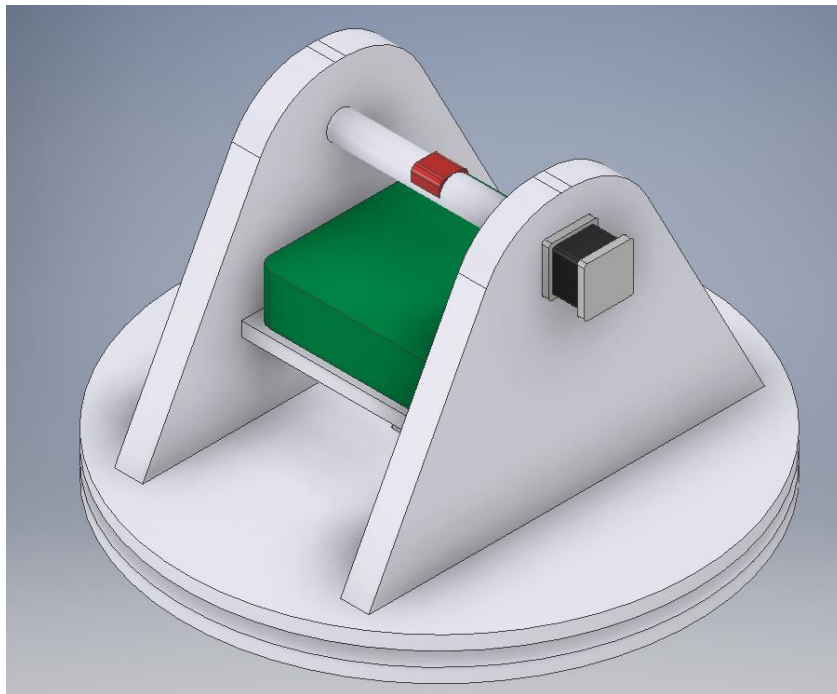
Figure 49: Inventor Model of Chassis (Top Corner View)
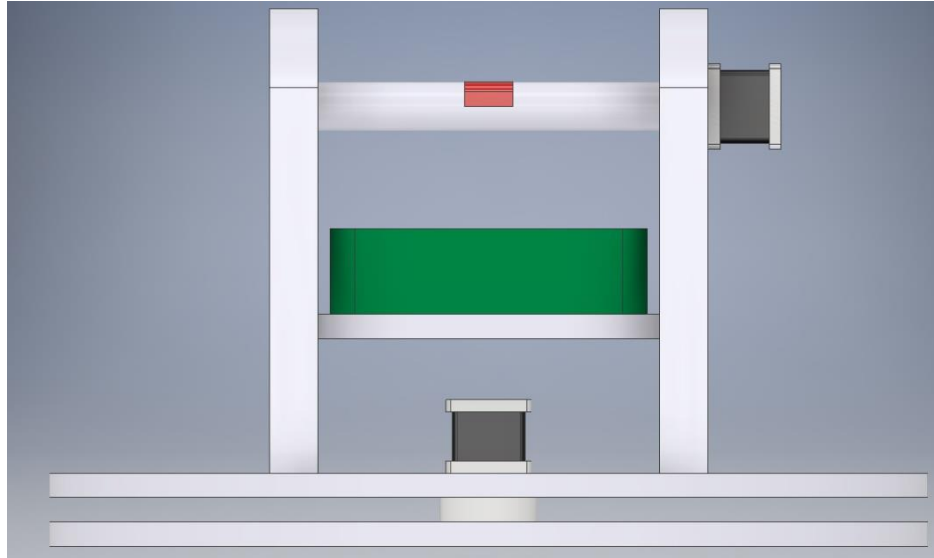
Figure 50: Inventor Model of Chassis (Front)

5.1.3 Controller Communication Design

Being that this system is comprised of two controllers, it is imperative that both of them are able to communicate freely to one another and also that they are able to perform each of their tasks. To assure that the two controllers (NVIDIA Jetson Nano and ATMEL ATMEGA328) are able to communicate effectively, this design will be using a UART communications scheme between the two. In order to achieve this, on the hardware side, this will involve wiring the two together. The Jetson Nano features a header (J41.x) which includes specialized lines for UART communications using a 3.3V TTL signal. The ATMEL ATMEGA328 features dedicated TX and RX lines that operate on a 5V TTL signal and are located on pin 1 and pin 0, respectively.

To ensure the communications are sound, the RX of the Jetson Nano will be connected to the TX of the ATMEGA328, and vice versa. A ground pin on the Jetson Nano will also be tied to the ATMEGA328's ground, ensuring that there is a common ground between the two sub-systems. Once this wiring is complete, and the software settings are set to equivalent levels in each system (baud rate, number of bits, parity), the communications will almost be ready for commencement.

The final step to ensure proper communication between these two controllers is to include voltage-level shifters between the two communication lines. The ATMEGA328's UART scheme uses a 5V TTL signal, while the Jetson Nano utilizes 3.3V logic. These voltage level shifters ensure that communication between the two controllers will function as expected while also ensuring that no lines will be compromised (fried) in the process.

5.1.4 Wi-Fi Communications Design

This design requires a reliable Wi-Fi communication, as a requirement of the system is to be able to display a live video feed to an external device. The requirements also extend to being able to disable/enable the system remotely, meaning that communications will need to travel both ways.

The integration of Wi-Fi communications is made simple in this system due to the Wi-Fi module that was chosen for this task. The COMFAST CF-WU810N that was selected for this application is perfect as it is simply a small USB dongle. It will be interfaced with the Jetson Nano by simply being inserted into a USB port on the carrier board (J32.2). Once this is complete only software will be required to establish a reliable Wi-Fi connection with the external device.

5.1.5 Sensor Implementation Design

Since this design is dependent on a reliable imaging solution it is crucial that the Intel RealSense camera module, shown in Figure 51, is configured correctly.

This is made very simple, however, as the Intel RealSense camera is interfaced with a USB 3.0 cable and a powerful software developer kit that is cross-platform. This makes connecting this camera to the Jetson Nano convenient as it features four USB 3.0 ports located directly on the carrier board. All that is required here is to connect the male end from the Intel RealSense camera module to the female USB connector (J32.1) on the Jetson Nano carrier board, then configure the SDK to create a 3-D point cloud to give range information. Overlaying the detection location with the point cloud yields range to target, and after recording temporally, the time of arrival can be calculated based on a simple velocity calculation for the target drone.

The power for the camera will also be drawn from this USB connection via the Jetson Nano, so no external power source will be required. The camera will be mounted on top of the launching mechanism as such that the center of the image frame is pointing at the direction as to where the net will be launched. Figure 51 below shows the mounting point and connection necessary to run the camera.
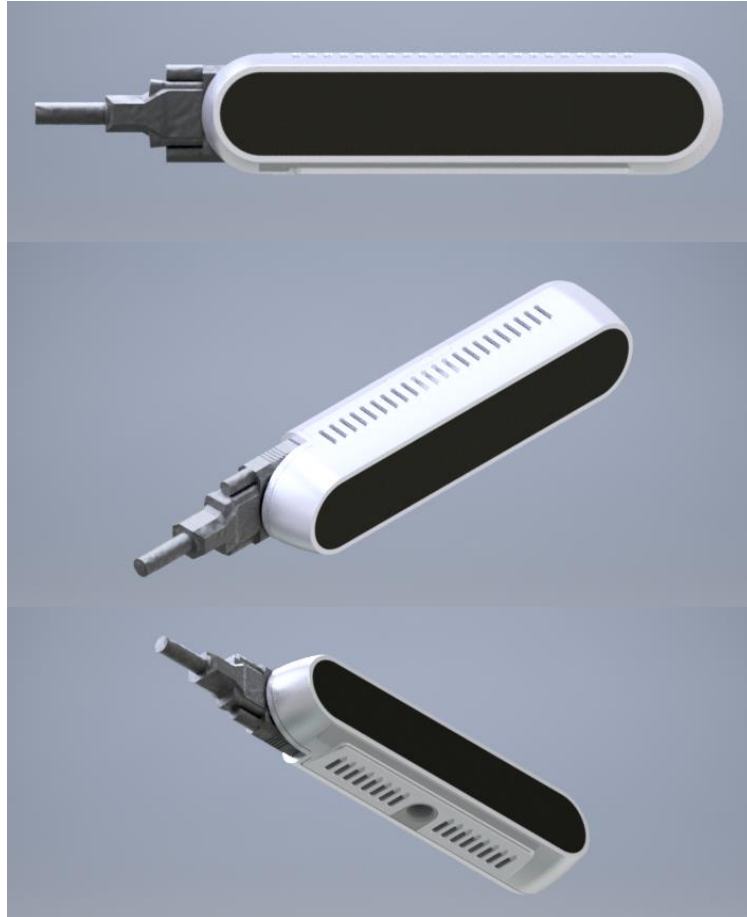
Figure 51: Inventor Model of Camera (Multiple Views)

5.1.6 **Turret Motion Design**

The motion of the turret system is critical to mission success as this will control the accuracy in which the mine will be able to fire upon the target. Guaranteeing that the targeting is accurate will require input to the ATMega328, from the Jetson Nano, to ensure the location of the firing mechanism is in line with the location of the target. The input from the Jetson Nano will be relayed to the ATMega328 via the UART communication scheme that was discussed in Section 5.1.3.

Following the input from the Jetson Nano, the ATMega328 will then be required to step the motor to the correct position to ensure that the target is in the engagement location. To do this, the ATMega will be connected to the Big Motor Driver, which will, in turn, be connected to the Nema 17 Bipolar stepper motor. Since this design features two motors in order to support 3D targeting, two motor drivers and two motors will be required to accomplish this task.

Motor Control Design

To power the motors, a 12V power source will be connected to the VCC of the motor driver and the 12V power source's ground will be connected to the GND on the motor driver. The next step, after motor power is considered, is to connect the control lines from the ATMega328 to the motor driver's inputs. Since the motor selected for this design is bipolar in make, it will require four control lines per motor driver to stop them. Because of this digital pins 2, 3, 4, 5, 6, 7, and 8 will be tied to IN1, IN2, IN3, and IN4 on the first motor driver and the remaining to IN1, IN2, IN3, and IN4 on the second motor driver, respectively.

In order to create motion, the final step is to wire each motor driver to its motor in question. The first motor will be used to control yaw, and therefore will be connected to motor driver one. Here, the positive and negative terminals of each phase (A, A-, B, B-) must be connected to the motor drivers. Similarly, for the pitch control, the positive and negative terminals of each phase will be connected from motor driver 2 to motor 2.

With this configuration in place, the motors will be able to control the position of the net launcher in both the yaw and pitch rotation planes. This will, therefore, allow the three-dimensional targeting that is pivotal to this design and overall mission success.

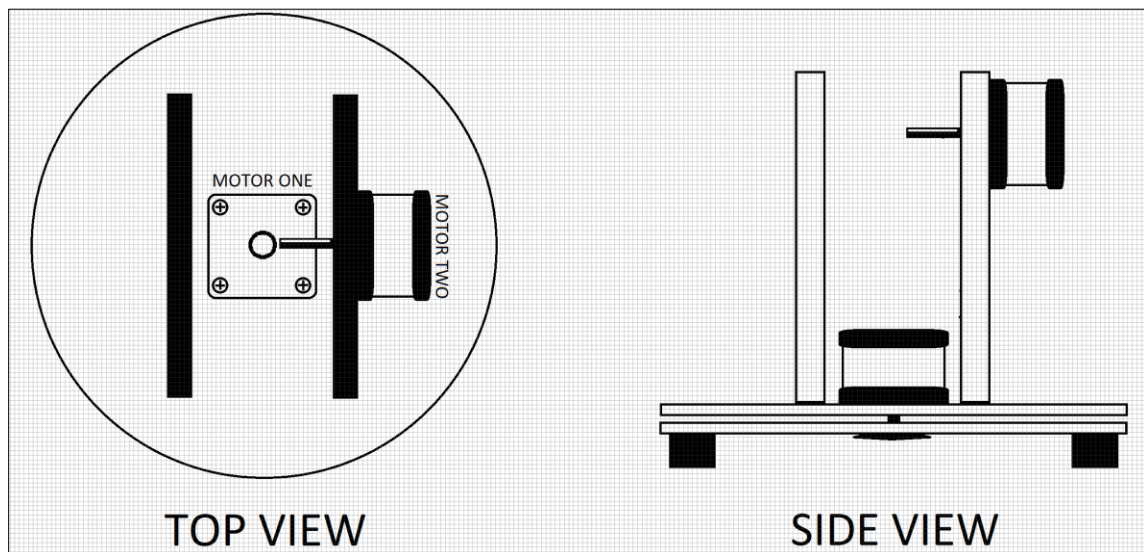**Figure 52: 3D Motion Concept. Motor One (Yaw) and Motor Two (Pitch)**

5.1.7 CO2 Net Launcher Design

For the primary disruption device, a CO_2 powered net launcher will be implemented on the mine. The net launcher is composed of three primary components: The CO_2 canister adapter along with brass tubing, a valve that will trigger the device to fire, and the net deployment system. All three main

components will be connected via brass piping of which will serve as pressure regulation for the propulsion system for the net. The prototype will end up mostly being utilized on the final design with a slight variation being in the triggering system to make the device function fully autonomously to seek and disable the target within the blast radius. The hardware used to construct the CO2 net launcher is shown in Table 29 below.

Item	Description
15 Count Crossman 12 Gram CO2 Cartridges	CO2 Cartridges
Paintball Quick Change 12 Gram Co2 Adapter	CO2 Cartridge Adapter
6'x6' 1" Mesh Net	Net
10' 1/4" PVC Pipe	Net Deployment Tube
DERNORD Stainless-Steel Heavy-Duty Ball Valve	Mechanical Valve
Everbuilt 1/4" Brass 90* Elbow	Brass Piping Turns
Everbuilt 1/4" Brass 3" Straight	Straight Tubing
Everbuilt 1/2" to 1/2" Adapter	Couples CO2 Adapter to Elbow
Everbuilt 1/4" Coupler	Between Ball Valve and PVC

Table 34: Net Launcher Part List

CO2 Canister

The main propulsion source for the new launcher is compressed carbon dioxide (CO_2) in which can be readily purchased for a relatively low cost. For this application, it was decided to use single-use twelve-gram CO_2 canisters. These 12g canisters are sold for roughly ~$0.50 per 12g cartridge and will supply around 5-8 shots per canister. When the launcher is triggered and CO_2 is released, the adapter, as well as the brass tubing, will drop in temperature due to the sudden release in temperature. For this reason, the triggering mechanism but be timed such that it does not remain open any longer than needed to ensure no components exceed their thermal operational limits. The disposable single-use canisters require an adapter to pierce the thin metal seal as well as adds a ½" threaded male adapter to allow further components to be added in unison with the adapter. The adapter allows for faster refilling as it only requires the user to unthread the piercing valve, place a new, unopened CO_2 cartridge in, and replace the piercing valve and tighten until the seal on the cartridge is pierced. These 12g cartridges were used over a larger supply tank as they allow for faster reloading, save space, and will not rely on a regulator as they do not contain near as much compressed gas as the larger refillable tanks. The CO_2 adapter will be connected to the other components via brass piping. Brass piping was chosen as it allows for 1000psi of working pressure of which is plenty of working pressure considering this application.
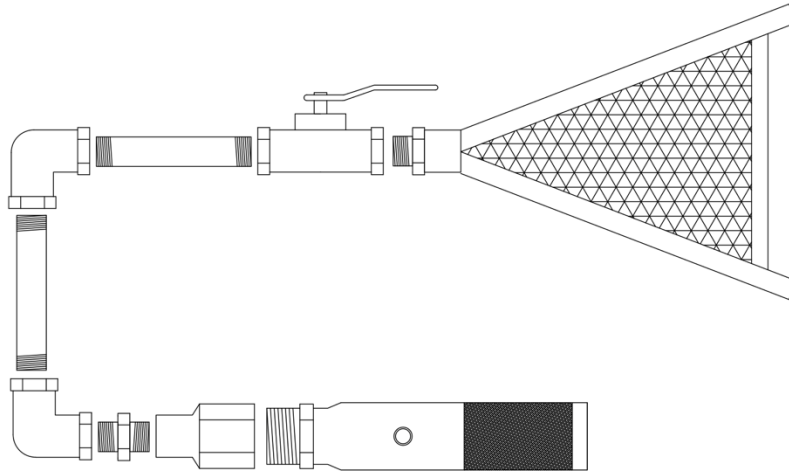
Figure 53: Net Launcher Overall Hardware Initial Concept

The brass tubing used to construct the net launcher serves the purpose of pressure regulation as well as discussed previously in Section 3.6.2. Using the derived equation, the pressure within the system is fully dependent on the volume of the space occupied by the CO_2. This results in the length of the tubing sections being the key variable for adjusting the pressure for deploying the net. Also, as seen in Figure 53, the brass piping is also used to route the gas in a way such that the device can occupy the least amount of space possible to stay within the size limitations of the customer. By utilizing two 90 degree couplers, the size of the disruption device can be reduced to roughly half of the overall length while still maintaining all of the necessary components. Since all of these components are under great pressure once the 12g CO_2 canister is punctured, Teflon tape will be used to guarantee a secure seal between all of the components. It must be noted that when applying the Teflon tape to the male threads of the tubing, the direction of application is important to ensure the tape does not 'unwind' while the two components are tightened together. The quick-change 12g CO_2 adapter, Crossman 12g canisters, and brass tubing and couplers are all used together to form the final system used for successfully propelling the net to capture the UAV.

Triggering Valve
There will be two different valves utilized for the net launcher for testing purposes versus the final product. For prototyping, a mechanical ball valve will be used between the net deployment system and the pressurized CO_2 canister. This mechanical ball valve will allow triggering to occur without the need for any electrical systems, therefore, simplifying the design process. The ball valve chosen is the Dernord Stainless-Steel Heavy-Duty Ball Valve with ¼" threads to allow further attachment to the rest of the launchers systems. This ball valve is rated for 1000psi allowing ample working room for the designing process. By turning the valve 90 degrees, the valve will open allowing the pressurized gas to flow out of the valve and propel the weights attached to the net to disperse the net in an open manner. After the net launcher functions the way it is intended to via testing and

105

prototype iterations, this ball valve can be substituted for one that can be actuated via power provided from the PCB.

The final iteration of the net launcher with have an electronic solenoid in place of the mechanical ball valve. This solenoid will receive a signal from the ATMega328 triggering the normally-closed valve to open and release the pressurized gas. This solenoid will require power to actuate the valve of which will be provided by the PCB terminal block outputs. Once the Jetson Nano detects the target with a high enough confidence to meet the threshold, the Nano will send a signal to the ATMega328 on the PCB to turn this pulse into the trigger command; sending a voltage to the solenoid to quickly open and reclose the valve. This triggering command will be a sudden, short pulse to ensure that the solenoid does not remain open any longer than needed so that temperatures of the system do not drop to any critical lows as well as ensuring the limited CO_2 in the canister is not wasted. Implementing the electronic solenoid is a crucial component for success as this allows for autonomous triggering and operation for the net launcher system.

Net Deployment System
The final and main part of the Net Launcher is the net deployment system that will deploy the net in a way that allows for maximum coverage. This part will be constructed using a PVC pipe that will be cut to make four, equal-length tubes that will all be aiming outward from one another for form four barrels. These four barrels will be joined with a ¼" brass coupler that will allow the net deployment system to be attached to the previously discussed triggering valves. Each of these four PVC barrels will be attached to one another via dowels and plexiglass to allow the net to be contained between the barrels. The net will have four small metal weights, one attached to each corner, which will be placed in each barrel to serve as the 'bullets' for the mine. When triggered, the pressurized gas will be released and dispersed within each barrel; propelling the weights outward from one another simultaneously. Since these weights are attached to the four corners of the net, this will deploy the net along with the weights. To ensure that the CO_2 propels the weights efficiently, each weight must create a seal between it and the inner diameter of the barrel. This seal can simply be made by wrapping electrical tape around the weights; adding more layers as needed without creating too tight of a seal that would obstruct the weight from propulsion entirely. Having each of the barrels facing outward from one another ensures the proper expansion of the net to provide the largest deployment possible while also providing a space for the rest of the net to be held before being triggered.

Utilizing the largest net possible while also being able to deploy it successfully is a crucial component of the system. A 6'x6' net with a 1" mesh was chosen from *TheNetGunStore.com* as this completely encapsulates the given blast radius if fired directly vertical. This net is also one that is used with commercial net guns such as the one shown in Figure 33, therefore, it can be assumed it should have no issues with being propelled through the air. The biggest concern is with the drag that the net will create upon deployment; making the net not travel the required

106

distance to reach the target. This will be considered heavily when designing the piping lengths for pressure regulation to ensure there is enough pressure to propel the net as fast as possible to maximize the accuracy of the mine in case of a fast-moving target.

Reloading
This net launching system only allows for one deployment before needing to be reloaded. Before loading, it is important to ensure there is no damage to any components, all tubing and couplers are tight and secure, and the valve is in the CLOSED position. To being reloading the system, each of the weights on the net are inserted into their respected barrels; ensuring they are pushed fully into the barrel using a probe. Next, the net is folded precisely into the space allotted between the barrels. Folding the net correctly allows for safe and successful expansion when the weights are deployed. Finally, the CO2 adapter is unscrewed from the launcher to release the empty CO2 cartridge. A new 12g CO2 cartridge is loaded into the adapter and is threaded back onto the fitting until the thin metal seal is punctured and the brass piping is pressurized. One of the tubings is pressurized, the launcher is armed and should be treated with extreme caution.

5.1.8 **PCB Design**

The printed circuit board (PCB) will contain all of the primary components for power distribution for all external processors and peripherals as well as an onboard microcontroller for sending and receiving various signals to execute the task at hand. The design for the PCB needs to be as efficient as possible while only containing the components necessary to achieve proper power and signal distribution to reduce the overall size and cost to manufacture the PCB.

Power Distribution
Since the PCB will be responsible for providing sufficient power to the ATMega328, Jetson Nano, as well as all of the peripherals, it is critical to have a large enough supply power for the entire system. The PCB will simplify the need for multiple external power sources as all power distribution will take place within the board. The issue that arises with sharing a main central power supply is that each component is rated to be operational under specific power conditions. To achieve the desired power for each component, linear voltage regulators will be used to divide the supply power amongst all of the components. Table 35 shows various common linear voltage regulators that can be implemented on the PCB for powering the internal systems. Since an external power supply will be used for converting the 120VAC wall power into a stable 12V DC signal, the first input stage into the PCB will be the 12V, 6A power from the external supply. This input power will be further regulated and divided amongst multiple components either integrated within the PCB or via output terminals to allow external peripherals to be attached.

The ATMega328 that is being used on the PCB for peripheral control can be run on either 3.3V or 5V DC power. For this application, the ATMega328 chip will be

powered with 5V while running at 16MHz to utilize the maximum processing potential offered from the microcontroller. To step down the incoming 12V power from the external supply to the 5V expected from the ATMega328, the LM7805CV linear voltage regulator will be used. The LM7805 regulator outputs typicals. 5V with a max current of 1.5A which is more than ample power for the ATMega328. Since the ATMega328 is not responsible for powering any of the subsystems directly, this dedicated power to the chip is solely for processing power and sending low-power signals to the peripherals.

Linear Voltage Regulators	STMicroelectronics LM7812CV	STMicroelectronics LM7805CV	National Semiconductor LM1084IT-5.0	Texas Instruments LP2985-33
Max. Input Voltage	35.0V	35.0V	30.0V	15.0V
Min. Input Voltage	19.0V	7.0V	6.5V	4.5V
Dropout Voltage	2.0V	2.0V	1.5V	1.2V
Typ. Output Voltage	12.0V	5.0V	5.0V	3.3V
Max. Output Current	1.5A	1.5A	5.0A	0.8A

Table 35: Comparison of Various Linear Voltage Regulators

The Jetson Nano has three main sources of input power: via micro USB, barrel jack connection, as well as dedicated pins on the GPIO header. For this application, the Jetson Nano will receive power from the PCB via the barrel jack connection. This input to the Jetson Nano can support 5V and 4A max which allows for more processing power in comparison to the 2.5A that can be delivered via micro-USB. From Table 35, it can be seen that the LM1084IT-5.0 can regulate the 12V input from the external power supply down to 5V while providing up to 5A maximum current. This will supply the Jetson Nano with ample power to process all of the sensor data being collected in real-time. While using this method of power, it is critical that the J48 header on the Jetson Nano is bridged using a 2.54mm jumper pin. Placing this jumper on J48 on the Jetson Nano ensures that the Nano knows to pull power from this barrel jack rather than the micro USB input.

A similar process will be implemented to distribute power to the motor driver for the stepper motors as well as the solenoid for triggering the net launcher. Utilizing these linear voltage regulators is a very simplistic way of stepping down the input voltage, however, this comes with a very important tradeoff. When the voltage is stepped down, this 'extra' power is dissipated as heat from the regulators. This is what makes a linear voltage regulator much more inefficient than a switching regulator. The upside to using the linear regulators versus a switching regulator comes with the simplicity, cheaper cost, and a lower ripple in which results in a

less noisy signal [67]. Since the mine will run off of traditional wall power versus using a battery to power the systems, the added power consumption from the linear voltage regulators is not a critical factor and they will be utilized on the final design for the mine.

Decoupling
Switching within circuits happens very quickly and can create numerous voltage and current spikes within the circuits which in return creates added noise within the signals. The signal to noise ratio (SNR) is typically measured in decibels and is desired to be around 25dB. One method to reduce the amount of noise is by adding capacitors within the circuit, also known as decoupling. For this PCB design, capacitors were used primarily for decoupling after any sort of voltage regulation. Placing a 10uF capacitor after each regulator ensures that the ripple voltage produced at the output is reduced as much as possible to create the most stable signal possible without altering the output voltage. Similar to how rectification works as discussed in section 3.10.1 while weighing out options for incoming power supplies, capacitors can be used to smooth out a signal; filing in the gaps between voltage spikes by discharging the capacitor between peaks. This same method is applied at the 16MHz crystal used for the ATMega328. Adding a capacitor between each terminal of the crystal and the central ground is used to filter and reduce any noise that may interfere with the performance of the ATMega328 chip.

External Connections
The PCB will be designed to be the central unit for the overall mine system, therefore requiring multiple outputs to provide power to all of the external components as well as input signals to allow communication between the ATMega328 and Jetson Nano is crucial. For power, terminal blocks will be added onto the PCB to allow connectivity to the Jetson Nano, stepper motors, and triggering the solenoid. Terminal blocks are the best solution for this application as they allow for quick and easy connections to be made without having to permanently bond the PCB to the peripherals. This will greatly reduce the time needed for revisions as well as troubleshooting since terminal blocks eliminate a great number of connections that would need to be resoldered if there is a faulty part in function with the PCB. Since partitioning is critical within the design, these power terminal blocks will be located apart from the signals that are being transmitted between the ATMega328 and the Jetson Nano. The communication signals to and from the ATMega328 will be terminated on the PCB via a terminal block as well in which will routes these signals through a logic level shifter before reaching the ATMega or Jetson Nano. This is necessary for UART communication as the Nano requires 3.3V logic while the ATMega requires 5V logic.

5.1.9 Breadboard Testing

Before the PCB schematic is sent to the manufacturer for prototype manufacturing, breadboard testing will be conducted in order to determine whether or not the circuit delivers the power required to each component in a safe and efficient

manner. Testing on the breadboard is a crucial step when doing circuit design as simulations do not always account for non-ideal situations when dealing with components virtually versus the physical component within the circuit. The main objective for breadboard testing for the mine is to provide power to the ATMega328, Jetson Nano, and the general power for the GPIO rail that will be implemented on the final PCB to power the stepper motors as well as the triggering solenoid.

Before testing, it is crucial to calculate the expected power consumption under a full load. This can be achieved using the data sheets provided by each component's respective manufacturer in which specify many important parameters that are needed when designing circuits. These parameters include but are not limited to input voltages, operating currents, maximum rated currents, operational temperatures, frequency responses, etc. Using the datasheets, the maximum current and operating voltages for each component were recorded in Table 36 below. These parameters can be used to calculate the maximum power consumption from each component using the equation $P=IV$ to ensure that no component draws more power than allotted from the external power source.

Component	Operating Voltage	Typ. Current	Max Current	Max Power
ATMega328	5V (@16MHz)	0.05A	0.2A	1W
Jetson Nano	5V	2A	4A	20W
Solenoid	12V	0.05A	0.5A	6W
Stepper Motor(x2)	12V	0.4A/Phase	1.6A Total	19.2W
TOTAL:	-	-	6.3A	48.2W

Table 36: Power Consumption Calculations

After obtaining all of the crucial components for the PCB and their respective power consumptions, the breadboard construction can begin to ensure each part works as advertised and that the circuit was designed correctly. Figure 54 below gives an exploded view of all of the components being implemented on the breadboard. Laying out all of the components before constructing the circuit is a very helpful technique to ensure all of the parts needed are accounted for while also speeding up the building process as everything is well organized and readily available. Along with all of the components, a multimeter is shown in Figure 54 which is a very important instrument when breadboarding to measure all of the voltages and currents traveling throughout the circuit once the external power is supplied.
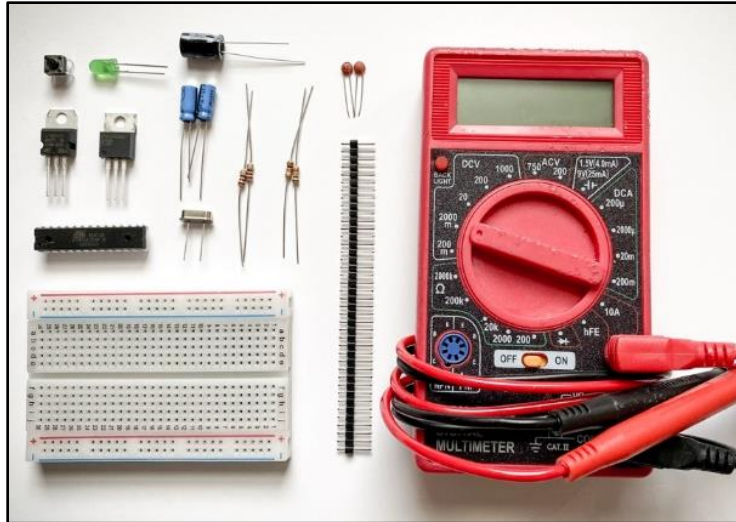
Figure 54: Breadboard Components, Exploded View

After following the schematic shown later in Figure 59, the final breadboard was constructed and ready to be tested. Utilizing the main header and footer power rails on the breadboard allowed for a much easier building experience in regard to routing the various regulated power around the circuit. As seen in Figure 55 below, the top leftmost corner of the breadboard was dedicated to power regulation. The red and black jumper wire leads to the left of the board were used to connect a 12V power supply to the circuit, which was then processed through the LM7805 and LM1048 regulators. The regulators implemented on the breadboard used a 3-pin TO-220 configuration which allows for easy connectivity to the breadboard. After regulation, the ATMega328 is powered via the 5V/1.5A regulator while the Jetson Nano has the dedicated output power shown by the orange and white jumper cable leads towards the top of the breadboard. These leads allow for easier measurement utilizing a multimeter along with multiple alligator clips during the testing phase.
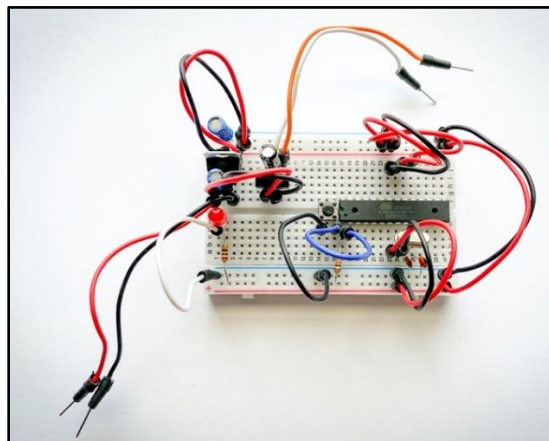

Figure 55: Assembled Breadboard for Prototyping

After the breadboard prototype was assembled and the connections were made to a Keithley 2230-30-1 DC power supply, the power supply was set to a 12V output on channel 1. An LED was included on the breadboard as an indicator for when the circuit is live; placed after the 5V regulator in series with a 220ohm resistor. Turning the power supply on illuminates the LED to show power is flowing through the circuit which allows for testing to begin to determine if the desired outputs are achieved. Using a Tektronix DMM4050 multimeter, the output voltages were measured at the dedicated Jetson Nano outputs (orange and white leads) as well as at the VCC and GND pins of the ATMega328. The output measured at the Jetson Nano was determined to be 4.9878V and the voltage at the ATMega328 VCC pin with respect to the common ground was 5.0702V, concluding that the breadboard testing was successful to provide sufficient voltages to the primary components on the board. Resistors were used to simulate a load across the Jetson Nano outputs, allowing 2.514A of current to be drawn before exceeding the resistors maximum power ratings in which would cause damage to the resistors or even the other components within the circuit. While this is not the full 4A that the Jetson Nano can draw under a full load, this is more than the current that can be provided via Micro USB to the Nano, therefore, concluding that the Jetson should not encounter any issues regarding power limitations.

5.2   Software Design

Section 5.2, Software, outlines any software implementation within the design. It covers how we are going to design the algorithm for object detection and tracking, setting up the Wi-Fi peer to peer connection, etc. The software design will later be integrated with the hardware design. The goal of the software is to first load in the camera feed using OpenCV. We want to take the captured video frame by frame in order to process it. The capture frame will be compared to the trained object detection/ classification model (we will need to train the own object detection/classification model). If a drone classification is made, we will pass it to the tracking algorithm. In the meantime, a metadata overlay will be applied Using a KCF tracking algorithm we will follow the drone and activate the firing mechanism using a prediction algorithm.

5.2.1 Software Flowcharts

This section will outline the software flow for both the NVIDIA Jetson Nano that handles the computer vision, and neural network computation, and the ATMEL ATMEGA328 which handles motor control.

NVIDIA Jetson Nano Flowchart
Figure 56 outlines the software block diagram. We first take in a live video feed from the camera that will be pre-processed (normalized, filtered, etc.) using OpenCV in Python. After we pre-process the video, we will use TensorFlow to detect any objects in the frame. A bounding box will place around the object and a classifier will be placed on the object. We will place a confidence percentage, as well as class, on each object detected. Depending on the object, the main function

will send a signal over to the PCB to move the motor or fire at the target. If no objects are detected, it will loop through the object detection until it finds something. Live video will be sent to the land station as a video is captured.
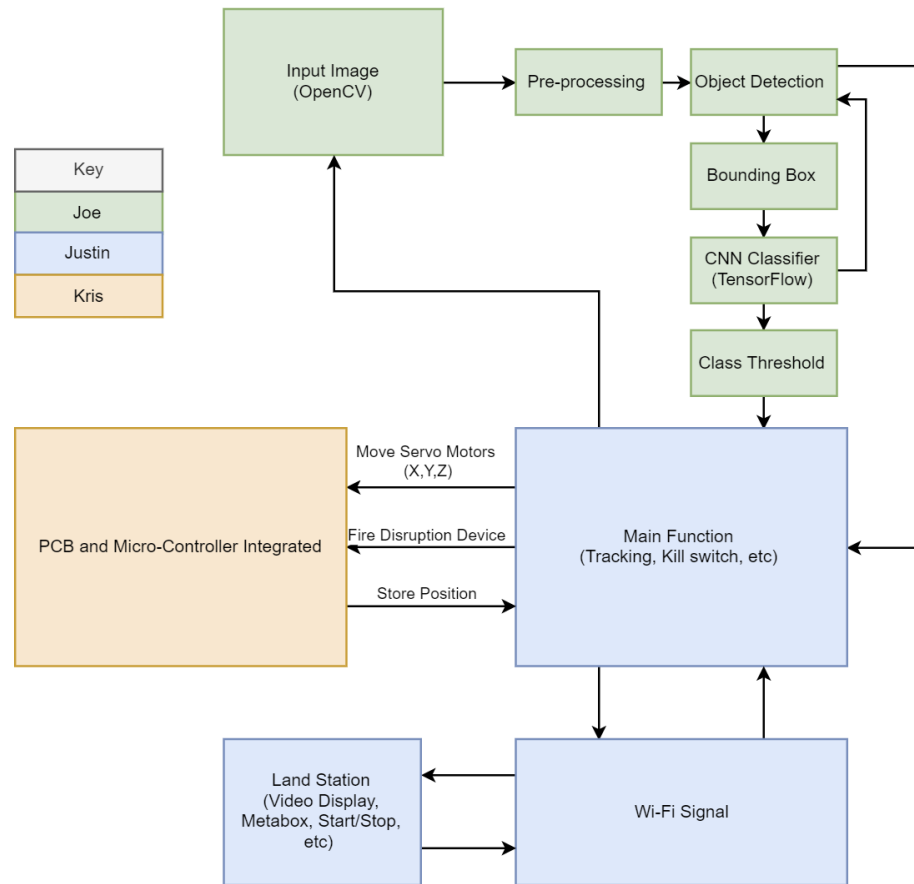

Figure 56: Software Flow Chart for the Jetson Nano

ATMEGA Software Flowchart

For the main control hub, the ATMEGA as referenced in Figure 57, we start with receiving and decoding the UART (x,y,z) coordinates. Then, based on if a new coordinate triplet is returned, i.e. the computer vision running on the Nano has detected a drone for a given time step, then we proceed to adjust the motors left, right, up, and down to match the detection location to the center of the frame. Based on experimental evidence, we can incorporate logic to aim the net launcher in front of the current location of the detection location. If the z coordinate is under 3 feet, then the firing mechanism will be enabled. The interception of the drone should happen as far from the system as possible in order to account for the deployment delay of the net. If new coordinates are not received, i.e. the computer vision has lost the drone, then the software enters a waiting state, whereupon five seconds of waiting, the system transition to a Scanning state, where it can structurally look for new targets. Both the Visual Servoing and Scanning states

output control signals to the two motors and firing mechanism (as seen in Figure 57 below).
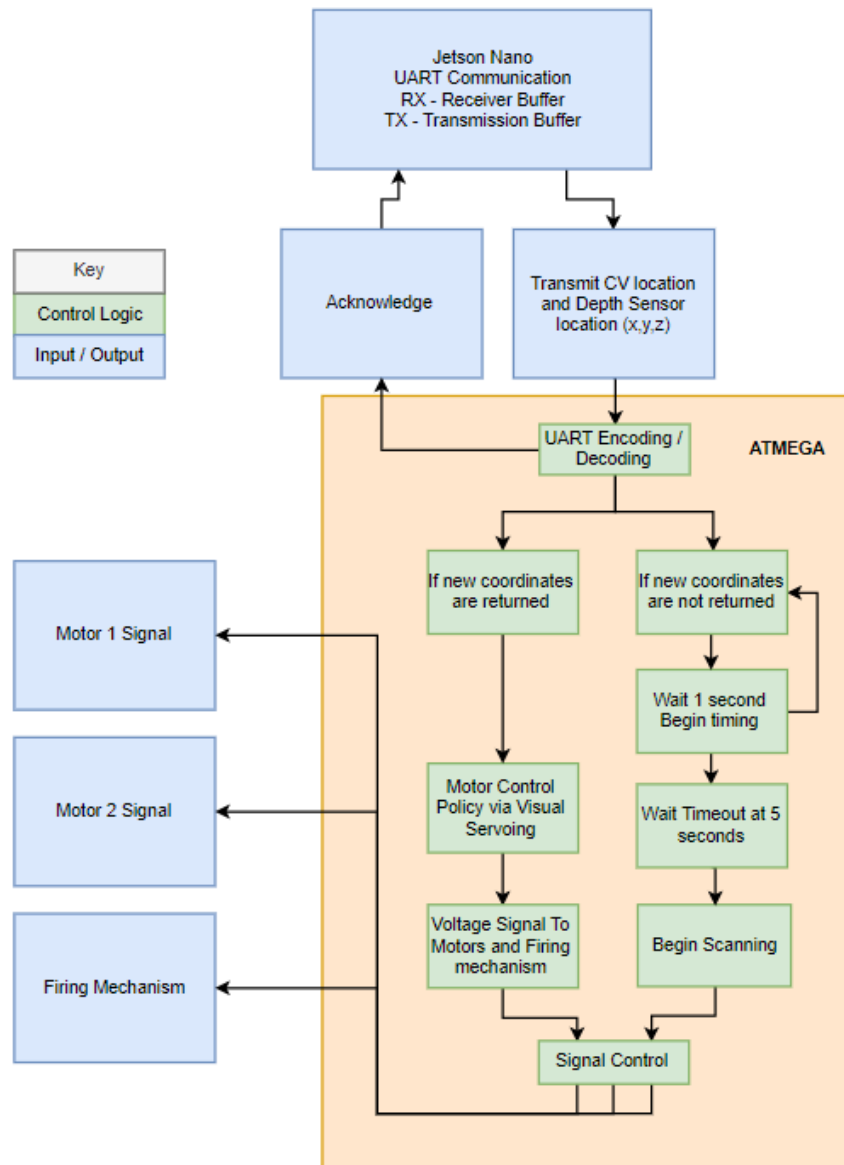
Figure 57: Software Flow Chart for the ATMEGA328

5.2.2 Object Detection and Recognition

Implementing a Faster R-CNN object detector with a transfer-learned MobileNet-v2 convolutional neural network backend provides intelligent bounding box nomination, and classification. The network was trained in MATLAB with parameters and techniques specified in the technology comparison. The network is then exported into the ONNX file format and optimized for Nvidia GPUs with TensorRT and serialized. The engine is loaded in its optimized format in the main

114

Python script that uses OpenCV to read image frames, apply image pre-processing, and continue to pipe the detections down the computer vision pipeline.

5.2.3 Tracking

Implementing a KCF tracker in python with OpenCV allows for temporal correlation between detections with a regressive bounding box. This helps to smooth detection locations over time and establish smooth tracks. KCF tracking should be easy to implement since OpenCV 3.1 has a built-in implementation. It will take in the processed (classified and bounded) frame and initiate the tracking around the bounding box

5.2.4 Turret Movement

Once the target has been successfully located and tracking has commenced, it is imperative that the turret is able to move with the target and attempt to keep it located within the center of its line of sight (LOS). This will be achieved via the ATMEGA328 but will require location info sent from the Jetson Nano.

To achieve this feat, the Jetson Nano will relay information about the target's exact position in a frame via a UART communication scheme. This transmission will be handled at a relatively low baud rate, most likely 19200, which should be more than fast enough to relay the information between frames. The information sent will consist of the position of the target's bounding box center in relation to the center of the frame. Being that the goal is to align the center of the launching mechanism with the cameras center point, this should be enough information to allow accurate firing and ultimately disabling of said target.

The information sent via UART from the Jetson Nano will inform the ATMega of how off-center the target is, in terms of angle in the yaw and pitch rotation planes. This angle will then be converted into an exact amount of steps that the motor should take in order to center the target within the camera LOS. This will then be used to control the motor driver, via the Arduino Stepper library, which will, in turn, ensure the motors translate the targeting system to the correct position.

5.2.5 Enabling Launch Sequence

Being that UART communications already exist to relay the angle between the center of the bounding box and the center of the frame, the system will also be able to utilize this communication to relay when firing is necessary. This is where the selection of the Intel RealSense D415 camera module becomes necessary.

Since the requirement of the system is to not fire upon target unless it is in the target zone cylinder (3' radius x 10' height), the ATMega must know when the target has entered this range. The RealSense D415 will be able to locate this third position coordinate (depth) of the target via its included SDK libraries and stereo camera configuration. Once this depth is calculated it will then be sent, along with the angle information, to the ATMega328 chip. If this depth is appropriate, and within the required firing zone, then the ATMega will send a high signal to the solenoid. This will, in turn, cause the launching mechanism to be activated, crippling the target and causing an abrupt end to its flight.

5.2.6 Interface

This section will document interfaces that the user will use. These interfaces will be on the land station when conducting the final presentation.

Metadata GUI
Simple bounding boxes can be overlaid onto the live camera feed, which is returned by the object detector. Class labels and class confidences are determined by the most confident class returned by the classifier, and range to target will be estimated by the range to the center of the detection boxes. These statistics will be incorporated in a simple GUI and saved to local storage on the microSD card in a data structure. Figure 58 displays an example of what the land station GUI interface will look like.

Figure 58: Live Video Feed GUI

Land Station Commands
The land station will have the commands for the kill switch and the startup/ power-down sequence. Since we will be running the program in Python the startup sequence will the run icon on the IDE and the power down sequence will just be exiting out of the Python script. The kill switch will just be pressing, ctrl + z or the character 'q'. This will force quit out of the python script. The live video window will no longer show, and the mine will be powered off. The mine is run entirely on a python script so the easiest and most effective way to work the commands was to use the python shortcuts.

6.0 System Integration

With the software block diagram drawn out as well as the hardware, the goal is to integrate all the components into a seamless design. For the DOMINANCE mine, there will only be one PCB that connects the signal computer from the Jetson Nano into the servo mechanism. This section outlines the thought process that occurred when integrating the system into a singular design. The goal of the integration was to match or improve upon the initial design represented in the block diagram, Figure 1.

6.1 Controller Pin Usages

This section contains a list of the pins that are utilized on each controller, along with a description of the function that each pin serves. There will be a dedicated table for each controller: the Jetson Nano Developer Kit and the ATMega328.

NVIDIA Jetson Nano Developer Kit
Below is a table that lists the pins (and ports) that will be used on the Jetson Nano Developer Kit. Since the Jetson Nano module will still be attached to the carrier board in this application, actual pins from the 260 pin SO-DIMM connector will not be referenced here, but rather the ports and connections that are located directly on the carrier board. All of these port names were referenced via NVIDIA's user guide for the developer kit [68].Table 37 lists the pinout descriptions for the Jetson Nano Developer Kit.

Jetson Nano Dev Kit Connection	Connection Description
Power Jack (J25)	Power connection resulting from voltage regulator delivering 5V 4A
USB-A Port 1 (J32.1)	Connected to Intel RealSense camera module for imaging purposes
USB-A Port 2 (J32.2)	Connected to WiFi module for wireless live feed and control purpose
GPIO Pin 8 (J41.8)	TX: Used for UART communication with ATMega328
GPIO Pin 9 (J41.9)	GND: Connected to ATMega328 GND to ensure common ground
GPIO Pin 10 (J41.10)	TX: Used for UART communication with ATMega328

Table 37: Jetson Nano Developer Kit Pinout Descriptions

ATMEL ATMega328
Below is a table listing the pins of the ATMega328 chip that this design will utilize. Pin names come directly from the pinout listed in the ATMega328 datasheet, but specific names located in the description (i.e. Digital 1 / D1, VCC, etc) are referenced by the names given to them in an Arduino implementation. This is appropriate, however, as the chip will utilize Arduino software and function accordingly. Table 38 lists out the pinout description for the ATMega 328.

ATMega328 Pin Number	Connection Description
1	RESET: Connected to VCC (5V) through resistor
2	RX: Used for communication with Jetson Nano
3	TX: Used for communication with Jetson Nano
4	D2: Connected to motor driver one for use as IN1
5	D3: Connected to motor driver one for use as IN2
6	D4: Connected to motor driver one for use as IN3
7	VCC: Connected to 5V 1.5A power source
8	GND: Connected to system ground
9	Crystal: Connected to 16MHz Oscillator
10	Crystal: Connected to 16MHz Oscillator
11	D5: Connected to motor driver one for use as IN4
12	D6: Connected to motor driver two for use as IN1
13	D7: Connected to motor driver two for use as IN2
14	D8: Connected to motor driver two for use as IN3
15	D9: Connected to motor driver two for use as IN4
16	D10: Connected to solenoid controlling CO_2 release
20	AVCC: Connected to VCC (5V 1.5A source)
22	GND: Connected to Jetson Nano for common UART ground

Table 38: ATMEL ATMega328 Pinout Descriptions

6.2 **PCB Schematic**

Located on the following page is a representation of what will be included in the initial PCB design that was elaborated upon in Section 5.1.8. The design will feature all circuit routing and power step down for the power distribution system. Also to be included in the PCB design is the connection for the ATMega328 chip which will also features traces to terminal bloacks that will allow the motor drivers to be easily connected via signal and power. Other connections include a dedicated power output for the Jetson Nano, UART connections along with logic level shifters for communication from the Jetson Nano and ATMega328 chip, and the connection to the solenoid for triggering the net deployment system. The PCB allows for simplified connections to be made while also providing power to all the subsystems in the overall design.

Figure 59: PCB Schematic
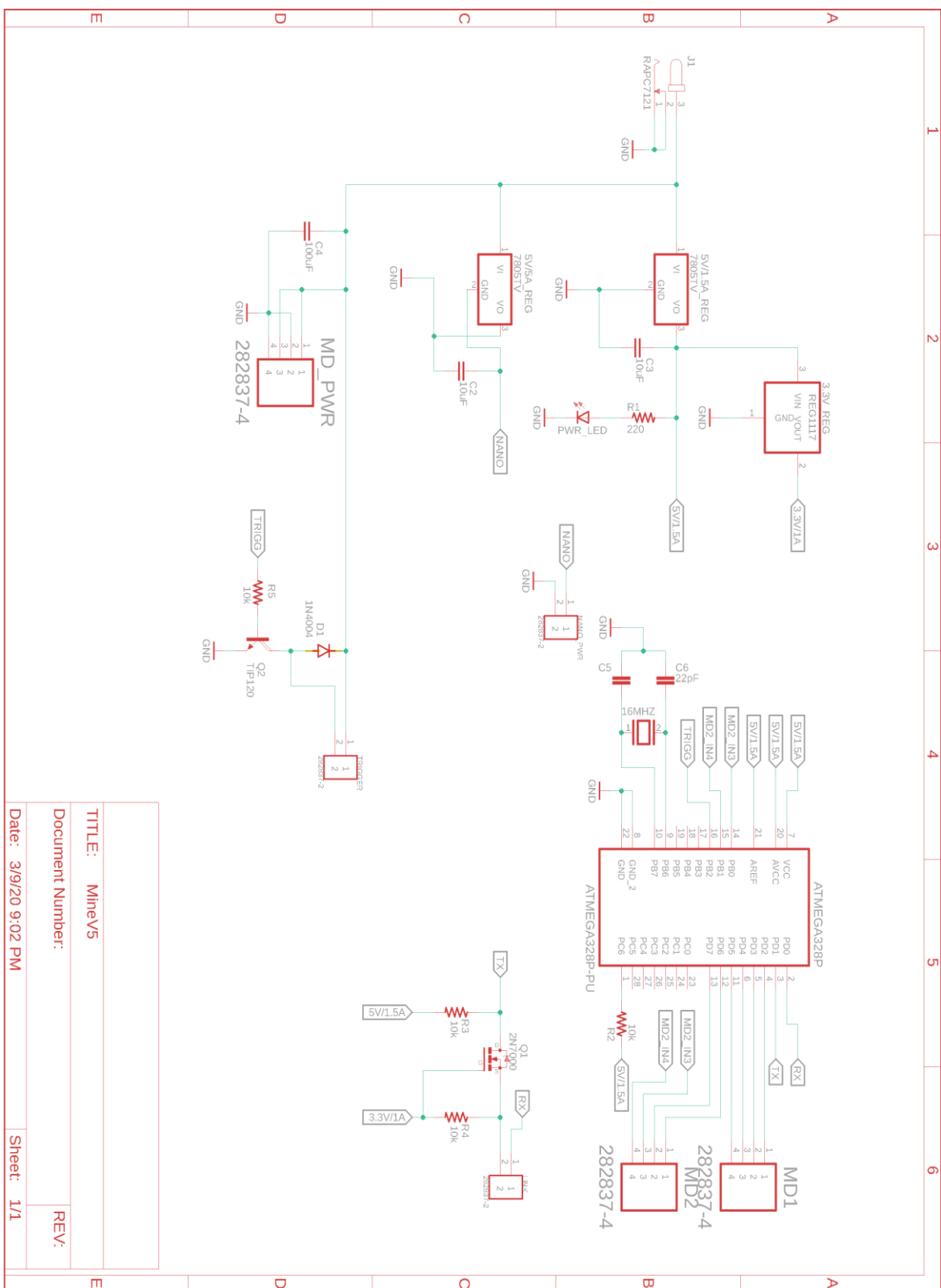
6.3 Hardware and Software Integration

This section will further detail and summarize the integration of the hardware components, the integration of the software components, and the overall hardware-software integration in the completed assembly.

6.3.1 Hardware Integration

This section will focus on integrating all hardware components including the controllers, turret movement mechanism, and net launcher. Referring to the hardware flowchart located in Section 5.1.1 will supply a broad overview of the hardware integration plan, but here a slightly more in-depth view will be given.

Supplying Power to the System
The first step in this hardware integration to supply power to the system. The power source to be utilized is a 12V 6A power supply that will be connected straight to wall power (120VAC 60Hz). The output of this supply will then be connected to the PCB, via a barrel jack, and be sent to the branches of the power distribution system. Here there will be three main lines: A 12V line branching straight from the supply to the motor drivers, a 12V line being sent to a voltage regulator that will step it down to 5V 1.5 A for the ATMega328 power, and a final 12V line branching to another voltage regulator that will supply the Jetson Nano with a 5V 4.5A source.

Connecting the Controllers and their Components
To connect the controllers for UART communications, and to their respective components, as detailed in Section 5.1. The steps to connecting the controllers are simple and involve connecting their ground lines so that ey feature a common reference, and then connecting the TX of one device to the other and vice-versa. These are the only steps required (in hardware) to communicate between the two controllers.

Once the controllers are correctly wired and able to talk, it is imperative that the sensors and their modules are then successfully connected. In terms of the Jetson Nano, this will require the Intel RealSense camera module's male USB-A connector to be connected to the J32.2 USB-A female connector on the Jetson Nano Developer Kit. The final component to pair with the Nano is the COMFAST WiFi module and can simply be inserted into the second female USB-A connection point on port J32, J32.1. After these steps, the Jetson Nano has been fully configured, hardware-wise, and its integration step is complete.

In tandem with the configuration of the Jetson Nano, the ATMega328 must also be correctly integrated into the system. To achieve this it's remaining components must be correctly wired to the chip. This includes an oscillator, power connections, solenoid, and motor drivers. The power is connected to VCC and AVCC of the ATMega328 chip while the ground wire is connected to the two GND pins. Once this is complete, the oscillator must be connected to the appropriate crystal pins, pin 9 and pin 10. This is what allows the chip to function properly at its expected

16MHz clock speed, and without it, this subsystem would not function at al. Next is the solenoid which will simply be connected to pin 16 of the ATMega. The solenoid will be triggered with a HIGH signal from the controller, and will easily be controlled via Arduino's "digitalWrite(10, High);" command. The final component to connect to this control scheme is the two motor drivers. This was heavily detailed in Section 5.1.6, and consists of connecting the Arduino-mapped digital pins 1-9 to the IN1-IN4 connections of each motor driver. This will allow full control of the motors via the circuitry included in the Big Easy Driver.

Wiring the Motors to the Motor Drivers
Connecting the motors to the motor drivers involves connecting the correct controls to each phase of the motor. Since the motors used in this design are bipolar two-phase motors both the positive and negative terminals to ensure the correct stepping of the motors. Here the A- and A+ wires from the motor must be connected to correct A- and A+ ports on the motor driver. The same must be completed for the B phase of each motor. Once this has been completed the motor is to be tested via a full rotation of all its steps and be verified that it is stepping at an accurate $360°$. Once this is verified the system is fully powered and wired correctly. The final step is to attach the components to the chassis and secure them.

Securing Components to the Chassis
Once all previous components have been integrated, the final step is to attach everything to the chassis and test. The motors are to be mounted on the chassis assembly as is displayed in
Figure 49. Motor two is to be connected to the base of the chassis with the output shaft pointing directly downwards. This will then be secured to the base via a fastener and will enable the yaw rotation in the system. To achieve pitch rotation in the system the second motor must be attached one of the bracing supports that extend upwards from the base. This motor will be screwed directly into the plate via holes and settings designed in the CAD model of the frame.

Once the motors are secure the next step is to connect the net launching mechanism to the output shaft of the pitch controlling motor. This will let the launcher follow the path of the motor output shaft and create a very reliable pitch control of the launcher. The launcher is now fully secured and integrated with the system. Following this is attaching the Intel RealSense camera module to the top of the launching mechanism, as is shown in the aforementioned figure above.

Finally, the electronics will be mounted to the base of the chassis. This includes the Jetson Nano and PCB. Once this is complete the hardware is completely integrated and the software integration is ready to be initiated.

6.3.2 **Software Integration**

First, we instantiate a Python runtime environment hosted on the Jetson Nano. This environment handles both the computer vision function calls, primarily through OpenCV libraries, and Deep Neural Network computation, primarily through TensorRT, CUDA, and cuDNN libraries. All are instantiated in a single environment. This instance will take in camera data, through OpenCV, and run the deep neural network image processing. Alongside this process, Depth will be processed by the on-board video processing unit on the RealSense camera, then ported via USB 3.0 to the Jetson, that input is handled by the RealSense SDK and incorporated into the Python runtime environment. So, both Image data and depth data will be ported into the same environment. After the bounding box prediction is generated, new x, y, z coordinates are generated. These are used in conjunction with past coordinates to produce a time of arrival, and range to target directly on the Jetson Nano. Confidence values are already produced at the bounding box stage, so all information to be written to the GUI can be communicated via wifi to the ground station at this point. Detection video will be saved in the background for later review.

The coordinates are communicated to the ATMega328 via UART connection between the module and the Jetson Nano Developer Kit. On the ATMega328 chip itself, mapping is done to perform visual servoing based on the received x, y, z coordinates to the control the motors. A simple feed-forward system suffices for the control policy, as new values are constantly piped in from the Jetson Nano. If no new values are sent via UART, i.e. the computer vision algorithm loses the target. Then, after five seconds, the module moves to a structured scanning of the surroundings in order to try and queue on new targets. Voltage signals from the module are translated to the stepper motors to move them.

7.0   **Testing (Unit and System Level)**

Testing will occur at each level to ensure we will have a safe and working disruption device. The following section will discuss how we will test the software and hardware implementations of the design.

7.1   **Unit Testing**

This section will detail the unit testing that will occur throughout the development process. The overall system has been broken down into multiple subsystems that are all to be tested prior to full integration. All of these tests have been completed as of this point. The unit testing will function as follows.

7.1.1 **Hardware**

For hardware unit testing, the system was broken into three five major subsystems: the PCB design, camera subsystem, WiFi communication subsystem, net launching subsystem, and motor control subsystem.

PCB Design Unit Testing
The first portion of this testing consisted of using a breadboard in tandem with the components designed to be placed on the breadboard. This testing was further explained in Section 5.1.9 and consisted of testing the power outputs from the regulators and power supply. All of these voltages checked out with the expected values.

Once the voltages are verified the next step is to test the connection to the ATMega328 connection via the breadboard. This will require the flashing of the ATMega328 with Arduino software. Once this is complete, and all inputs/outputs are functioning as expected, the breadboarded version is then ready to be tested in the full system. If this functions as expected, then the PCB is ready to be integrated into the system and tested in the exact same fashion.

Camera Subsystem Unit Testing
The camera will be simple to test as a live video feed, dynamic depth calculations, and proper actions via the included libraries will verify its functionality. This subsystem will be tested using a Jetson Nano that is powered via a reliable power supply. The camera will be connected to the Nano, and then the live feed will be verified to be reliable and free of blemishes. If this is completed and the unit passes the visual testing the camera will then be subjected to a depth testing using the SDK libraries included with the purchase of the module.

To confirm the depth testing, multiple objects will be placed around the scene and the distance to the objects will be compared to the actual distance from the sensor. If these distances are relatively close, and the values were derived from the SDK, then the module will be considered to be functioning properly and will be sent to the full-scale integration test. If not the module will be shipped back to the

manufacturer and a new module will be requested as a replacement for the faulty equipment.

WiFi Communication Subsystem Unit Testing
The testing for this subsystem will consist of inserting the COMFAST WiFi module into a Jetson Nano that is powered via a reliable power source.. If the module is able to communicate with the device via the WiFi module then the test will be deemed a success, and the module will be ready for full-scale integration testing. If the module is not able to communicate with the device, however, then the system will be debugged until the issue arises. Once this occurs the issue will be eradicated and then unit testing can begin once again.

Net Launcher Subsystem Unit Testing
The testing of this subsystem will take place after the full launching mechanism has been developed. The main difference in testing is that, instead of using the electronically controlled pressure valve (solenoid), initially a mechanical ball valve with a lever will be used. This will be beneficial in the fact that it will allow the system to be fine-tuned and tested more efficiently than if it were to be connected to an Arduino from the start. The variables being examined here are the trajectory of the net and the velocity in which it travels. Obtaining a proper combination of these two factors will consist of changing the weights attached to the net and changing the tightness in which the weights are contained in the firing cylinders.

Once this testing has been completed, and the results are repeatable and satisfying to the design requirements, the mechanical ball valve will then be replaced with the electronically controlled pressure valve. This valve will then be connected to an Arduino Uno and testing will occur to confirm that the signal from the Arduino is able to trigger the valve to launch the net. If this functions as expected, then the net launching mechanism is ready to be integrated into the full-scale system and tested.

Motor Control Subsystem
The motor control subsystem was initially tested using the motor driver in tandem with an Arduino Uno. The second step of unit testing for this subsystem will consist of abandoning the Arduino and testing via the bread boarded PCB design. This will verify that the design is still valid using the Arduino-flashed ATMega328 chip. Once this is validated this subsystem will be ready for full-scale integration testing

7.1.2 Software

Unit testing will occur throughout the development process. For the software implementation, we will develop each algorithm separately and unit tests them by running new data sets to see if they can work. Once it is established that they can work independently, we will integrate the algorithms and run tests on it again. We will divide the software system into three parts: the camera SDK, object detection / deep learning, and control policy.

For testing the stereo camera with the RealSense SDK, testing can easily measure the true distance from the camera to a floor marking and place objects at various distances to measure what the reported values are in the point-cloud against the true distance. Testing also needs to be conducted on how size in x and y attributes to uncertainty in depth perception.

For the object detection / deep learning component, unit testing will be done beforehand on the acquired dataset from the data collects at Lockheed Martin's facilities. The custom data set serves as a testbench and benchmark for classification and localization capabilities. Factors to be examined are the confidence level, center position of detections, and false alarm rate.

The motor control policy will be implemented on the ATMega238 chip, which can be tested and adjusted by experimental evidence. This control policy is dependent upon the performance of the CO_2 net launcher, thus control policy will have stochastic elements. Adjusting the correct firing angle based on the given x, y, z coordinates will be tuned experimentally over the effective range. Testing will be structured in 1-foot increments in each direction to capture the full effective range from the 3-foot radius to the 10-foot ceiling.

7.2 Full-Scale System Testing

System-level testing will occur after the development process. This will be the final testing before the demonstration. The goal is to fully integrate the components and run a thorough dry run of the device utilizing a live target. The list of requirements will be examined in depth once more and met requirements will be checked off accordingly. This will not only be relevant in terms of validating the functionality of this system but will also allow the customer to see that all of their aspirations for this design have been met. The plan is to mimic the obstacle course on test day.

8.0 **Project Operation**

This primary goal of this section is to provide an "owner's manual" for the DOMINACE land mine. This section discusses how to operate each major subsection of the mine; set up, net launching, start up and shut down, as well as creating a wide local area network.

8.1 **Setting up the Mine**

The DOMINANCE mine will be simple to setup, but must be configured correctly. The first step in this procedure is to attach peripherals (mouse, keyboard, monitor) to the Jetson Nano so that the system can be booted properly and the computer vision algorithm will be loaded.

Next the user is to attach the micro-USB cable to the Jetson Nano so that power will be supplied. Upon powering on of the system it is appropriate to run the executable CV algorithm as well as attach the PCB power source (12V 8A) so that the motors and solenoid are ready for operation.

Now that the mine is ready for deployment it is appropriate to unplug all peripherals and allow the only two incoming wires to remain the power sources for the Nano and PCB. The mine is now operational and will look for drones to begin tracking within its respective FOV.

8.2 **Creating a W-LAN**

The DOMINANCE mine will be able to send live video feed and metadata back to the land station (laptop) using a local area network set up by the router. We will discuss how we establish a connection between the three devices.

8.2.1 **Setting Up the Router**

The first step is to set up the router. Since we will not be using an Internet Service provider, we can just power on the router set up the wireless router communication. All we need to determine if the router's IP address. It will not be necessary to set up any additional security for the router.

8.2.2 **Setting Up the Land Station Communication**

Once we establish a LAN connection, all we need to do is connect the device that will be communicating with each other. The lands station will now need to enable file sharing in order to receive data from the mine [69]. Below are the steps:

1. Go to Start>> Control Panel >> Network and Internet >> Network and Sharing Center >> Advanced sharing settings

2. Select "Turn on network discovery"

3. Select "Turn on file and printer sharing"

4. Click "Save Change"

Figure 60, provides an image of what the configuration should look like.

Network discovery

When network discovery is on, this computer can see other network computers and devices and is visible to other network computers.

◉ Turn on network discovery
◯ Turn off network discovery

File and printer sharing

When file and printer sharing is on, files and printers that you have shared from this computer can be accessed by people on the network.

◉ Turn on file and printer sharing
◯ Turn off file and printer sharing

Figure 60: Network Discovery/ File and Printer Sharing

8.2.3 Setting Up the Mine Communication

Setting up the mine connection to the local area network will be simple and straight forward. We need to simply connect the Wi-Fi module to the corresponding IP address. Once this connection is made, we are ready to begin transmission.

8.3   Launcher Mechanism

This subsection will outline the step-by-step procedure to load the CO2 canisters, as well as load the net into the net launcher, and how to prime the launcher correctly before the system is ready for deployment.

8.3.1 Loading CO2 Canister

Before loading the 12g CO2 canister into the respective adapter, it is crucial to check all brass piping and fittings to ensure they are fully tightened with Teflon tape applied at each connection as well ensure that the ball valve is in the "closed" position. This is entirely for safety reasons as the system ungoes high pressure once the CO2 is enguaged. The canister holder is then unscrewed from the base counter clockwise until the canister holder is separated from the adapter fitting. A 12g CO2 cartridge is then loaded into the canister holder and threaded back onto the adapter fitting and tighted until the 12g canister is pierced and the launcher is armed.

8.3.2 **Loading Net Launcher**

To begin loading the net launcher, the net is first laid out flat to ensure no knots or tangles are present. Each counterweight is then gathered into one hand while the other hand grabs the center of the net; stretching it out to make the net gather tightly together. The center of the net is then placed into the space between the four barrels and folded over itself until the net is folded entirely leaving only the counter weights exposed from the bunch. Finally, each counter weight is loaded into its respected barrel with extreme caution ensuring none of the weights 'cross' over eachother. If any of the weights are place in an incorrect barrel, the net will not deploy correctly and will tangle itself upon launch. After ensuring the net is loaded correctly and the weights are fully sunk into each barrel, the net launcher is loaded and ready for deployment.

8.3.3 **Priming the Trigger**

The final step before the device is ready to fire involves setting up the triggering mechanism. The ball valve arm is place against the solenoid actuator and the spring (rubber bands) are stretched around the end of the valve arm, ensuring they are tight and pulling the arm against the solenoid. The solenoid is then ready to be actuated in which will release the ball valve arm, allowing the valve to spring open and release the CO_2; propelling the weights from the launcher.

8.4 **Software**

This subsection will outline the step-by-step procedure to launch the software code and how to activate the E-stop mechanism. After initialization, the main function, written in MATLAB, will connect to the Jetson Nano over an isolated WIFI network. After connection, the software will call the camera object on the Nano and start streaming frames to the host laptop. Frames are not scheduled, only called as needed.

8.4.1 **Software Activation**

After the script is started on the host laptop, and the connection to the Jetson Nano initialized, the main loop begins. A frame is grabbed from the camera through the video4linux library, and sent wirelessly over ssh to the host computer. Next, the Faster R-CNN is run on the image to return a position of any drone within the frame. If there is no drone, then another frame is grabbed. If the object detector finds something, a bounding box is overlaid onto the input image. The position is compared against the 15% threshold for finding the center to compute whether the mine is pointing ON TARGET or OFF TARGET. The difference between the bounding box's position and the center of the frame are sent to the C++ script on the Nano to actuate the motors. The Time of Arrival counter beings. As long as the distance is within firing range (10 feet), the main loop iterates and another frame is grabbed. A real time clock begins after the first frame is grabbed, and will continue to count down for 5 seconds until the time of arrival counter hits 0. This timer is reset if the object detection breaks during that 5 seconds. If there are 5

seconds of continuous detections, in firing range, and the mine is pointing at the object (within 15% of the center of the frame) then the main function will branch off to call the python script to trigger the firing solenoid through the GPIO pins.

8.4.2 E-Stop Activation

Our E-Stop correctly ends all processes on the Jetson Nano. Each script, for solenoid firing, and motor control cleans up GPIO voltages upon each call, so no additional actions are required other than breaking out of the main function, and clearing the ssh connection to the remote Jetson Nano.

8.5 Power Down

This subsection will outline the step-by-step procedure to exit out of the software tool and power down the mine.

8.5.1 Software Shut Down

Since the software tool is an executable running on a command promt, pushing the buttons "ctrl + z" will close out of the program and stop the software. No furture steps are necessary to shut down the software script.

8.5.2 Power Off

With the software script powered down it now safe to power down and disarm the entire mine.

A. If the launcher **has been deployed** with CO2 fully dispated, all that is necessary is to unplug the 12V power supply from the PCB.

B. If the launcher **has been not been deployed** and there is still a full CO2 canister, it is necessary to:

    1) Remove the net along with all four counterweights from the net launcher.
    2) Gently manually actuate the ball valve; releasing all pressure within the system.
    3) Unplug the 12V power supply from the PCB.

9.0 Administrative

This section will include details for multiple administrative portions of this project, such as the initial milestones that were constructed and budgeting information.

9.1 Initially Constructed Milestones

Listed here are the milestones that were initially constructed to aid in time management for the development of this system. This focuses not only on senior design 2 development milestones but also for paper submission milestones required for senior design 1.

9.1.1 Senior Design One

Being that Senior Design One is focused on picking, researching, planning, and documenting the project that will ultimately be implemented and built during Senior Design 2, most of the milestones listed here will consist of documentation deadlines for various submissions over the course of the semester. Submission dates were updated prior to the completion of this document and are accurate to the day. Projected component procurement dates are also listed in this table but delays in the ordering system pushed this task further into senior design 2. Table 39: Senior Design One Milestones outlines the timeline of Senior Design One.

Requirements / Tasks	Start Date	Completion Date
Group and Project Selection	August 26, 2019	September 9, 2019
Initial Project Document – Divide and Conquer	September 9, 2019	September 20, 2019
Initial Project Proposal	-	September 23, 2019
Updated Project Document – Divide and Conquer Revision	September 21, 2019	October 4, 2019
Senior Design Project Documentation – 60 Pages	October 5, 2019	November 1, 2019
Senior Design Project Documentation – 100 Pages	November 2, 2019	November 15, 2019
Select and Procure Components / Materials	November 2, 2019	January 6, 2019
Senior Design Project Documentation – 120 Pages (Final)	November 16, 2019	December 4, 2019
Initial Design Presentation (LM Corp.)	-	December 2, 2019

Table 39: Senior Design One Milestones

9.1.2 Senior Design Two

Senior Design Two focuses on the building and implementation of the actual prototype and the testing and redesigning that comes with this task. Table 40 outlines the timeline of Senior Design two and denotes whether the presentation and demonstration dates are mandated through the University of Central Florida or Lockheed Martin Corporation.

Requirements / Tasks	Start Date	Completion Date
Preliminary Design Review (LM Corp.)	-	January 8, 2020

Test Components / Parts	January 6, 2020	January 13, 2020
Design Initial Software Infrastructure	January 6, 2020	February 19, 2020
Assemble Initial Hardware Prototype	January 14, 2020	January 28, 2020
Design Final Software Infrastructure	February 20, 2020	March 1, 2020
Integrate Hardware and Software	March 2, 2020	March 20, 2020
Test and Redesign (if necessary)	March 21, 2020	April 12, 2020
Customer Demonstration (LM Corp.)	-	Canceled
Customer Presentation (LM Corp.)	-	April 13, 2020
Senior Design 2 Presentation (UCF)	-	April 15, 2020
Senior Design 2 Showcase (UCF)	-	Canceled

Table 40: Senior Design Two Milestones

9.2 **Financing and Estimated Budget**

This section outlines the projected costs that will be incurred during the prototyping of this design. Lockheed Martin Corporation has granted the DOMINANCE Mine Team with a budget of $700, including an extra $350 for prototyping costs. This allows an overall development budget of $1050.

LM Corporation Budget	Allowance (in dollars)
Baseline Budget	$700.00
Additional Prototyping Budget	$350.00
Total Budget	$1050.00

This budget also does not consist of any replacement components required if they were to be damaged or destroyed. This is strictly a unit cost.

Part Name	Quantity	Price Per Unit
Jetson Nano Dev Kit	1	$98.00
ATMEL ATMega328	1	$6.99
Intel RealSense d415	1	$149.00
64GB MicroSD Card	1	$13.99
PCB Manufacturing	5	$17.99
12V 6A Power Supply	1	$10.99

NEMA 17 Stepper Motor	2	$7.63
Big Easy Driver	2	$19.95
Net Launching Mechanism	1	~ $100.00
CO_2 Cartidges (15 Count)	1	$6.97
6' x 6' Mesh Net	1	$36.00
Chassis Construction	1	$37.48
Wires,Headers,Connectors	1	~ $60.00
Total Costs		$565.90

Table 41: Estimated Budget Breakdown

10.0 Conclusion

The DOMINANCE Landmine project not only challenged the knowledge but the teamwork skills. As a team tasked to develop a fully functioning disruption device with a list, given from the customers, of specified engineering requirements to meet. There was a need to figure out how to design, research and develop the mine.

Although the DOMINANCE mine was intimidating at first, it became easier to tackle once the planning of the design was made as well as the dividing of tasks. It was decided that the divide and conquer method would be the best approach to complete the project. Two Electrical and Computer Engineer (ECE) students were tasked to accomplish the hardware design while two other ECE students were tasked to develop the software. It would be able to easily integrate the two groups once the design process was completed.

The overall goal of the design was to it an easy to use and effective disruption device while meeting the specified customer requirements. Many iterations of designs were considered while developing the device. Through unit testing was accomplished once a developed working prototype was made. It was important that a focus on meeting the requirements, tasked to us, was made.

One of the biggest accomplishments of the DOMINANCE mine project was victoriously integrating the software detection and tracking algorithm onto the PCB and Jetson Nano. This was the hardest task but was accomplished with careful planning and teamwork.

11.0 **Appendices**

The final section consists of the appendix. This section consists of references that were used throughout the paper. It has been cited in IEEE format. We also provide emails sent for copyright permission to use specific images.

11.1 **Appendices**

[1] J. Dobbin, "HP," 24 February 2019. [Online]. Available: https://store.hp.com/us/en/tech-takes/gpu-vs-cpu-for-pc-gaming. [Accessed 3 December 2019].

[2] I. Automotive, "medium.com," Medium, 9 August 2018. [Online]. Available: https://medium.com/@intellias/the-ultimate-sensor-battle-lidar-vs-radar-2ee0fb9de5da. [Accessed 18 October 2019].

[3] Realizator, "raspberrypi," 28 June 2018. [Online]. Available: https://www.raspberrypi.org/forums/viewtopic.php?t=216940. [Accessed 3 December 2019].

[4] C. E. W. Kusworo Adi, "DISTANCE MEASUREMENT WITH A STEREO CAMERA," International Journal of Innovative Reaseach in Advanced Engineering, 6 November 2017. [Online]. Available: https://ijirae.com/volumes/Vol4/iss11/05.NVAE10087.pdf. [Accessed 5 November 2019].

[5] dasmehdixtr, "kaggle," 2019. [Online]. Available: https://www.kaggle.com/dasmehdixtr/drone-dataset-uav#0008.txt. [Accessed 3 December 2019].

[6] J. Hui, "Medium," 6 March 2018. [Online]. Available: https://medium.com/@jonathan_hui/map-mean-average-precision-for-object-detection-45c121a31173. [Accessed 3 December 2019].

[7] OpenCV-Python Tutorials , "OpenCV-Python Tutorials," [Online]. Available: https://opencv-python-tutroals.readthedocs.io/en/latest/py_tutorials/py_feature2d/py_shi_tomasi/py_shi_tomasi.html. [Accessed 3 December 2019].

[8] P. G. R. G. K. H. P. D. Tsung-Yi Lin, "arxiv," 7 Feburary 2018. [Online]. Available: https://arxiv.org/pdf/1708.02002.pdf. [Accessed 4 December 2019].

[9] D. A. D. E. C. S. S. R. C.-Y. F. A. C. B. Wei Liu, "arxiv," 29 December 2016. [Online]. Available: https://arxiv.org/pdf/1512.02325.pdf. [Accessed 4 December 2019].

[10] E. Forson, "Towards Data Science," 18 November 2017. [Online]. Available: https://towardsdatascience.com/understanding-ssd-multibox-real-time-object-detection-in-deep-learning-495ef744fab#targetText=Single%20Shot%3A%20this%20means%20that,forward

%20pass%20of%20the%20network&targetText=Detector%3A%20The%20networ k%20is%20an,also%2. [Accessed 4 December 2019].

[11] A. S. Walia, "Towards Data Science," 10 June 2017. [Online]. Available: https://towardsdatascience.com/types-of-optimization-algorithms-used-in-neural-networks-and-ways-to-optimize-gradient-95ae5d39529f. [Accessed 3 December 2019].

[12] V. Bushaev, "Towards Data Science," 22 October 2018. [Online]. Available: https://towardsdatascience.com/adam-latest-trends-in-deep-learning-optimization-6be9a291375c#targetText=Adam%20%5B1%5D%20is%20an%20adaptive,for%20 training%20deep%20neural%20networks.&targetText=The%20algorithms%20leve rages%20the%20power,learning%20rates%2. [Accessed 3 December 2019].

[13] A. Nagpal, "Towards Data Science," 13 October 2017. [Online]. Available: https://towardsdatascience.com/l1-and-l2-regularization-methods-ce25e7fc831c. [Accessed 3 December 2019].

[14] Mathworks, "Mathworks," [Online]. Available: https://www.mathworks.com/help/deeplearning/ref/trainingoptions.html#bu80qkw-3_head. [Accessed 3 December 2019].

[15] Mathworks, "Mathworks," [Online]. Available: https://towardsdatascience.com/l1-and-l2-regularization-methods-ce25e7fc831c. [Accessed 3 December 2019].

[16] A. E. Orban, "arxiv," 2018. [Online]. Available: https://arxiv.org/pdf/1701.09175.pdf#targetText=Skip%20connections%20are%20e xtra%20connections,more%20layers%20of%20nonlinear%20processing.. [Accessed 3 December 2019].

[17] OpenCV, "OpenCV," [Online]. Available: https://opencv-python-tutroals.readthedocs.io/en/latest/py_tutorials/py_video/py_lucas_kanade/py_lucas_ kanade.html. [Accessed 3 December 2019].

[18] OpenCV, "OpenCV," [Online]. Available: https://docs.opencv.org/3.4/d2/dff/classcv_1_1TrackerKCF.html. [Accessed 3 December 2019].

[19] OpenCV-Python Tutorials , "OpenCV-Python Tutorials," [Online]. Available: https://opencv-python-tutroals.readthedocs.io/en/latest/py_tutorials/py_video/py_lucas_kanade/py_lucas_ kanade.html. [Accessed 3 December 2019].

[20] I. Starepravo, "Intellias," 3 May 2018. [Online]. Available: https://www.intellias.com/sensor-fusion-autonomous-cars-helps-avoid-deaths-road/. [Accessed 23 September 2019].

[21] J. A. Lopez, "Instructables," July 2012. [Online]. Available: https://www.instructables.com/community/At-room-temperature-how-much-pressure-does-a-12g-/. [Accessed 15 October 2019].

[22] A. Chilton, "Azo Sensors," 15 October 2014. [Online]. Available: https://www.azosensors.com/article.aspx?ArticleID=339. [Accessed 4 November 2019].

[23] M. Larabel, "Phoronix," 30 March 2019. [Online]. Available: https://www.phoronix.com/scan.php?page=article&item=jetson-nano-cooling&num=3. [Accessed 2 October 2019].

[24] "Noctua," Noctura, 15 Feburary 2019. [Online]. Available: https://noctua.at/en/which-is-the-best-fan-for-the-nvidia-jetson-nano. [Accessed 3 October 2019].

[25] EL-PRO-CUS, "EL-PRO-CUS," [Online]. Available: https://www.elprocus.com/how-does-bluetooth-work/. [Accessed 3 December 2019].

[26] JIMBLOM, "Sparkfun," August 26 2013. [Online]. Available: https://learn.sparkfun.com/tutorials/bluetooth-basics/all. [Accessed 3 December 2019].

[27] J. Martindale, "Digital Trends," 25 November 2019. [Online]. Available: https://www.digitaltrends.com/computing/what-is-wi-fi/. [Accessed 3 December 2019].

[28] wifibond, "wifi-bond," 8 April 2017. [Online]. Available: https://wifibond.com/2017/04/08/802-11-association-process/. [Accessed 3 December 2019].

[29] "TechDifferences," 16 August 2017. [Online]. Available: https://techdifferences.com/difference-between-bluetooth-and-wifi.html. [Accessed 3 December 2019].

[30] B. O. Khurram Shahzad, "Semantics Scholar," 2014. [Online]. Available: https://www.semanticscholar.org/paper/A-comparative-study-of-in-sensor-processing-vs.-raw-Shahzad-Oelmann/66f44e31fbf91aa1bb60559ed824c791e7cd922a. [Accessed 3 December 2019].

[31] B. Merriman, "Hardware Studio," 5 July 2018. [Online]. Available: https://techdifferences.com/difference-between-bluetooth-and-wifi.html. [Accessed 3 December 2019].

[32] Orenda, "Medium," 14 February 2017. [Online]. Available: https://medium.com/@fiberstoreorenda/do-you-know-the-difference-between-hub-switch-router-b74c2e8a8143. [Accessed 3 December 2019].

[33] J. Phu, "Our PCB," 28 September 2018. [Online]. Available: https://www.ourpcb.com/multilayer-pool.html. [Accessed 26 October 2019].

[34] SfuptownMaker, "SparkFun," 28 July 2014. [Online]. Available: https://learn.sparkfun.com/tutorials/pcb-basics/all. [Accessed 16 November 2019].

[35] CircuitBasics, "Circuit Basics," 30 January 2016. [Online]. Available: http://www.circuitbasics.com/make-custom-pcb/. [Accessed 29 October 2019].

[36] A. Designer, "Altium Resources," 3 April 2016. [Online]. Available: https://resources.altium.com/pcb-design-blog/identifying-minimum-trace-spacing-and-trace-requirements-in-altium. [Accessed 10 October 2019].

[37] "PCB Cart," 12 December 2018. [Online]. Available: https://www.pcbcart.com/article/content/pcb-partitioning-design-rules.html. [Accessed 21 November 2019].

[38] NVIDIA, "NVIDIA Jetson Nano System-on-Module Data Sheet [PRELIMINARY]," NVIDIA, 14 October 2019. [Online]. Available: https://developer.nvidia.com/embedded/downloads#?search=Data%20Sheet. [Accessed 18 October 2019].

[39] R. Pi, "Raspberry Pi 4 Model B Datasheet," Raspberry Pi (Training) Ltd., June 2019. [Online]. Available: https://www.raspberrypi.org/documentation/hardware/raspberrypi/bcm2711/rpi_D ATA_2711_1p0_preliminary.pdf. [Accessed 19 October 2019].

[40] Intel, "Intel Neural Compute Stick 2 Data Sheet," Intel, 14 July 2019. [Online]. Available: https://www.intel.com/content/dam/support/us/en/documents/boardsandkits/neural-compute-sticks/NCS2_Datasheet-English.pdf. [Accessed 20 October 2019].

[41] G. Coral, "Coral Dev Board Datasheet," Google, August 2019. [Online]. Available: https://coral.ai/docs/dev-board/datasheet/. [Accessed 19 October 2019].

[42] C. 101, "ATMega328P Microcontroller," Components 101, 4 April 2018. [Online]. Available: https://components101.com/microcontrollers/atmega328p-pinout-features-datasheet. [Accessed 19 October 2019].

[43] TI, "Mixed Signal Controller: MSP430G2x53," Texas Instruments, 16 May 2013. [Online]. Available: https://www.ti.com/lit/ds/symlink/msp430g2553.pdf. [Accessed 20 October 2019].

[44] 3. Matter, "3dhubs," [Online]. Available: https://www.3dhubs.com/knowledge-base/fdm-3d-printing-materials-compared/. [Accessed 3 December 2019].

[45] Dorhea, "Amazon," [Online]. Available: https://www.amazon.com/dp/B07DNSSDGG/ref=sspa_dk_detail_2?psc=1&spLa= ZW5jcnlwdGVkUXVhbGVyPUExQURQT1gyWjc5VlZQJmVuY3J5cHRlZ ElkPUEwNDAyNjMzMVQ3Rlc0S0ZJQTVXNSZlbmNyeXB0ZWRBZElkPUEw OTE2Nzc4MjdZUkNJRzZNRlk4NSZ3aWRnZXROYW1lPXNwX2RldGFpbDIm YWN0aW9uPWNsaWNrUm. [Accessed 3 December 2019].

[46] R. Pi, "RaspberryPi.org," Raspberry Pi (Training) Ltd., 2017. [Online]. Available: https://www.raspberrypi.org/documentation/hardware/camera/. [Accessed 8 November 2019].

[47] I. RealSense, "intel.com," Intel, January 2019. [Online]. Available: https://www.intel.com/content/dam/support/us/en/documents/emerging-technologies/intel-realsense-technology/Intel-RealSense-D400-Series-Datasheet.pdf. [Accessed 9 November 2019].

[48] "The Net Gun Store," [Online]. Available: https://thenetgunstore.com/products/spider-net-gun-package. [Accessed 3 December 2019].

[49] "Animal Care," 2019. [Online]. Available: https://www.animal-care.com/product/coda-all-purpose-net-gun/. [Accessed 3 December 2019].

[50] S. Online, "omc-stepperonline.com," StepperOnline, 18 August 2018. [Online]. Available: https://www.omc-stepperonline.com/download/17HS13-0404S1.pdf. [Accessed 19 November 2019].

[51] Wantai, "wantmotor.com," Wantai Motors, 14 January 2011. [Online]. Available: https://oceancontrols.com.au/files/datasheet/sfe/SFM-002_42BYGHM809.PDF. [Accessed 19 November 2019].

[52] B. Schmalz, "schmalzhaus.com," Adafruit, 10 November 2016. [Online]. Available: http://www.schmalzhaus.com/BigEasyDriver/. [Accessed 19 November 2019].

[53] H. Technology, "handsontec.com," Handson Technology, [Online]. Available: http://www.handsontec.com/dataspecs/L298N%20Motor%20Driver.pdf. [Accessed 19 November 2019].

[54] Geekworm, "RPI Wiki," 12 September 2019. [Online]. Available: http://raspberrypiwiki.com/index.php/Wireless_USB_adapter. [Accessed 3 December 2019].

[55] Comfast, "Comfast Wifi," 2019. [Online]. Available: https://comfastwifi.us/comfast-cf-wu810n-mini-usb-wireless-adapter-dongle. [Accessed 3 December 2019].

[56] E. Systems, "Espressif," 2019. [Online]. Available: https://www.espressif.com/sites/default/files/documentation/0a-esp8266ex_datasheet_en.pdf. [Accessed 3 December 2019].

[57] tp-link, "tp-link," [Online]. Available: https://www.tp-link.com/us/home-networking/wifi-router/tl-wr841n/. [Accessed 3 December 2019].

[58] tp-link, "tp-link," [Online]. Available: https://www.tp-link.com/us/home-networking/wifi-router/tl-wr940n/. [Accessed 3 December 2019].

[59] linksys, "linksys," [Online]. Available: https://www.linksys.com/us/p/P-E2500/. [Accessed 3 December 2019].

[60] IEEE, "IEEE802," 14 June 2002. [Online]. Available: http://ieee802.org/15/Bluetooth/802-15-1_Clause_05.pdf. [Accessed 3 December 2019].

[61] IEEE, 26 June 1997. [Online]. Available: http://ant.comm.ccu.edu.tw/course/92_WLAN/1_Papers/IEEE%20Std%20802.11-1997.pdf. [Accessed 3 December 2019].

[62] V. Beal, "webopedia," [Online]. Available: https://www.webopedia.com/TERM/8/802_11.html. [Accessed 3 December 2019].

[63] "acqnotes," [Online]. Available: http://www.acqnotes.com/Attachments/Briefing%20Introduction%20to%20Software%20Configuration%20Management%20Training.pdf. [Accessed 3 December 2019].

[64] N. Davis, "All About Circuits," 20 October 2017. [Online]. Available: https://www.allaboutcircuits.com/news/ipc-standards-the-official-standards-for-pcbs/. [Accessed 2 November 2019].

[65] Python, "Python," 5 July 2001. [Online]. Available: https://www.python.org/dev/peps/pep-0008/. [Accessed 3 December 2019].

[66] CUI, "CUI," [Online]. Available: https://drive.google.com/drive/u/0/folders/1TmN3s78RHhmNvLoNpZul5aa4NxEY fIv3. [Accessed 3 December 2109].

[67] Renesas, "Renesas," 16 March 2011. [Online]. Available: https://www.renesas.com/br/en/products/power-management/linear-vs-switching-regulators.html. [Accessed 28 November 2019].

[68] NVIDIA, "NVIDIA Autonomous Machines," NVIDIA, 18 March 2019. [Online]. Available: https://developer.download.nvidia.com/assets/embedded/secure/jetson/Nano/docs/ NVIDIA_Jetson_Nano_Developer_Kit_User_Guide.pdf?6xZL1a0S_Nh7rciTa1RY br2z6CpXELkjr4CglxgMP94HKwZu59_Y6v_HTPr3e7JR7zLz4ouSMD7sM3lfO Vlc9mKhQxgX8g73suTp69A3Qr7wdVdFFnZdrpVD2AJi0H5Ze. [Accessed 15 October 2019].

[69] A. Smith, "doityourself," 1 June 2017. [Online]. Available: https://www.doityourself.com/stry/set-up-lan. [Accessed 3 December 2019].

[70] A. Rosebrock, "pyimagesearch," 30 July 2018. [Online]. Available: https://www.pyimagesearch.com/2018/07/30/opencv-object-tracking/. [Accessed 3 December 2019].

[71] B. R. J. J. M. Michael George, "Science Direct," 2017. [Online]. Available: https://www.sciencedirect.com/science/article/pii/S1877050917328363?via%3Dihu b. [Accessed 3 December 2019].

[72] OpenCV-Python Tutorials , "OpenCV-Python Tutorials," [Online]. Available: https://www.sciencedirect.com/science/article/pii/S1877050917328363?via%3Dihu b. [Accessed 3 December 2019].

[73] dasmehdixtr, "kaggle," [Online]. Available: https://www.kaggle.com/dasmehdixtr/drone-dataset-uav. [Accessed 3 December 2019].

11.2 Copyright Permissions
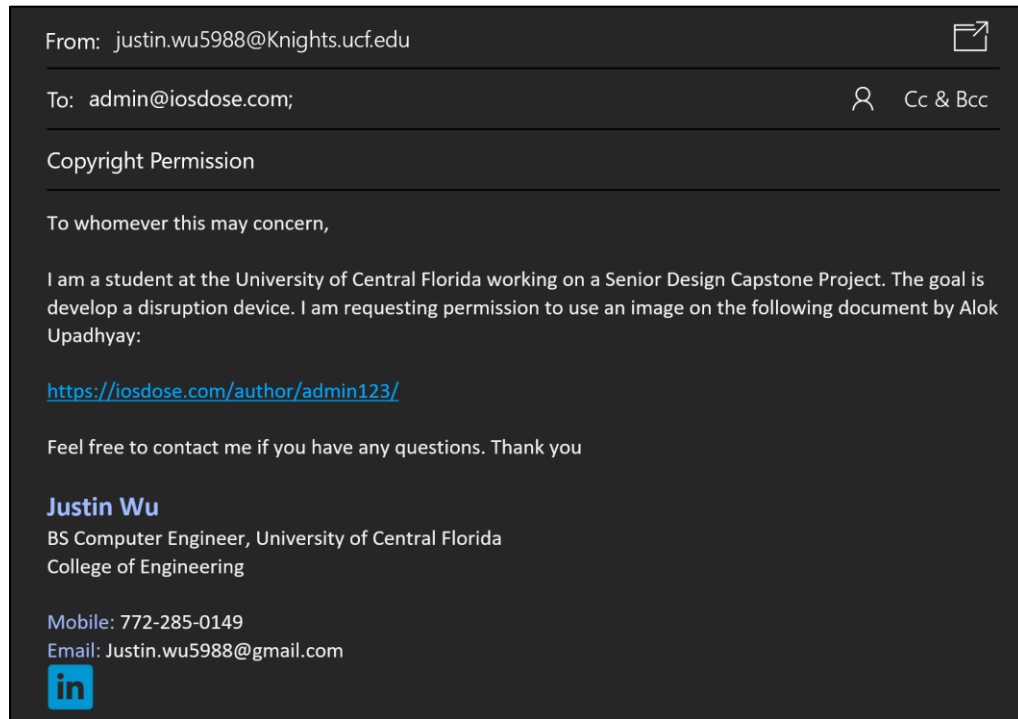
Figure 61: Image Permission Request
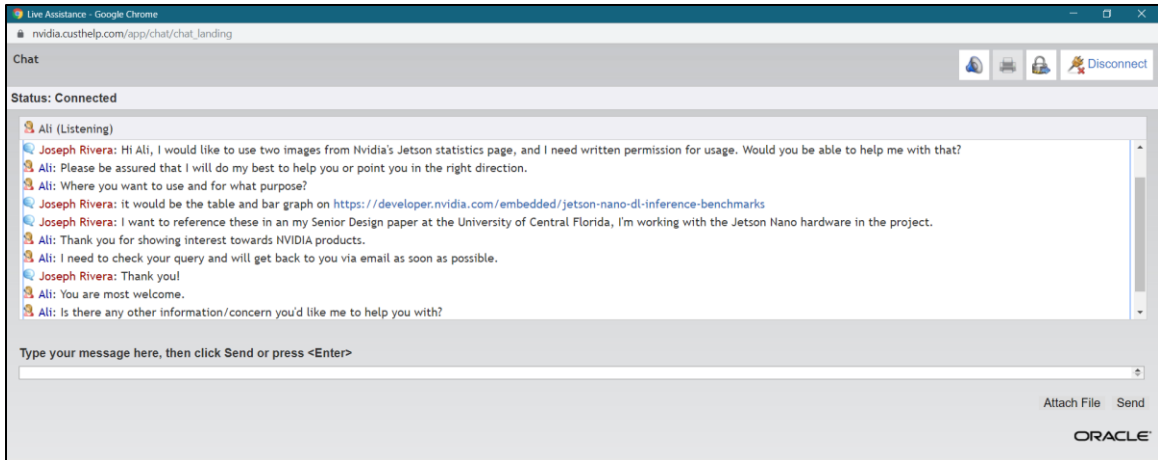
Figure 62: Image Permission Request
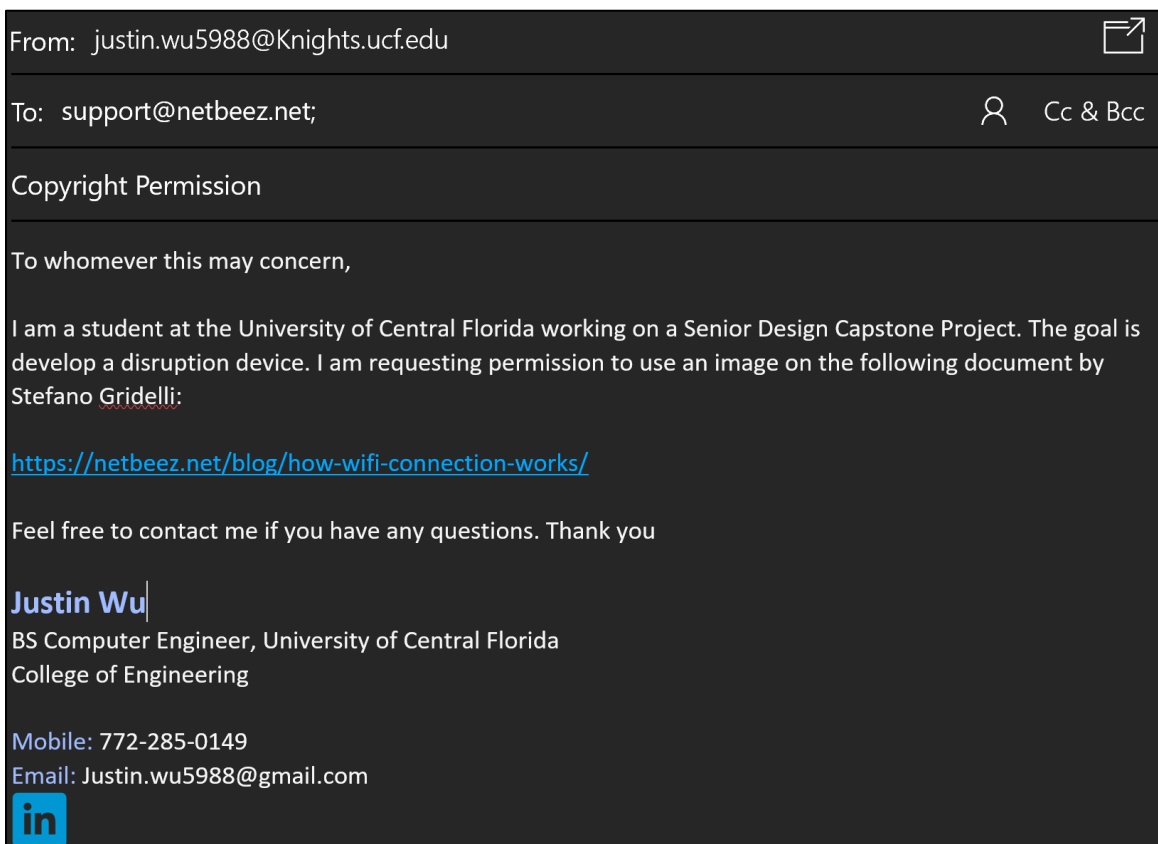
Figure 63: Image Permission Request

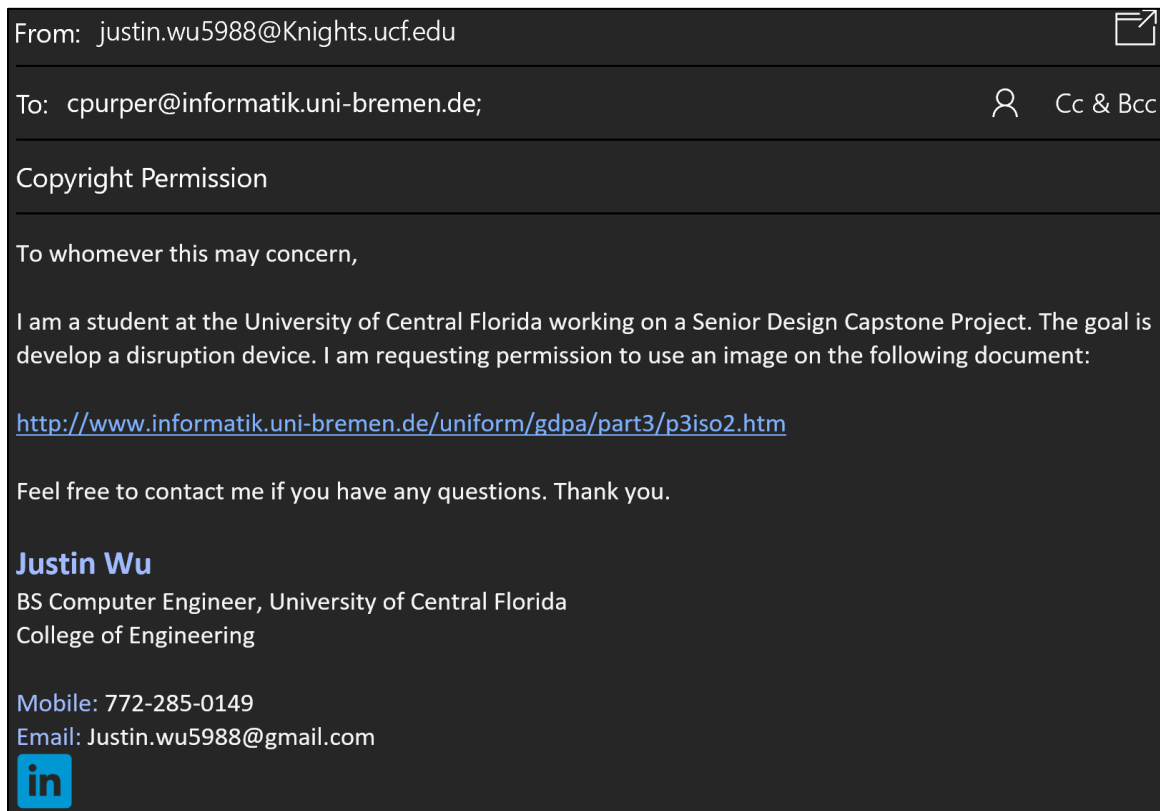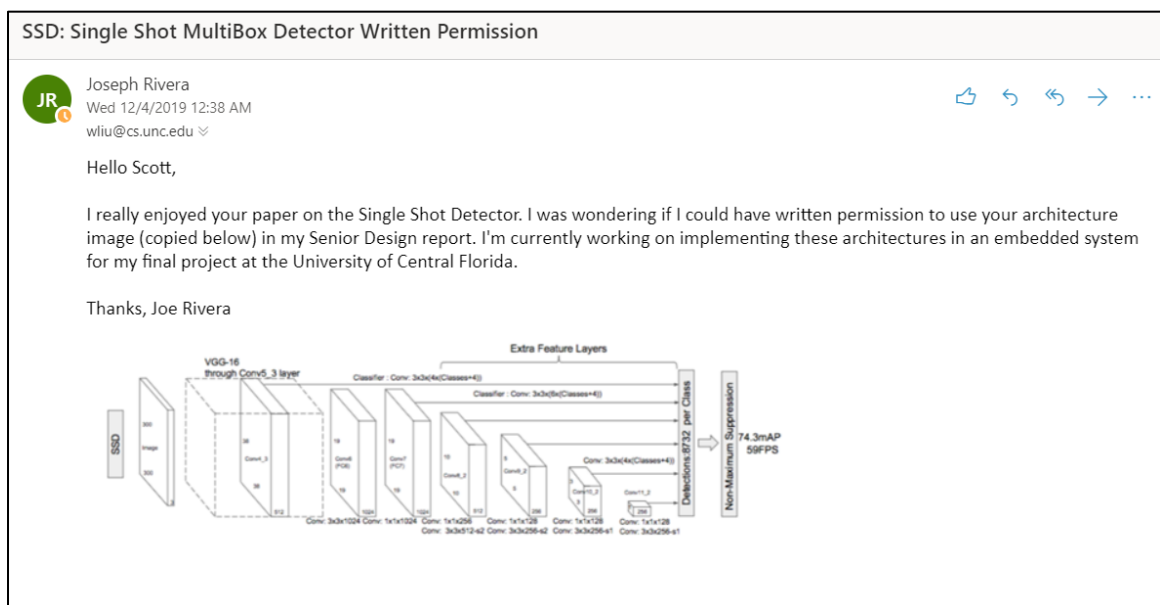**Figure 64: Image Permission Request**

Figure 65: Image Permission Request

Figure 66: Image Permission Request
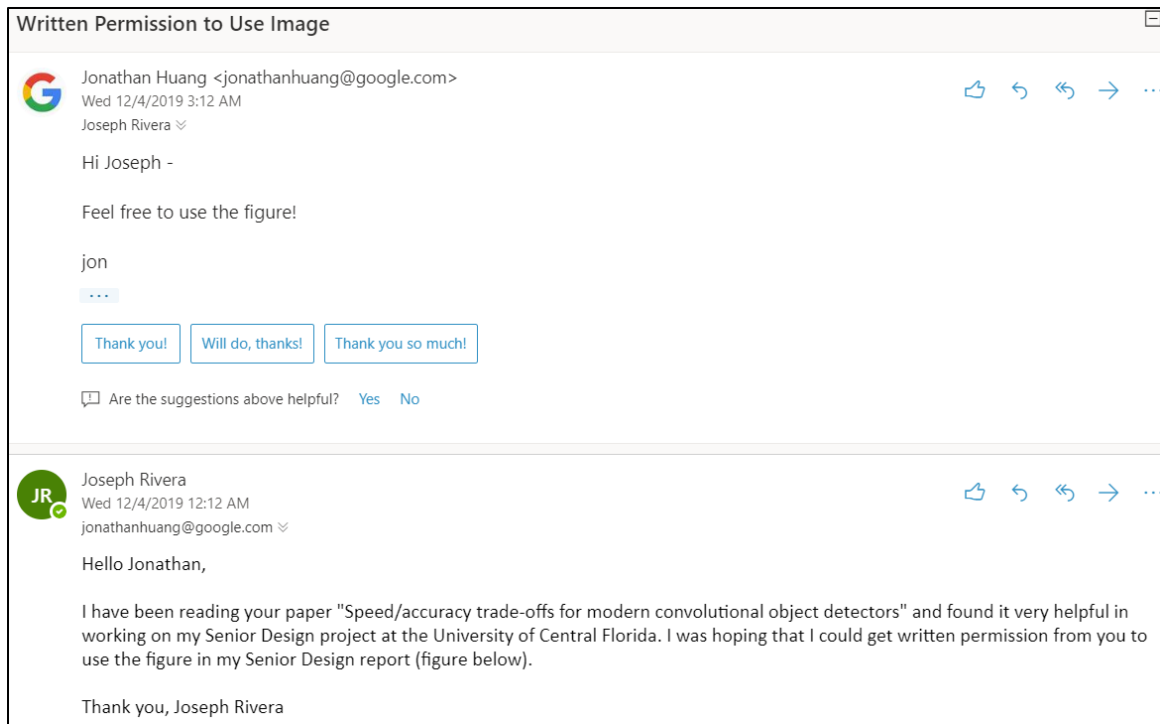

Figure 67: Image Permission Request

Written Permission to Use Image

Jonathan Huang <jonathanhuang@google.com>
Wed 12/4/2019 3:12 AM
Joseph Rivera

Hi Joseph -

Feel free to use the figure!

jon

...

Thank you! | Will do, thanks! | Thank you so much!

Are the suggestions above helpful? Yes No

Joseph Rivera
Wed 12/4/2019 12:12 AM
jonathanhuang@google.com

Hello Jonathan,

I have been reading your paper "Speed/accuracy trade-offs for modern convolutional object detectors" and found it very helpful in working on my Senior Design project at the University of Central Florida. I was hoping that I could get written permission from you to use the figure in my Senior Design report (figure below).

Thank you, Joseph Rivera

Figure 68: Image Permission Acknowledgement

Written Permission to Use Figures

Joseph Rivera
Wed 12/4/2019 12:47 AM
walt.stuart@mathworks.com; joseph.rivera@lmco.com

Hi Walt,

I'm currently working on a Lockheed Martin sponsored Senior design project at the University of Central Florida (organized b Jonathan Tucker in Applied Research), and I was wondering if I could have written permission to use this figure from the Mat documentation in our final paper.

Thanks, Joe Rivera

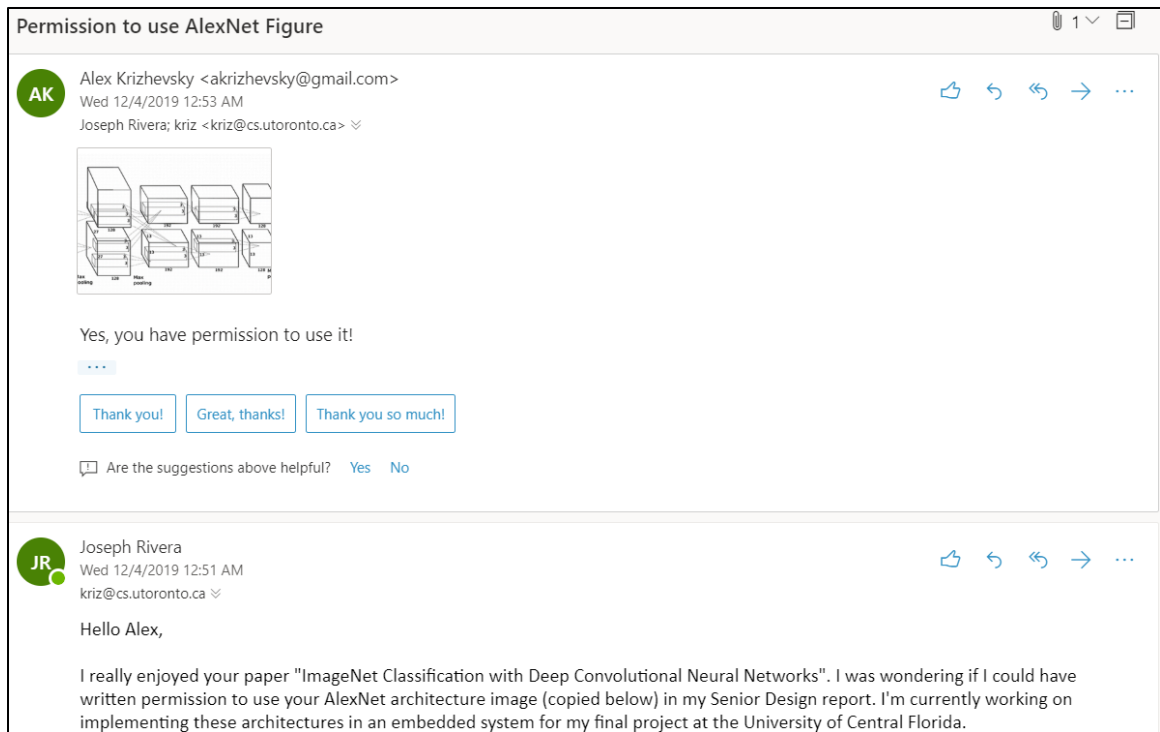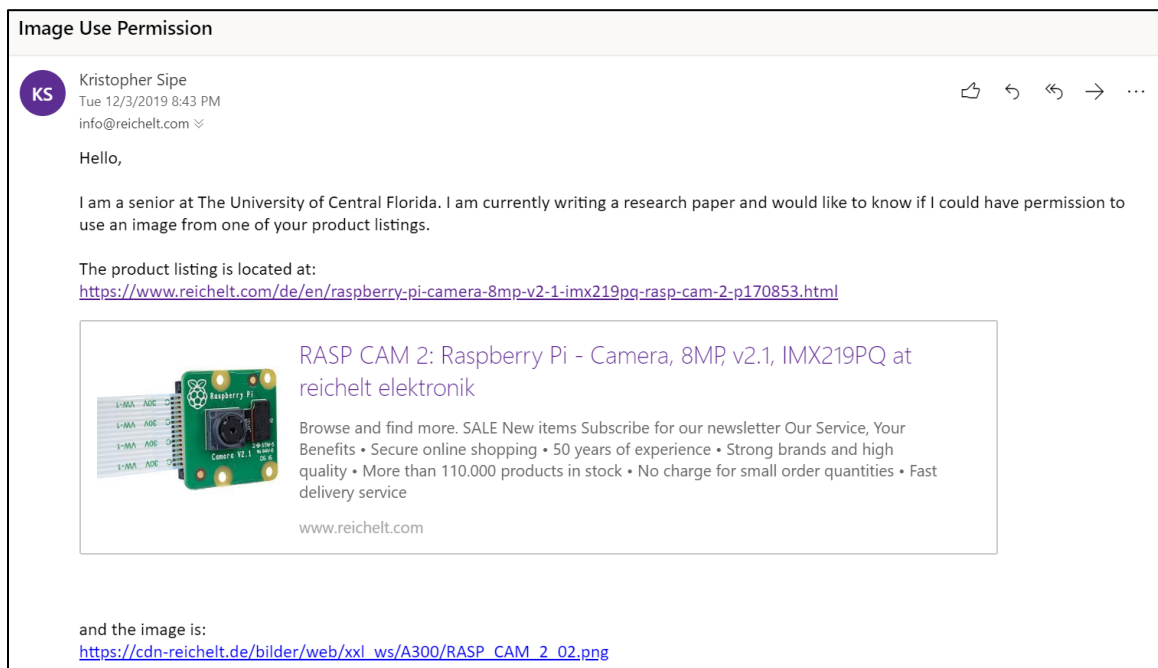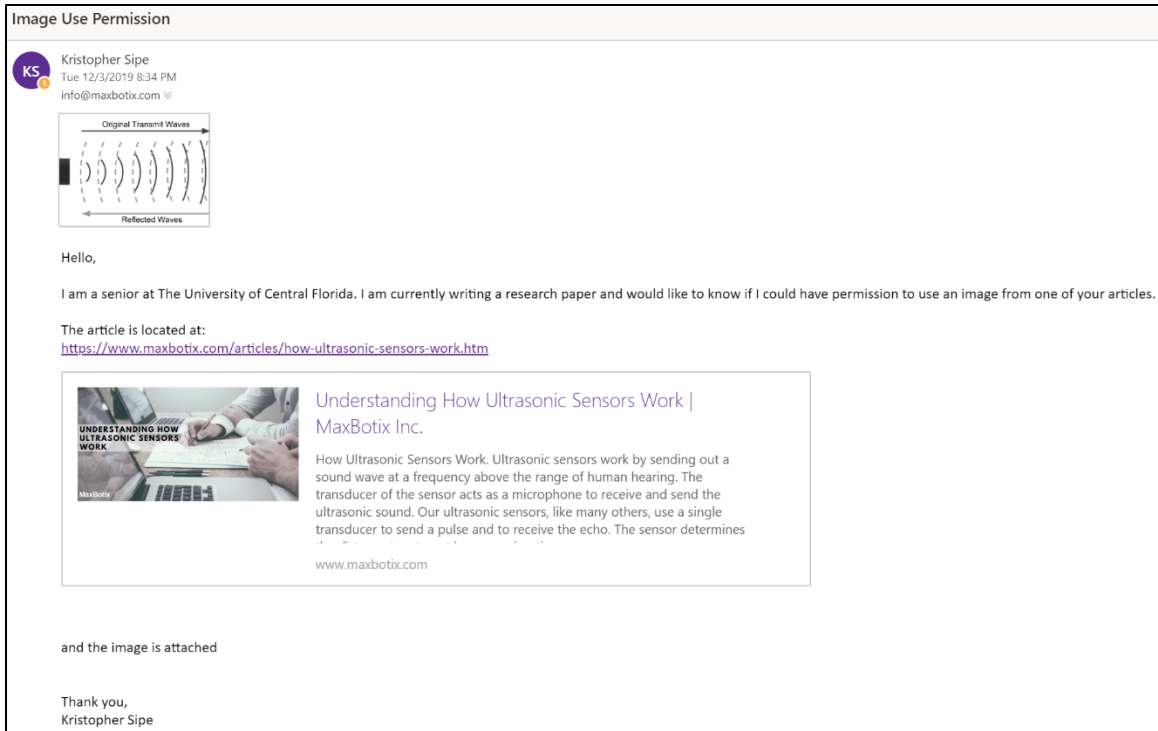**Figure 69: Image Permission Request**

Figure 70: AlexNet Image Permission Acknowledgement

Figure 71: Image Permission Request

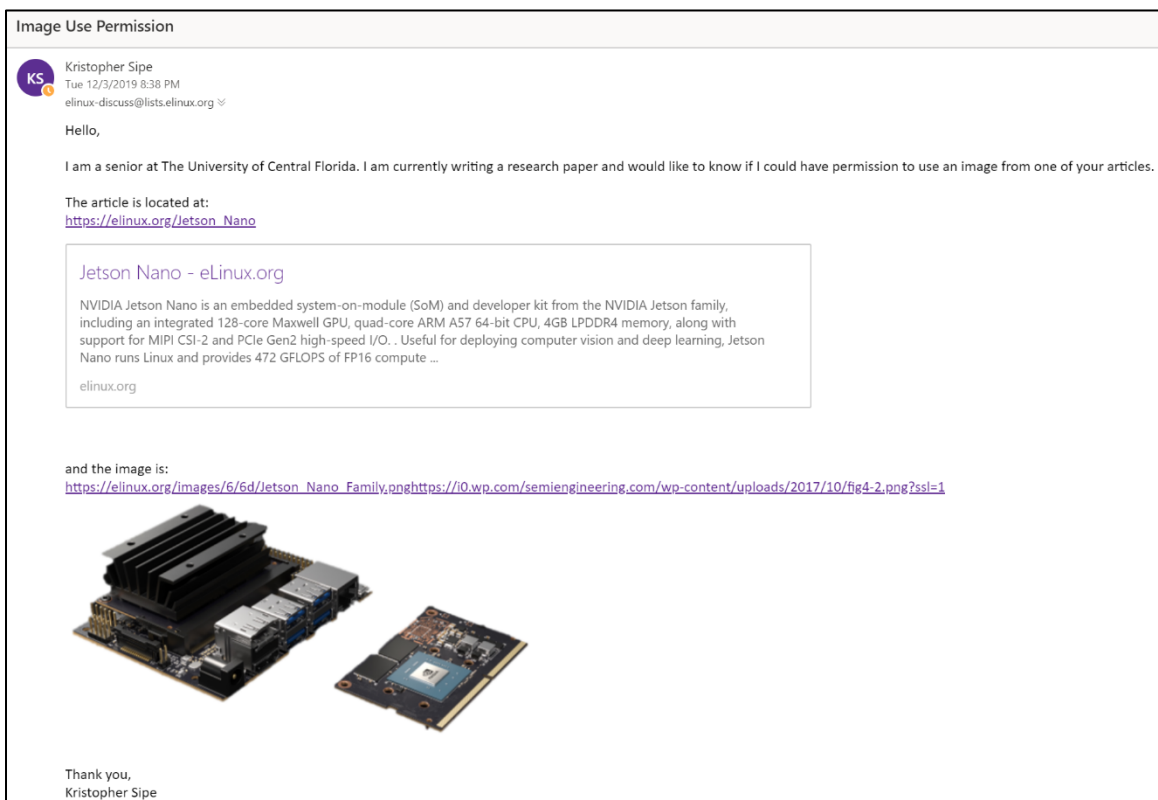**Figure 72: Image Permission Request**
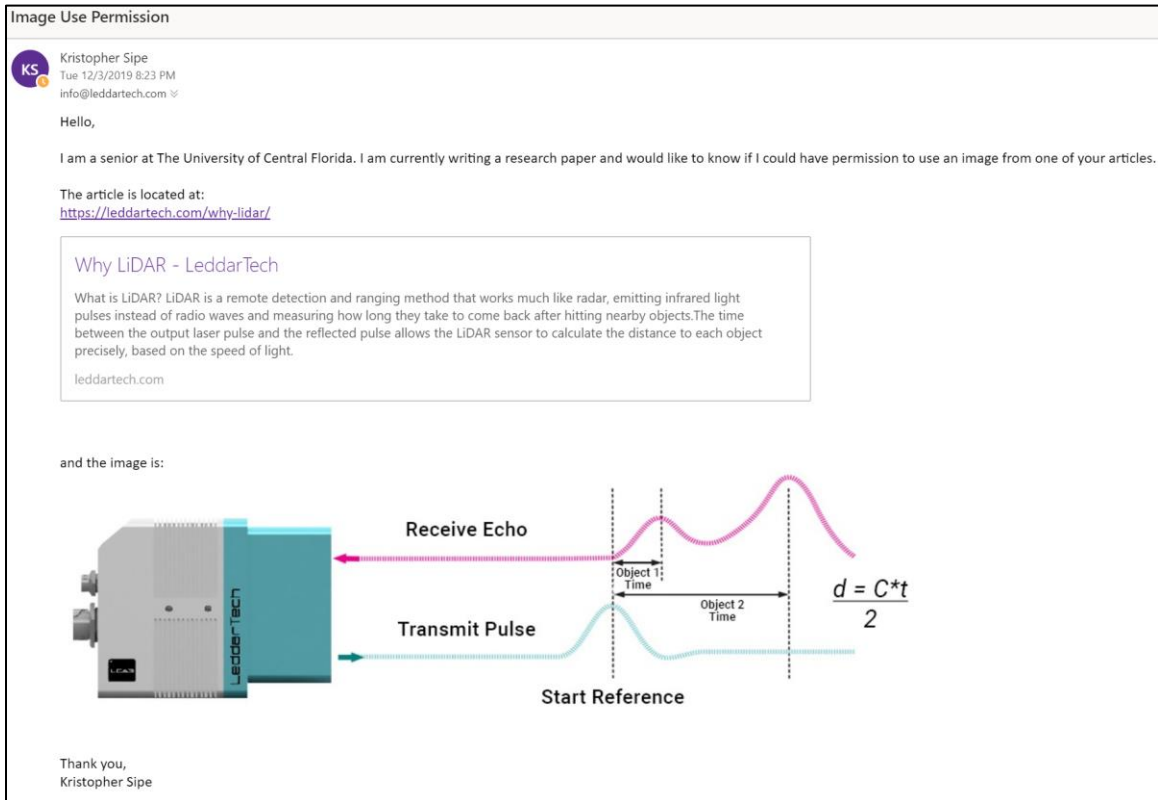

Figure 73: Image Permission Request
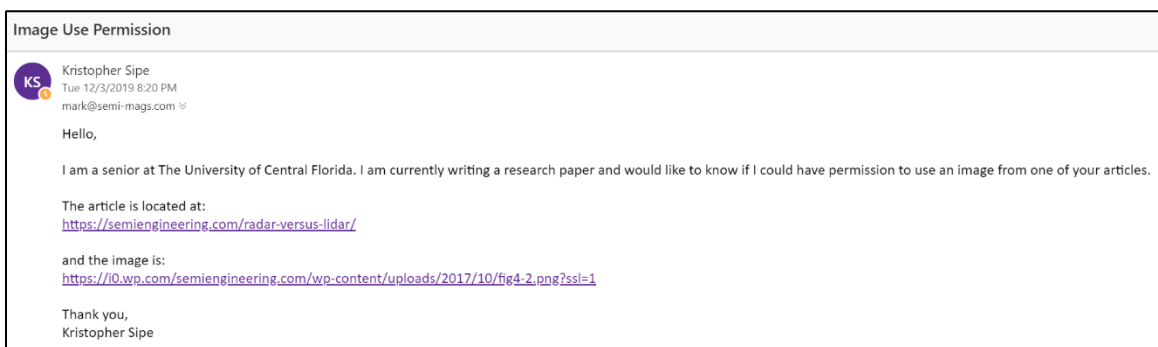
Figure 74: Image Permission Request

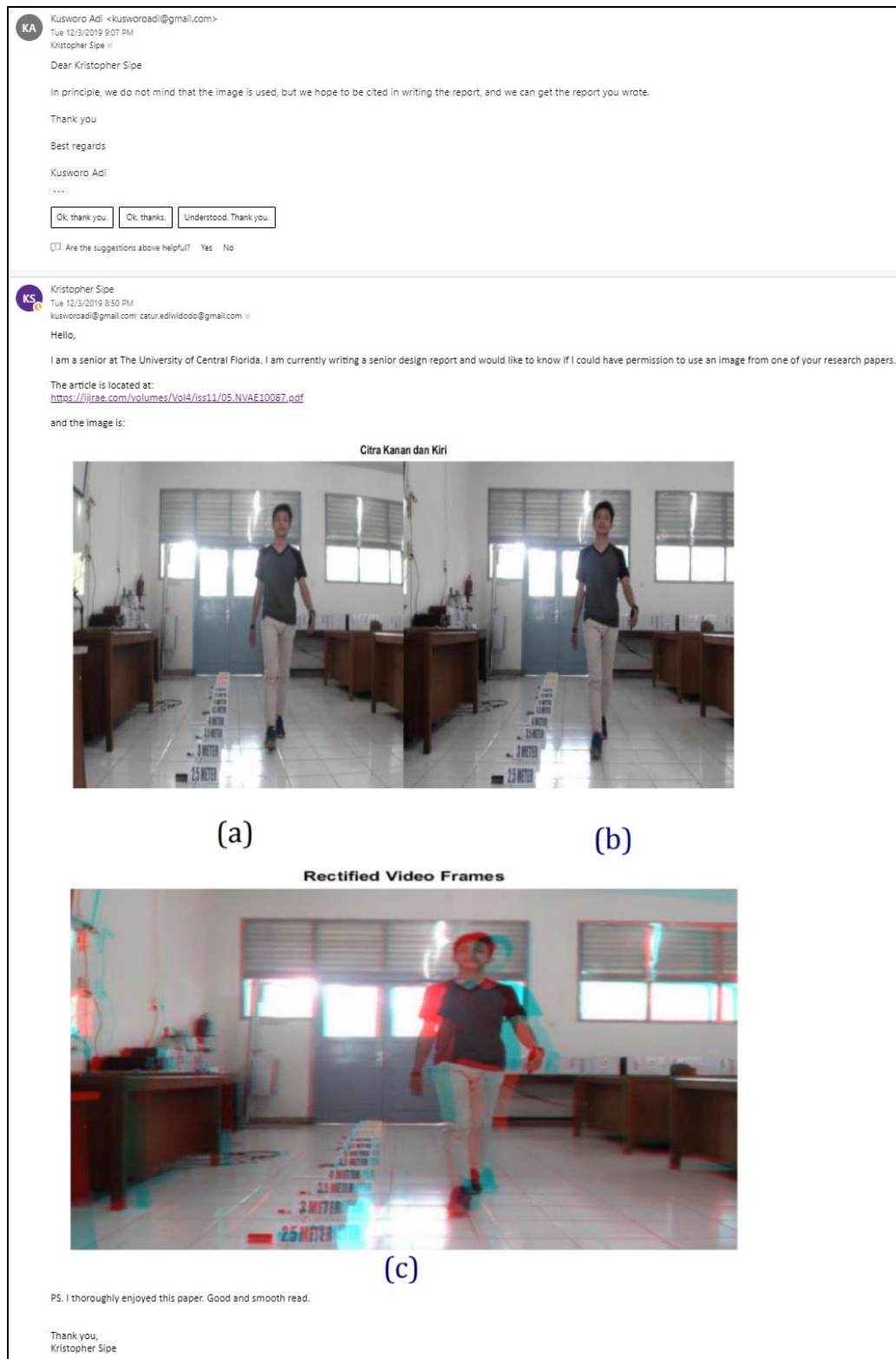**Figure 75: Image Permission Request**

Figure 76: Image Permission Request

Permission to Use

Joseph Rivera
Wed 12/4/2019 3:26 AM
goppold@mediamarktsaturn.com ⌄

Hello Josef,

I really enjoyed your paper "An improvement of the convergence proof of the ADAM-Optimizer". I was wondering if I could have written permission to the image of your optimizer comparison (copied below) in my Senior Design report. I'm currently working on implementing some of these optimizers in training a CNN for my final project at the University of Central Florida.
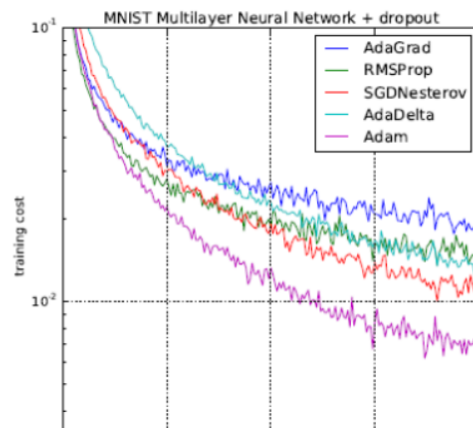
Thanks, Joe Rivera

Figure 77: Image Permission Request